POLITECNICO DI TORINO

MICHIGAN STATE UNIVERSITY

DIPARTIMENTO DI ING. MECCANICA E AEROSPAZIALE

Master of Science in Automotive Engineering

SELECTIVE BINDER CURING: A NOVEL HYBRID 3D PRINTING TECHNIQUE

TESTING, DESIGN AND ASSEMBLY OF A PROTOTYPE

Advisor: Prof. **Luca Iuliano**

Co-Advisor: Dr. **Patrick Kwon**

Laureando: **Luca Milocco**

March 27, 2019

TABLE OF CONTENTS

List of Figures

List of Tables

Chapter 1

INTRODUCTION

1.1 PRINCIPLES OF ADDITIVE MANUFACTURING

In the conventional production processes, components are created through several machining steps, all characterized by a common characteristic: the material removal from a solid block or a semi-finished part. As a result, it is often referred as Subtractive Manufacturing.

In contrast, additive manufacturing (AM) is the technical term that refers to as a process by which components are built up adding layer-upon-layer of material.

"It is also the formalized term for what used to be called rapid prototyping and what is popularly called 3D printing. In other words, the emphasis is on creating something quickly and that the output is a prototype or basis model from which further models and eventually the final product will be derived." "In a product development context, the term rapid prototyping was used widely to describe technologies which created physical prototypes directly from digital model data." [10, p.1]

Likewise ATSM defines AM as "the process of joining materials to make objects from 3D model data, usually layer, as opposed to subtractive manufacturing methodologies" [13]

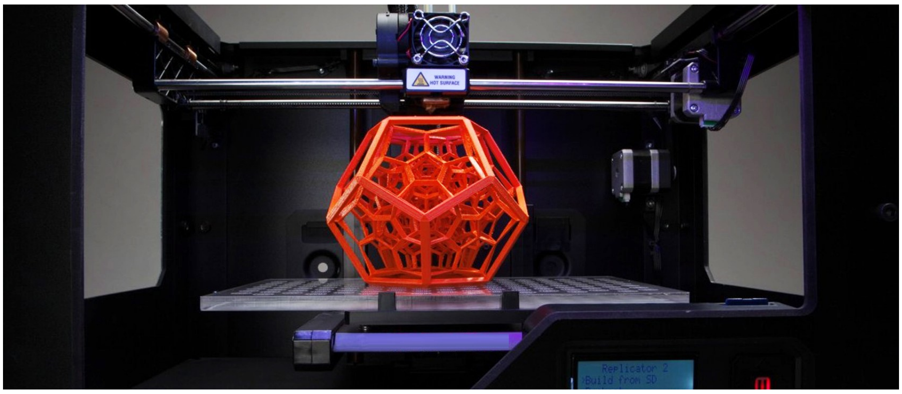

Figure 1.1: Example of a AM process

However, the term has become inadequate to describe this technology.

Modern techniques have their foundations in four key patents: vat photopolymerization, powder bed fusion, material extrusion, and binder jetting. [9]

Their first applications were in the area of rapid prototyping and, only in a second moment, tooling. Even though these continue to be exploited, the technological development has led to the birth of several new techniques and to a general improvement of performances (in terms of output quality, time reduction, number of suitable materials[1], etc.) such that they are becoming more and more a reliable series production alternative.

For instance, in the aerospace industry, where aircraft components often have complex geometries, AM technologies represent an ideal solution. In the medical sector, with highly personalized and micro-accurate applications in orthodontics, prosthetics, orthopaedics, etc., AM processes are already widely employed. [2]

As a result, the ASTM F42 committee underlined the need for using the word Additive Manufacturing, in replacement of the old RP[2] and other synonyms, also in order to distinguish the process from subtractive manufacturing techniques [13].

From a manufacturing point of view, AM technologies have given rise to a renovation which has the potential to become revolutionary in the way we are used to producing objects, hence it's considered one of the pillars of Industry 4.0.

Additive Manufacturing can have a strong impact in terms of: [2, 9]

- waste reduction
- cost reduction
- building and assembly process simplification
- lead time reduction
- supply chain simplification;
- industrial machinery reduction

[1]Such as metals, ceramics, composite etc.
[2]Rapid Prototyping

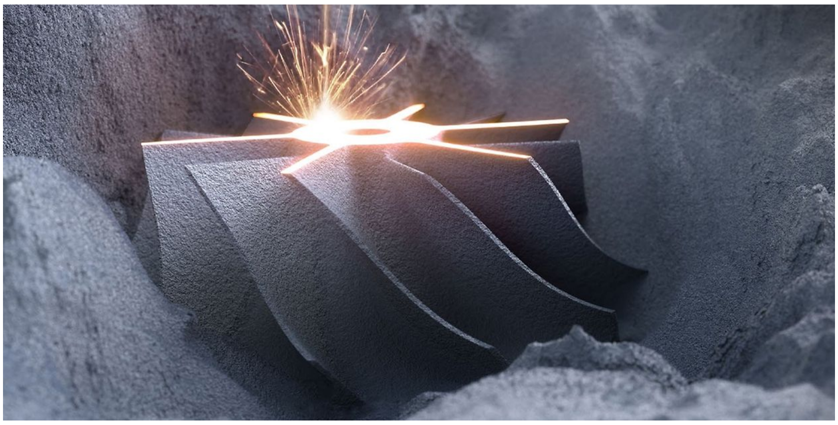

Figure 1.2: Example of a AM process application to aerospace industry

The basic principle of AM is that, starting from a CAD file, the object is virtually sliced in layers, the information is saved in an STL file, transferred to the AM machine and built through the deposition of material in layers (and/or energy to fuse the raw material).

Thus, one of the main benefit of AM is its simplification of the process planning while satisfying customized design requirements [4]. Conventional production requires a careful analysis of the part geometry, so as to determine the correct operations order, which are the required tools and the process parameters, whether additional fixtures may be needed etc. Whereas AM requires only some setups and a basic knowledge of the process and of the machine functioning. [10, p.2]

The production, in this way, becomes more streamlined, it is performed usually in a single step, no machine or tool change are needed, the level of experience necessary to operate the system, as well as the number of resources, are limited.

AM processes also allow the realization of complex-shaped parts that could not be produced as a single part with the classical manufacturing systems. In addition, the complexity of the process preparation is not directly proportional to the complexity of the component. Therefore, detailed and elaborated parts may simply require more precise positioning or additional support structures.

The accuracy of the AM machines is of course finite and, as a result, layers have a minimum finite thickness, which implies that final products can be only an approximation of the ideal models. For this reason, the thinner the layer thickness is, the more precise will be the final part, but with a significant increase in processing time.

Having said that, the aforementioned progress of the AM technologies has led to levels of accuracy which almost comply with the actual market requirements. On the other hand, there are still some deficiencies which have become a central focus of the recent research. Time and cost are certainly among the most important ones, in particular when we refer to throughput and productivity of a mass manufacturing process.

For these reasons, in many different applications (both for production or repair) a combination of subtractive and additive techniques produced reliable, efficient and cost-effective results.

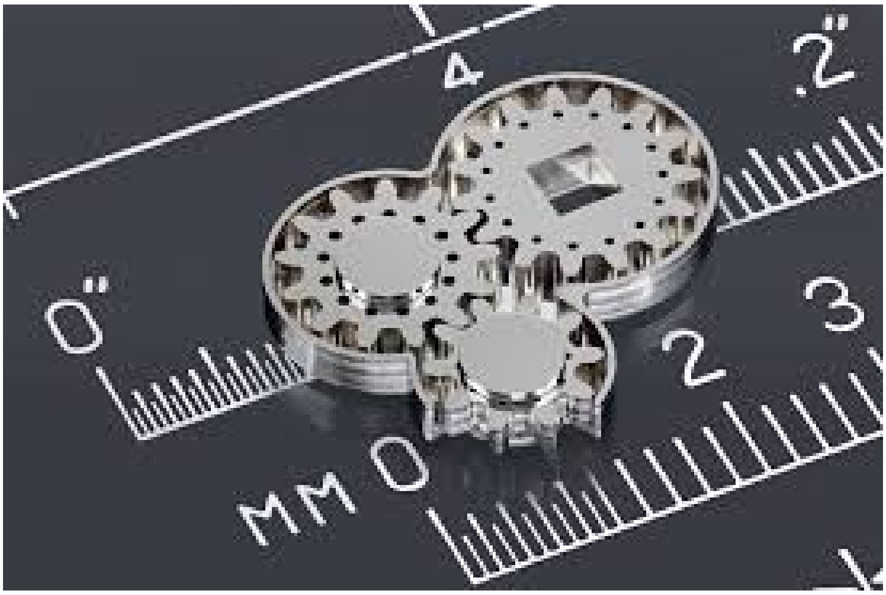

Figure 1.3: Level of precision achieved by the latest technologies, courtesy of Microfabrica

1.1.1 AM Generic Process Manufacturing

Despite the several production technologies that have been developed over the past decades, a common generic process characterizes all of them, and it can be schematized as follows: [10, 25]

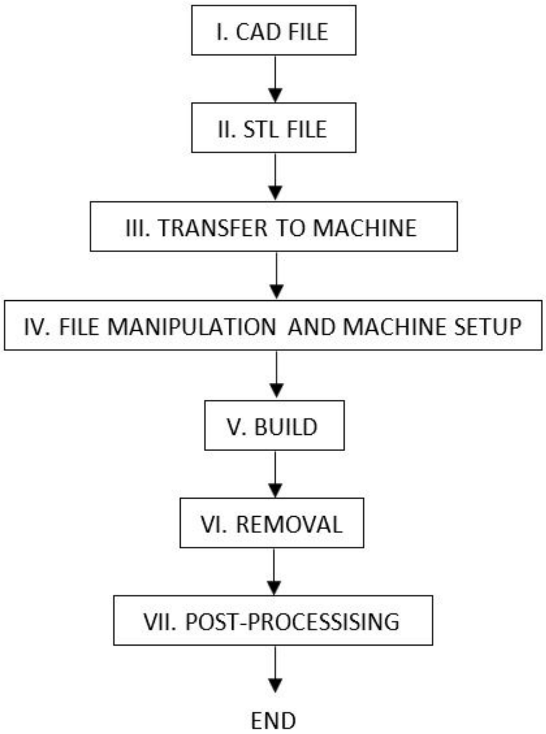

Figure 1.4: Schematization of a generic AM process

I. CAD FILE

The process has to start from the creation of a 3D solid surface or from its surface representation, either through the use of modelling software or via reverse engineering.

II. STL FILE

The information coming out from the CAD file has to be converted in an STL[3] file, which discretizes the solid or the surface representation in a set of triangles, preparing the information for the slicing procedure. This step has to be performed by additional software.

III. TRANSFER TO MACHINE

The file has to be transferred to the AM machine.

[3]Standard Triangulation Language

IV. FILE MANIPULATION AND MACHINE SETUP

The machine is to be prepared and the process parameters must be set, according to the desired result, in terms of process time and/or final quality, to the employed material, to the kind of technique etc.

V. BUILD

One basilar characteristic of the AM machines is their automation. They do not require any manual operation, except for the supply of material at the beginning, and, in case, during the fabrication, and an optional superficial supervision.

VI. REMOVAL

At the end of the process, the part has to be removed from the AM machine.

VII. POST-PROCESSING

The part may still require some post-processing operation, such as curing, polishing, cleaning etc.

After the AM process, parts could still need some specific treatment, such as painting or assembly, as in the case they are part of kits. It has to be highlighted that each of the AM techniques is maybe similar, but still different from any other. As a consequence, each of them could require some specific steps or particular attention over some aspects. Time, quality, cost, needed resources and other parameters vary according to the employed production method. At the end, components have to comply with the requirements of their initial design, which could be related to design, surface quality, mechanical properties, specific functionalities etc.

Unfortunately, AM processes still face great challenges, including the reduction of the building time and cost, while increasing the mechanical and superficial properties, as well as the portfolio of suitable materials and the building size of the machines.

What the AM also lacks is an optimal tradeoff among accuracy, cost, throughput, and size. With the technology existing nowadays it seems that the improvement of one parameter is inevitably accompanied by the worsening of an another one. [21, 27]

1.1.2 AM Classification

The available technologies in the market are numerous, therefore their classification could be problematic. One of the main and more generic approaches is to categorize the techniques according to the type of raw material [10, p.31]:

- LIQUID POLYMER: It is one of the most popular material, as well as the first to be applied in a commercial system (3D Systems Stereolithography). More precisely, the materials commonly employed are photopolymers, in other terms polymers that chemically react when exposed to a sufficient level of luminous energy. Anyway, also some applications characterized by the use of hydrogels, as well as liquid polymers have been efficiently employed.

- DISCRETE PARTICLES: They are normally powders graded in a relatively uniform shape and size. Similarly to the layer thickness, a small particle dimension is usually linked to improved final results. On the other hand it can be correlated to distribution and dispersion problems. It has also been demonstrated that a mix of different particle sizes could be beneficial in obtaining a higher final density of the component [5].

- MOLTEN MATERIAL: As the denomination states, their working principle is based on the melting of the raw material, usually achieved raising its temperature by a pre-heated chamber. Several different applications, which use this technology, can be found in the market, and they usually differentiate according to the employed heating system.

- SOLID SHEET: It can be considered one of the oldest and simplest AM application. The components are created through the bonding of different layers, obtained by cutting, usually with laser systems, sheets of various materials.

The classification could be refined, as made by Pham [22], who uses a two-dimensional classification method. The first is the type of raw material utilized, with the classification seen in the previous paragraph. The second is the method by which the layers are constructed. While the first technologies made use of single point source to gradually create the layers, nowadays systems made of multiple sources (2x single source and arrays of single source) or 2D surface systems [21, 16, 24] are often used in order to increase the system productivity.

It is worth to mention then the recent classification made by ASTM [13], which is becoming a world-spread standardization:

- VAT photopolymerization: Born with the first Stereolithography AM commercial system, it utilizes a light source, and in some cases an optic system, to selectively cure a liquid photopolymer kept in a container, technically called vat, creating layers of solidified material. The working platform is then shifted downwards or upwards, according to the developed technology, and the process is repeated cyclically.

- POWDER BED FUSION: They make use of an energy beam (most commonly a scanning laser or an electron beam) to selectively fuse the powder stocked in a container. Once the solid layer is created, the platform is shifted, a new powder layer is spread over it (often via a counter-rolling mechanism), and the process is repeated.

- MATERIAL EXTRUSION: The process is quite simple, as described by its technical name, the layers are created through the deposition of extruded material. It requires high operating temperatures so as to reach the melting point of the raw material and facilitate its flow.

- MATERIAL JETTING: Similar to ink-jet printing technology, it deposits droplets of material onto the previous layer via drop-on-demand inkjetting. A post-process phase, characterized by the heating or the photocuring of the material, is usually required so as to strengthen the component. [9]

- BINDER JETTING: The process has some similarities with the powder bed fusion systems. The layers of building powder are in fact created in the same way. However, instead of using an energy source to melt the material, a binder is selectively jetted on the powder. In-process and post-process heating phase are required to cure and then remove the binder from the created component (debinding), as well as to increase its final density.

- SHEET LAMINATION: It is the process described in the aforementioned classification, made according to the type of material utilized.

- DIRECT ENERGY DEPOSITION: Process that simultaneously deposits a material (usually a metal powder or wire) and provides energy (usually via laser or electron beam, as for powder bed fusion systems) to create a molten pool. A translating system provides the motion freedom necessary to create the desired shape. Therefore, DED machines are essentially 3D welding systems.

1.1.3 Vat photopolymerization

Most polymers are sensible to UV[4] radiations, some of them even to light in the visible range. In the case they are exposed to a sufficient quantity of energy, they undergo a chemical reaction, creating boundaries among particles, and becoming solid. This phenomenon is called photopolymerization.

Therefore the ASTM has defined the vat photopolymerization as the “additive manufacturing process in which liquid photopolymer in a vat is selectively cured by light-activated photopolymerization” [13]

Its origins date back to mid-1980s when C.C. Hull, while experimenting laser radiation on UV-curable materials, discovered he was able to produce 3D parts, giving birth to one of the earliest AM techniques: stereolithography (SL).

This term is now used to describe macroscale, laser scan vat polymerization techniques, which employ an energy source and two galvanometers to pattern the light. Otherwise, the generic term commonly used is VP[5]. [10, p.63] It is worth to mention that many other processes have been developed from the original SL, adopting different kinds of light source[6], transmission mean, motion kind etc.

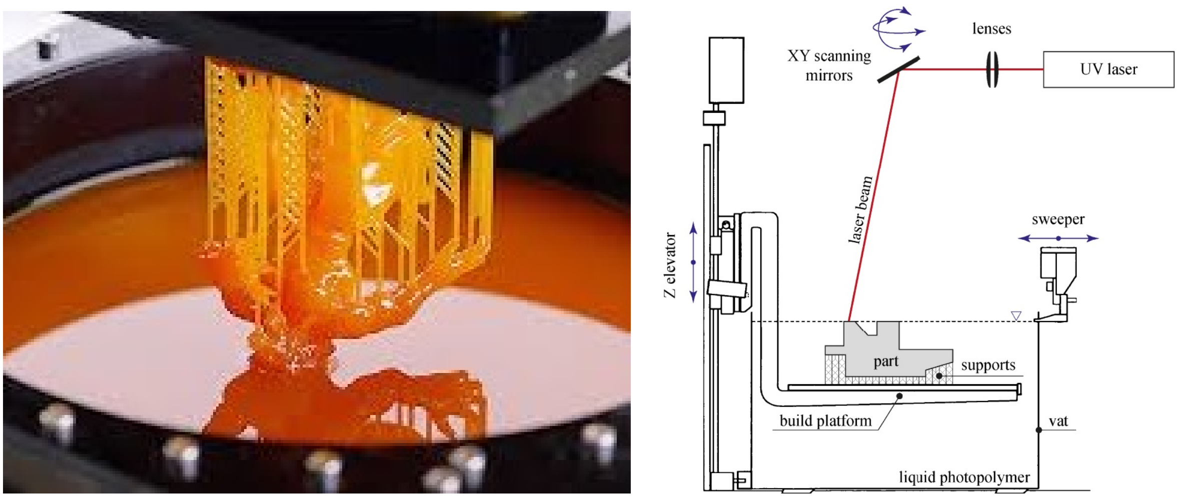

(a) (b)

Figure 1.5: Application example (a) and basic principle (b) of a SL process [2]

[4]Ultraviolet

[5]Vat photopolymerization

[6]X-rays, UV, electron beam, etc.

Also the materials used in SL processes have undergone some modifications. While at the beginning only low molecular weight resins, such as polyacrylate or epoxy macromers, were used, nowadays they can be substituted by new epoxy-based and hybrid polymers. There is also the possibility to fabricate pseudo-elastomeric components, by using a combination of specific resins with diluents, as well as polymer-ceramic composite objects. [2]

The basic SL process starts when the building platform is lowered into the vat and an ultraviolet laser is used to selectively cure the resin, thus creating a solid layer. The platform is then lowered by a layer thickness, the supply resin covers, often with the help of a blade, the cured layer and the process is repeated, until completion. [2]

During post-processing, the part has to be cleaned with chemical cleaners, the supports are detached and, in some cases, the placement of the part in a UV oven is required in order to obtain complete curing.

Since SL is a liquid-based process, there is no structural support during the building phase, but some parts may require additional support material to allow a correct fabrication, according to the chosen positioning and orientation. It is important to note that, basically, SL can process a single material, since the building platform is fully submerged in the vat, without possibility of material separation. [2]

One possible classification of vat photopolymerization processes is the following [10, 27]:

- Vector scanning SLA, where a light source is transmitted via an optic system, which includes lenses and galvanometers, to the building platform, moving inside the polymer-filled vat. The solidification process occurs in a point-by-point style, hence with high precision.

- Mask projection SLA, the energy source can still be a laser beam, but through the use of a DMD[7] or a LCD[8] the energy is dynamically patterned to a precisely-defined area of the surface. In this way it is possible to simultaneously cure an entire layer, or, with other words, in a planar-by-planar style. As a result, the building time is extremely reduced.

[7]Digital Micromirror Device

[8]Liquid-crystal Display

- Two-photon SLA, the process is similar to the vector scan, but the curing occurs at the intersections of two laser beams, without the need of optic system, with a high-resolution final product.

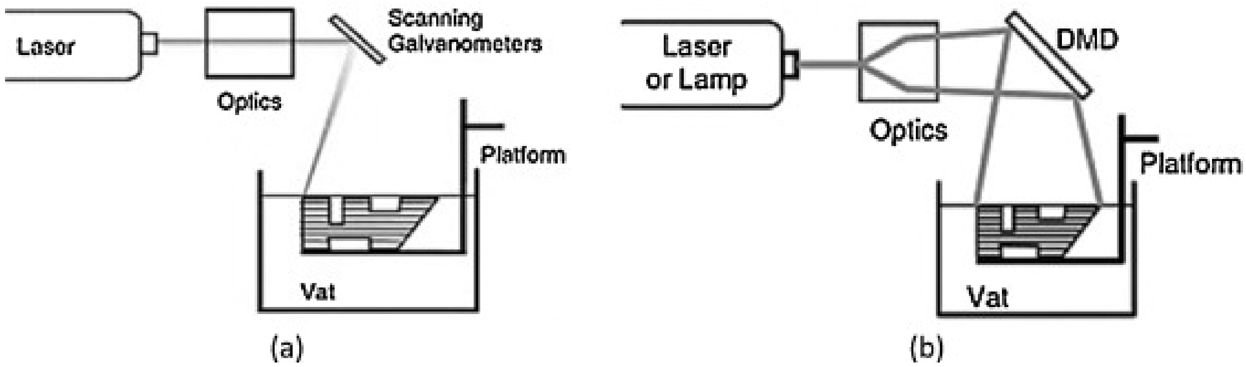

Figure 1.6: Vector scanning vs Mask projection [10]

1.1.4 Binder Jetting

The first version of a binder jetting AM machine was the Three-Dimensional Printing, invented by a MIT research group.

The basic principle of working is the selective jetting of a binder over a powder surface. This allows achieving a significant reduction of the material used to build the components, also because the powder which is not covered by the binder can be reused in following applications. After the deposition of the binder, the surface is exposed to a certain amount of thermal energy, commonly by means of heating lamps, in order to introduce adequate mechanical strength into the printed structure to withstand the shearing and gravitational forces, involved in the consequent printing process [19].

After the heating, a new layer of powder has to be spread over the previous one. Therefore, the building platform is lowered with a step equal to the layer thickness. The spreading mechanism is often constituted by a translating system and a counter-rolling cylinder or a static blade, with the powder taken from a supply-bed. From experimental results, the counter-rolling cylinder has shown better results in terms of powder spreading and compaction, hence it is often preferred [18]. Otherwise, a high-precision dropping system can be installed with similar results.

Since the printer head can contain several ejection nozzles, the entire width of the building bed can be jetted with binder in a single passage.

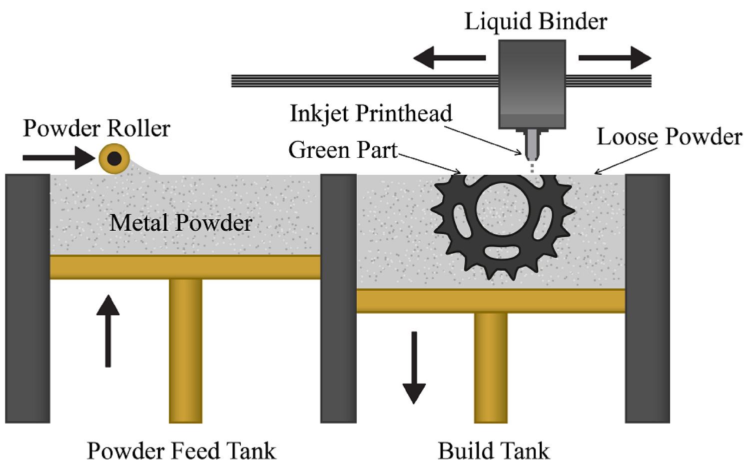

Figure 1.7: Example of a BJ process

Parts need to be removed from the powder bed and cleaned from the powder in excess. In order to obtain components with a high final density and good mechanical properties, an accurate and long post-processing is required. A sintering process could be necessary, as well as an infiltration of specific low melting metals[9], to improve the material properties, through complete decomposition of the binder and the formation of sinter necks between the powder particles. [1]

The geometrical qualities and the structural integrity of the green parts still strongly depend on the quality of the deposited binders and on their interactions with the powder bed.

BJ technology has been used with a wide range of metals and alloys, such as iron or steel, titanium, nickel, etc., often with the intentional purpose of having a porous structure, particularly for biomedical implants. [19]

The applications of BJ are highly dependent upon the material being processed: [10]

- Low-cost BJ machines use a plaster-based powder and a water-based binder to fabricate parts for visual purposes.
- Polymer powders are also available and they allow the creation of coloured components, with the same goal.
- With some particular elastomeric infiltrants objects can also bear some light-duty functional purposes.
- Metal components produced with BJ technique can have both functional and production purposes. Models and cores for sand casting can be produced with BJ machines and the process is particularly sizeable in the automotive and heavy equipment industries.

[9] Such as bronze

Chapter 2

MAIN IDEAS BEHIND THE PROJECT

2.1 OBJECTIVES OF A NOVEL HYBRID SYSTEM

Additive Manufacturing is attracting constantly increasing attention thanks to its capability to adapt to numerous applications, all different among each other, without specific and time-consuming changes in the process planning or in the employed resources. Furthermore, AM allows the realization of components which could not be easily produced through traditional manufacturing technologies.

For these reasons, one of the key elements of AM is its tremendous flexibility.

If the several techniques are singularly analyzed, some peculiarities, both as benefits and drawbacks, could be found in relation to each of the possible applications. In other words, all the technologies have specific potentials, which are particularly efficient under determined conditions or within precise applications. For instance, the primary advantages of printing technologies, such as material jetting, include low cost, high speed and easily scalable fabrication, together with the ease of using different materials (also with different colors). On the other hand, a few materials are suitable for MJ processes, the precision is not as good as for other technologies, etc. [10, p.198] Therefore, material jetting is particularly suitable for implementation where a quick, scalable aesthetic product is required, such in prototyping during product development.

Even though polymers are the materials most extensively researched, also due to the fact they have been utilized since the AM birth, metal components production is gaining greater importance. The most commonly employed metal alloys powders are: [7]

- Stainless steel
- Aluminum
- Nickel
- Titanium alloys

The most important technologies able to produce metal components are:

- Selective Laser Sintering or Melting (SLS or SLM)
- electron beam Melting (EBM)
- Binder Jetting (BJ)

BJ has received less attention in comparison with other AM techniques, primarily because the mechanical properties of products made by BJ machines are not as good as for EBM and SLS/M systems. The strength level of a part fabricated via BJ is usually inferior, mainly due to the prolonged thermal treatments such as annealing, curing and sintering, which can lead to a component not able to withstand any structural application. [7]

Another weakness of this technique is the density of the final products, which typically ranges from 50-90%. [23] However, as it can be read in [5, 6], great results (up to 99,6%) could be obtained via a three-step sintering process, together with the infiltration step exclusion, thanks to the addition of a small percentage of Boron to the initial metal powder.

Nevertheless, post-processing operations are extremely time-consuming, thereby limiting the productivity and the economic competitiveness of this technology.

Having said that, among the aforementioned techniques, Binder Jetting is for sure the most economical, thanks to the fact it does not employ any expensive energy source system, such as lasers or electron beam generators, together with their high precision positioning mechanisms. It also does not require precise control on the atmospheric conditions.

There is no need for support structure, since parts lie on the loose powder bed and the amount of deposited binder is limited, as well as the waste of material, thanks to the fact the unutilized powder can be re-used in other processes.

It is worth to note that scalability and ease of customization are only other two advantages attributed to BJ, but the list could be longer.

For instance, it does not have precise limitations for component or powder sizes and for the material choice[1], contrary to SLM and EBM. In fact, building material with high melting points cannot be easily processed with these techniques, due to the high quantity of energy required and to the significant cooling rate they would undergo, which can lead to high internal stress. In the worst case scenario, these can generate cracks in the internal structure, with consequent loss of integrity. [7, 11]

Conversely, BJ-AM products, because of the intrinsic characteristics of sintering process, do not suffer from extensive thermally-induced defects, such as significant distortions and unwanted grain growth. For the same reason, a mitigation of the residual stresses within the structure is usually observed. [18, 23]

In the end, BJ can be considered the most flexible and the most economical of these three technologies.

In order to try to reduce the constraints of this process, without deeply modifying the operations outlined by Dr. Do et al. [5] so as to preserve the good final quality and density, a solution capable of reducing, in particular, the manufacturing time has been investigated.

Analyzing the steps of a BJ process, they can be briefly summarized as a cyclic process including: powder layer creation, binder deposition and heating phase. The time needed for the completion of the last two steps certainly represents the greatest percentage of the whole process time. As a consequence, a solution has been sought, taking inspiration from the other AM technologies.

In our project, the basic idea was to merge in a novel hybrid machine the main structure and the building process of a BJ machine, together with a different system, able to replace the jetting and the curing mechanism for the binder.

The most suitable technology, also considering the feasibility of the modifications and parts replacements, was identified in the mask projection stereolithography.

[1] several metals and alloys, such as Al/CU/Ni/Fe/Co-base alloys, glass, sand

As mentioned before in chap. 1.1.3, mask projection is a technique that allows curing in a single phase the surface of an entire layer, thanks to the exposition of the photo-sensible resin to UV light, precisely patterned via accurate digital technologies. However, it must be highlighted that, while in Mask projection vat photopolymerization (MPVP) the UV photo-sensible resin is the primary building material, in our application it would have been used as source of structural bonding for the metal particles.

If successful, we would have been able to take advantage of the flexibility and cost-effectiveness of BJ systems, of the great outputs of the process designed by Dr. Do et al. [5], as well as of the curing rapidity of mask projection stereolithography.

In order to further reduce the fabrication time, the core idea was to completely get rid of the jetting phase. Instead of creating layers of dry powder and spraying the binder on it, it was thought to directly spread the composition of metal powder and photopolymerizable binder. The mixture would have been kept homogeneous by an external mixing mechanism, equipped with a discharge port for its deposition.

In this way, there would not have been the need for a high-precision jetting system and the mixture in excess could have still been collected and reused in following fabricating processes.

This idea was made possible by the dynamic projection of UV light sources, which allow to cure the desired cross-sections, hence moving from a selective binder jetting system to a selective binder curing one.

Following this proposition, the main focus of the project has been linked to the detailed study of this novel hybrid technique for metal components. Our first and main objective has been the demonstration of the fabricating process feasibility.

Since the photo-curable low-viscosity resin purchased for the project had not been used before in the engineering department of MSU, the product development started with the execution of some tests. These were mainly meant to understand its intrinsic properties and to assess the feasibility of the printing process.

In fact, using a UV-curable resin does not guarantee the success in creating solid components when mixed with metal powder. For this reason, many experiments have been performed, following a step-by-step procedure, trying to obtain components with a sufficient quality and, at the same time, looking out the ideal process parameters and the required tools for the process.

Therefore, many hours have been spent striving to obtain a reference for the optimization of the fabrication process, with special attention to the elimination or reduction of the most relevant issues encountered during this phase, which has been our second relevant goal for the entire duration of project.

Eventually, in order to reduce to execution time of future experiments, another significant part of the project has been dedicated to the design and building of a prototype, able to replace with accurate automation all the manual steps done during the first experimental phase.

Considering also the possible industrial application of this new technique, the prototype was also meant to practically test the correct functioning of the process and of the individual components.

As a result, a detailed design of a possible prototype, characterized by many revision cycles has been created. An accurate selection of then needed parts for the final assembly, considering all the possible constraints in terms of performance and compatibility, has been made. The parts that we were not able to purchase, in particular for budget limitations, were made out of different raw material at the university machine shop. All the electric and electronic connections among the components were carefully studied. A LabVIEW code was created, able to control efficiently all the mechanism while offering a clear user interface. The final assembly of the prototype was realized and the correct functioning has been tested.

Before proceeding with the actual activities of the project, so as to have a full understanding of the manufacturing process, it is important to have insights of some of the physical and chemical principles underlying the two manufacturing techniques we tried to merge.

2.1.1 Mask Projection Vat photopolymerization

The main advantage of vat photopolymerization technique is its ability to fabricate parts with smooth surfaces and high level of accuracy, with a total fabrication time relatively short. [2]

MPVP has the significant characteristic of displaying, and therefore curing, entire cross-sections onto the photopolymer resin surface through a dynamic digital mask. This is constituted by an LCD display or a DMD, whose function is to direct the radiation (usually of a UV lamp) according to the specifications[2] of the cross-section that needs to be created on that layer.

As a consequence, there is no need for accurate optic systems, as well as their motion mechanisms, in order to pattern the laser beams and generate vector scans. It is also quite obvious that the manufacturing time can be even more reduced, if compared to traditional technologies. The final part is obtained by spreading a new resin layer over the cured image, displaying the following one and continuing the process until the moment when all the layers are cured together.

However, it suffers from the typical issues concerning SLA processes [2, 16]:

- It often requires support materials, which adversely affect the surface quality.
- The volumetric shrinking of the irradiated is not negligible and induces compression stresses, which could cause distortions.
- It requires long and labor-intensive post-processing operations.

Another issue concerning mask-projection vat photopolymerization is the limited resolution of the projectors[3]. In order to obtain the highest precision possible in the final parts, a minimum pixel dimension is required. As a result, if there are precise accuracy requirements to comply with, the dimension of the part has to be limited to a certain threshold. [27]

[2]Stored as bitmaps

[3]Most commonly used commercial projectors have 1024x768 or 1920x1080 pixels resolution. Only thanks to the latest technology developments the 3840×2160 pixels format has been commercialized for a couple of years, but with extremely high purchasing costs.

Furthermore, some of the errors related to image projection cannot be neglected. For instance, due to inherent optic defects of the projection system, the light energy is not uniformly distributed, resulting in a certain amount of distortion. The light energy is not uniformly distributed within pixels as well. In fact, due to the diffractive nature of light, the pixel energy is not concentrated in a well-defined spot, but it is rather blended over a certain surface region. [27, 4]

Another common inconvenience is the so-called print through error. As a matter of fact, the residual radiation penetrating the cured surface causes unwanted polymerization. [16] In order to understand the principle behind it, as well as the characteristics of a general polymerization process, some mathematical considerations are needed. We need a model to represent the exposure of a resin layer.

One of the oldest and most well-known analysis is the one made by Jacobs [14], slightly modified in Gibson et al. book [10, pag.74-80].

The model makes use of the following nomenclature:

- $H(x, y, z)$: irradiance, defined as the radiant power of the beam per unit area $[W/mm^2]$
- E: exposure, possibly as a function of spatial coordinates $[mJ/mm^2]$
- E_c: critical exposure, exposure at which resin solidification starts to occur $[mJ/mm^2]$
- E_{max}: peak exposure of laser shining on the resin surface (center of laser spot) $[mJ/mm^2]$
- C_d: depth of cure $[mm]$
- D_p: depth of penetration of UV light into a resin until a reduction in irradiance of 1/e is reached $[mm]$

It must be underlined that the curing process occurs if and only if the exposure energy E is greater than the threshold exposure of polymerization E_c.

Starting from the considerations that the exposure energy received by the resin can be considered as the product of the irradiance and the time of exposure t:

$$E = H \cdot t \tag{2.1}$$

and that the energy would get attenuated as it enters the resin, according to the Beer Lambert's law, determining an exposure energy at depth z E_z equal to:

$$E_z = E \ exp(-z/D_p) \tag{2.2}$$

the model arrives at the conclusion that:

$$C_d = D_p \ ln(H \cdot t/E_c) \tag{2.3}$$

The model, therefore, considers that the depth of cure C_d is proportional to the logarithm of the exposure E with a threshold model for the resin cure.

According to Limaye and Rosen [16] the basic model just presented is fairly simple. The main weakness resides in the assumption that the attenuation through a cured layer is the same as that through the uncured resin, whilst it has been proved experimentally that the attenuation in the first case is significantly reduced.

Because of this Limaye and Rosen refined the model, considering two different values for the depth of penetration:

- D_{pS}: depth of penetration of UV light into a cured layer $[mm]$
- D_{pL}: depth of penetration of UV light into an uncured layer $[mm]$

At the instant when the exposure energy reaches the critical value, a thin film of cured resin will form on the surface, therefore changing the energy attenuation value, which will have to firstly pass through the cured resin and then through the liquid one. At the bottom of the cured layer, the exposure will be equal to the critical value. When the next dose of energy $H \cdot t$ will hit the surface (at $t + dt$), it gets attenuated through the cured layer, reaching its bottom with an energy level equal to $E = H \cdot dt \ exp(-z/D_{pS})$.

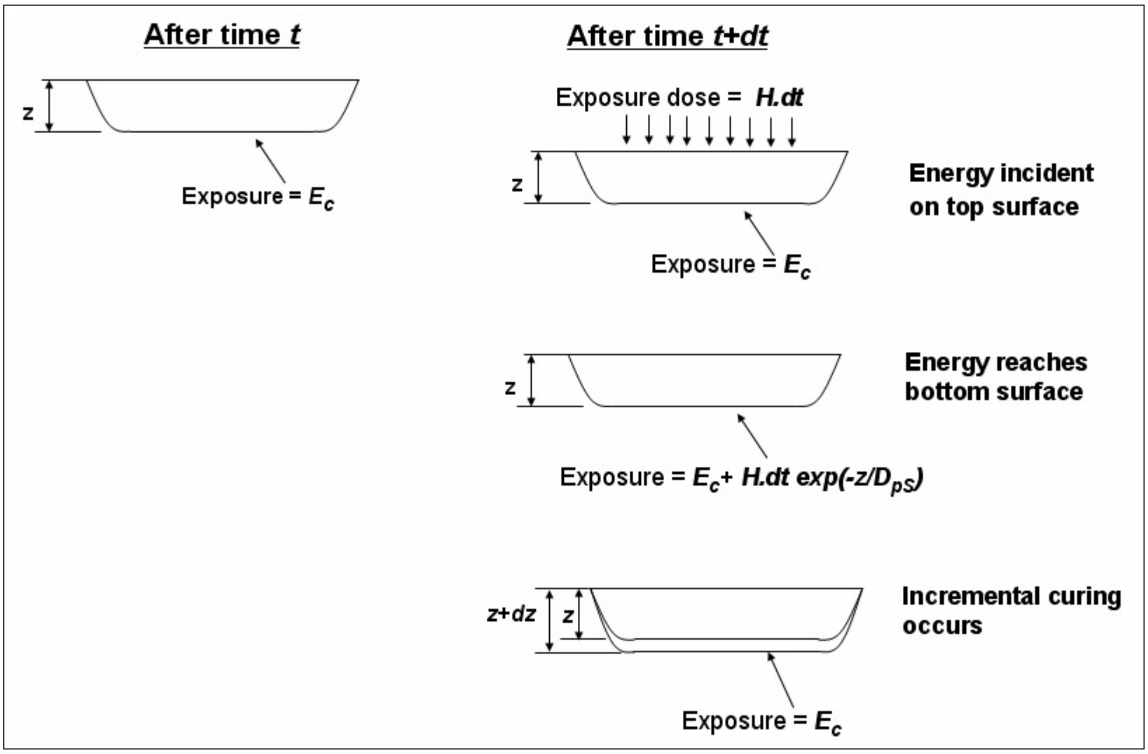

Figure 2.1: Modeling layer curing as a transent phenomenon [16]

There it adds up with the pre-existing energy, causing an incremental curing dz, expressed by the following I order differential equation, with initial condition $z = 0$ and $t = t_c$:

$$dz = D_{pL}\ \ln\left[\frac{H \cdot dt\ exp(-z/D_{pS}) + E_c}{E_c}\right] \tag{2.4}$$

It has also been proved, through a comparison between the experimental and the analytical results obtained starting from this equation, that the D_{pS} tends to infinity, indicating that a cured layer is almost transparent to radiation. [16]

Despite the fact that we will not use polymeric resin as primary material, but mixed with metal powder, thanks to these work we have a clear idea of the relation existing among the cure depth and several of the variables which influence it.

Other considerations useful for our project could be made analyzing the work of Lee et al. [15], where the main focus was on the investigation of the relation between the photocuring of the resin and the photoinitiator concentration.

In order to do so, the work started considering that among the several parameters which influence the final monomer-polymer conversions, photoinitiator concentration and light intensity play a primary role. As a consequence, they also influence the cure depth, which is then reflected on the manufacturing and final product characteristics. The cure depth is defined as the "depth to which a 3D gel network is formed during photopolymerization". "Since photon propagation through the medium is graded rather than discretized, gel is only formed up to the point at which the degree of cross-linking and polymerization is sufficient to form a solid gel network". In their examination, it was found out that as the photoinitiator concentration is increased, the cure depth initially increases, reaches a maximum for a precise photoinitiator concentration and then starts to decrease again.

In addition, the developed a mathematical model to relate all the variables involved, which at an intermediate step of the demonstration appears to be:

$$R_P = k_P[M]\left[\frac{\phi\epsilon I_0[PI]10^{-\epsilon[PI]z}}{k_t}\right]^{0.5} \tag{2.5}$$

where:

- R_p is the rate of polymerization.
- k_P is the kinetic rate constant for propagation.
- $[M]$ is the monomer concentration.
- ϕ is the quantum yield of the photoinitiator.
- ϵ is the molar extinction coefficient $(M^{-1}l^{-1})$.
- I_0 is the incident photonic flux or intensity at the surface (z=0).
- $[PI]$ is the molar concentration of photoinitiator (M).
- z is the depth.
- k_t is the kinetic rate constant for termination.

Which can be transformed with several mathematical steps into the definition of the cure depth:

$$z_c = \frac{2}{2.303\epsilon[PI]}\ ln\left(\frac{E_{max}[PI]^{0.5}}{\alpha\beta}\right) \tag{2.6}$$

where:

- E_{max} is the maximum energy exposure per unit area.
- α and β are variable that incorporate constants characterizing the chemical system and the photopolymerization processing conditions.

Unfortunately, we will not be able to apply these equations to our study case. This because:

- The resin used in our project has a different chemical composition and structure, which could have a relevant influence on the experimental outcomes.
- Most of all, our main interest is focused on the capacity of the resin to cure when mixed to metal powders. Therefore, the interaction between these two constituents and the proportions of the mixture itself are certainly not negligible in the curing behavior.

However, the relations just described are useful to let us understand that the concentration of the monomer and of the photoinitiator are extremely important parameters for a correct curing of the resin.

As a consequence, we can state that the amount of resin in the mixture is relevant not only so as to have a proper flowability and homogeneity of the mixture, but also because it is fundamental to have the proper rate of curing and cure depth. Therefore, there is a precise threshold for the minimum resin percentage. The greatest risk is to need a strong light source in order to balance an extremely low amount of resin, and hence of monomer and photoinitiator, or, in the worst case scenario, not being able to create enough cross-links to obtain a cured layer.

Also for this reason, the experimental phase has turned out to be fundamental in the assessment of the curing characteristics of the mixture.

2.1.2 Binder Migration

As mentioned before, the building material of our project is a mixture of polymeric binder and metal powder. Consequently, fully understanding the properties of binder migration in a porous material, such as our bed, made out of tiny metal particles, is particularly important to be able to avoid fabricating issues.

In traditional binder jetting processes, once the liquid droplets are deposited on the desired location, they will start to migrate into the powder pores under the influence of both capillary attraction and the surface tension-induced pressure gradient across the binder droplet meniscus, formed between the binder and air. [19]

Since the latter decreases as the binder penetrates further into the powder bed, it can be stated that the primary driving force is due to capillarity. For this reason, the intrinsic properties of the liquid binder, as well as its interaction with the powder, are of great interest.

After a certain degree of migration, the binder reaches an equilibrium state with null resultant capillary pressure. As a result, the equilibrium saturation, which determines the optimal saturation level, could be evaluated. The binder saturation level is defined as the ratio of the binder volume to the pore volume in a defined envelop of the powder bed. [19]

In a traditional BJ process, the equilibrium saturation has a significant influence on the final products quality. If the quantity of the binder deposited is much higher than the equilibrium saturation, it would overflow in undesired area, with the risk of solidifying regions which are not part of the initial design. On the other hand, a too low quantity would create problems in the bonding of the layers among each other.

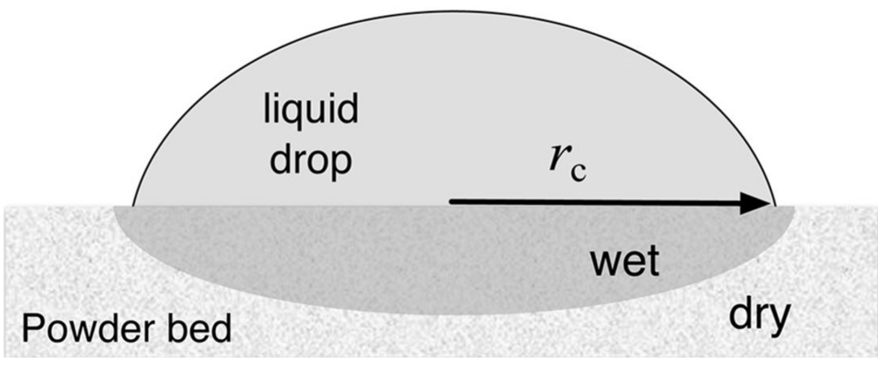

Figure 2.2: Droplet penetration into powder bed [17]

Our 3D printing technique is fairly different from a traditional BJ, hence some additional considerations should be made in order to have a clear understanding of the possible problems.

First of all, since the basic idea is to use a mixture of powder and binder instead of jetting the binder over the powder layers, the only driving force applied to the binder is the capillarity attraction.

A second important consideration must be done in relation to the equilibrium saturation. In fact, since in our printer the layer creation is related to the selective curing of the mixture and not to the selective deposition of binder, the problem of binder overflow does not exist. In our building platform, in fact, there is in theory no difference in composition between the material which is meant to be cured and the one which is simply spread during the layer creation but not cured. Since there is no mixture composition difference, there should be not a migrating effect among different areas of the building bed.

This is certainly true if, during the preparation of the mixture, the proportions are close to equilibrium saturation. On the other hand, if the quantity of the binder is too low, in addition to the obvious curing issues, a possible unwanted migration could arise. As a matter of fact, the binder positioned over the cured layers could be attracted by the capillarity force of the surrounding areas, where the binder has left empty spaces, flowing downwards, again because of the capillarity force created by the several interstitial volumes. However, the amount of binder should anyway be limited in order to have the highest metal final density possible. Therefore, the proper threshold should be sought with great attention.

Additionally, since the first observations on the mixing characteristics of the two constituents, a certain tendency to separate has been noticed, with the binder tending to flow over the metal particles after a certain resting period, mainly due to the difference in density. Consequently, not only the correct mixture composition is pivotal in the realization of good parts, but also the continuous blending of the compound is extremely important.

2.2 PRODUCT DEVELOPMENT PROCESS

In any company, the efficient management of all the activities is a key factor for the success of the company itself.

As a consequence, many different plans and procedures have been developed and have become mandatory as guidance for every part of a business activity, from the marketing implementation to the control of customer satisfaction.

The bigger is the company, the more detailed needs to be the plan and the working logic, so as to have the optimal coordination and synchronization of all the involved resources.

However, these principles and techniques, after the proper corrections, could be of the utmost importance even for a small project like ours. They are only generic schemes that have to be blended with the characteristics of every single project and actor, mixing together specific requirements, needs, procedures and experiences.

For this reason, the adoption of a model to follow during the development of the project, and more precisely the scheme offered by Pahl et al. [20], was thought to be pivotal, in order to have a reliable instrument to count on for the management of the several steps.

In Chap. 4 the authors clearly state that their method is more a guideline than a rigid prescription. For this reason, they suggest considering only the parts that may suit the application, giving however an idea of which should be the tasks, as well as their order.

They observe how each activity starts from the confrontation of the problem, gathering of all the available information and identifying the unknown variables. It is then followed by the definition phase, where the essential problems are clearly defined, in order to set the objectives, as well as all the constraints. The following step is the creation, where possible solutions are sought, discussed, varied, combined, and eventually defined through several decision steps.

They also underline the importance of iterative loops. In fact, in many different situations, the desired result cannot be obtained in a single step, due to its complexity or the time needed to develop it.

As a consequence, the separation of the tasks in several different sub-steps, with the relative objectives, times and requirements, could improve considerably the overall performance.

Each iteration, however, must improve or increase the value of the last working step results, in order to be valuable for the whole system. It is also important to keep the loops as short as possible, so as to be consistent with updated goals and have reliable intermediate outcomes.

This is extremely important for the design phase, where the requirements of the final product may be known since the beginning, but the integration and the interaction of the different components might need a constant refinement. In addition to this, it often happens to have several possible solutions for the same problem. Even in this case, the iterative loops, with sequences of identification, development, analysis and selection of the alternatives, results to be of extraordinary relevance.

Pahl et al. recommend the subdivision of the planning and design phase process in four different phases: (Fig. 2.3)

- Planning and task clarification: specification of information.
- Conceptual design: specification of principle solution (concept).
- Embodiment design: specification of layout (construction).
- Detail design: specification of production.

However, they also underline that it is not always possible to define a clear borderline between these, since they often require backtracking or simultaneous development.

The working steps of the different phase are shown in Fig. 2.3 and they have been followed as backbone for the development of the project. However, it must be noticed that many different secondary activities, which are not directly reported in the scheme, were necessary to obtain the required results of the different steps, such as:

- Collecting information.
- Problem understanding and assessment.
- Searching for solutions.
- Calculation and verification through analysis.
- Evaluation and discussion of the alternatives.

2.2.1 Planning and Task Clarification

Before developing a new product, the requirements and the results expected from it have to be clearly identified and defined. It this way it is possible to have a more precise subdivision of the objectives among the several sub-step more precise. This was done in Chap. 2.1, where, starting from the state of art of the Additive Manufacturing and of its existing lacks or deficiencies, the importance of the new technique we wanted to develop, as well as our main expectations regarding its performance, were underlined.

2.2.2 Conceptual Design

Starting from the abstraction of the essential problem of the product under development, establishing function structures, searching for suitable working principles and combining them in all the possible outcomes, a working structure, constituting the principal solution has to be defined. This often requires a concrete representation, with the choice of the preliminary materials, a rough dimensional layout and a consideration of the technological possibilities. Only then, in general, it is possible to assess the aspects of the solution and review the objectives and constraints. It often happens that more principle solutions coexist, complying with the prescribed requirements in a similar way. In this case, as well as among the possible variants of the same solution, the main kind of decision criteria are economic or technical, or a combination of them. The conceptual design is developed in Chap. 3.1 and Chap. 3.4.1

2.2.3 Embodiment Design

Once the principle solution is defined, the designers are required to identify and develop the construction structure (overall layout). Even for this task, many different variants could be generated and are to be assessed carefully through decision processes. By an appropriate combination and elimination of weak spots, the best layout can then be obtained, providing a mean to check function, strength, spatial compatibility and the base to the economic assessment of the final product. This is exactly the main content of Chapt. 3.2 and 3.4.2

2.2.4 Detail Design

During this phase the arrangement, the forms, the dimensions of all the individual parts, the materials etc. are finally laid down, followed by the creation of all the technical documentation required for the actual production. Also during this phase, difficulties and mistake could come to the surface, requiring the proper corrections and changes, which have to be performed always seeking for an improvement in quality, in performance or in economic efficiency. The detailed design of our project is presented in Chap 3.3 and Chap. 3.4.3

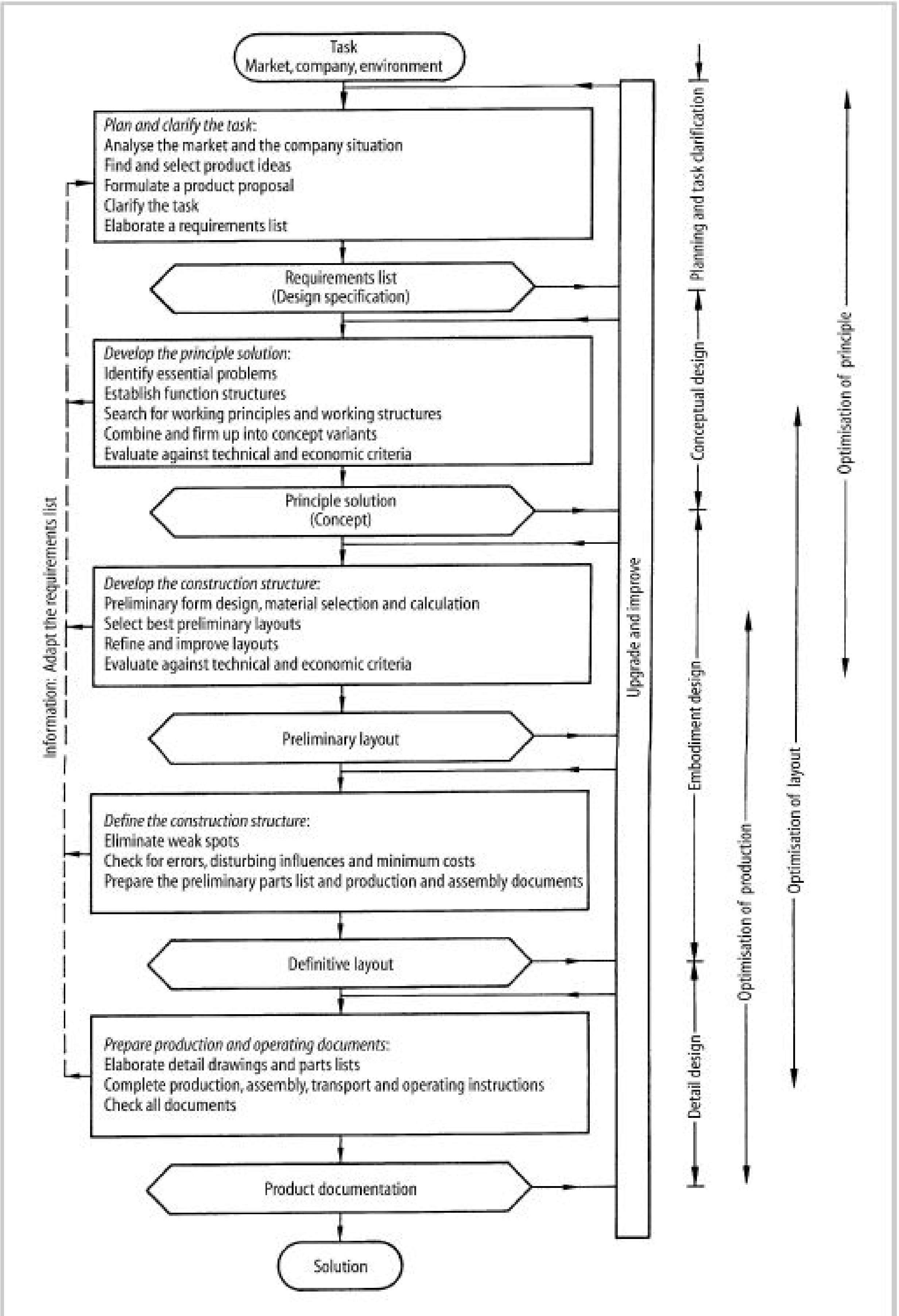

Figure 2.3: Steps in the planning and design process [20]

2.3 EXPERIMENTAL TESTS

2.3.1 Characteristics of the Binder

For the realization of the printer a new UV-curable resin, synonym CPS 1030 UV from Sigma-Aldrich, was purchased.

The properties of the resin are given in Tab. 2.1:

Supplier	Sigma-Aldrich
Resin name	CPS 1030 UV
Part code	900149-250g
Form	Liquid
Viscosity	55cP
Density	1,16g/mL
Storage T	2-8°C
Modulus (after curing)	750MPa
Elongation (after curing)	11%
Pencil Hardness (after curing)	6H
Curing wavelength range	380-500nm
Peak curing wavelength	380nm

Table 2.1: Resin properties

Since an economical SLA printer was available at the MSU laboratory, some samples were created in order to understand if it was powerful enough to cure the resin, which could have been useful for further experiments.

In Tab. 2.2 the parameters used for the creation of the samples are set out.

Printer Manufacturer	Anycubic
Model	LCD Photon
Technology	UV-LED Mask Projection Vat Photopolymerization
Sample Characteristics	5mm cube
Layer Thickness	0,1mm
Curing Time	10s
Initial Curing Time	50s for the first 10 layers

Table 2.2: Experiments parameters

The wavelength of the UV-light installed in the machine is equal to 405nm, therefore within the curing range of the resin and, also thanks to the small dimension of the samples, no defects were detected in their realization.

2.3.2 Components of the Mixture

The analysis on the suitable mixture for our project started by evaluating BJ printer present in the MSU laboratory, an ExOne x-1 ProLab. The consumables used by the machine are:

- PM-TSP-R116, a thermal support powder used during the furnace cycle.
- PM-B-SR1-04, an aqueous based binder.
- PM-C-R1-02, required for all automated and in-process maintenance routines, dissolves ExOne binder.
- Metal powder, chosen according to the required application.

It was then thought to create a mixture employing the following materials:

- CPS 1030 UV, our new low-viscosity UV photo-sensible resin used as binder.
- Isopropyl alcohol (IPA), equivalent to PM-C-R1-02.
- SS316 or SS420 metal powders.

Even though IPA has dissolving properties over polymeric materials, it was decided to mix it as primary component, since it has been noticed to have thinning properties, when used in small percentage. The r116 has not been used because of its toxicity and its little positive influence on the quality of the final result, which allowed us to operate without it.

A sample of a mixture with a good flowability was created and placed under a UV led lamp (30W 395nm) in order to test its curability, which started to occur after 20 sec. The mixture had the following weight percentages:

- SS316, approx. 85%.
- Resin, approx 12.5%
- IPA, approx. 2.5%.

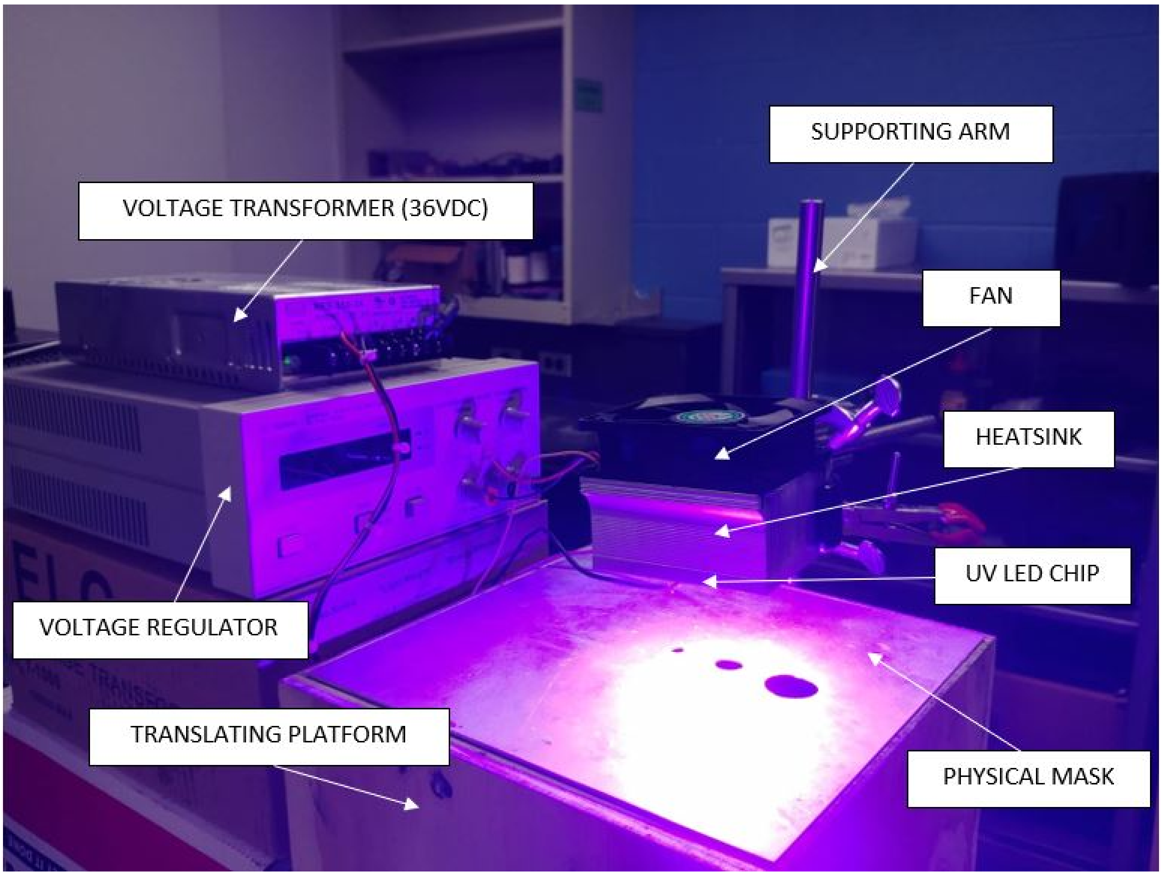

Figure 2.4: Components of the UV testing system

2.3.3 Process Parameters Experiments

Starting from the aforementioned mixture composition, some approximate experiments, related to the process parameters have been performed. In particular, the influence of two different variables has been considered:

- How the exposure time to UV-light can influence the shrinkage and the curing quality, in particular in terms of adhesion among different layers.
- Whether the exposure to a heating source after the curing, as done in common BJ printers, can influence the adhesion of the following layer.

Unfortunately, due to the bottom-up approach of the Anycubic LCD photon the experiments had to be made manually. In fact, the bottom-up approach implies that the building platform is completely immersed in the liquid resin, the light comes from the bottom and the platform is lifted step-by-step. This is made possible only thanks to the liquid resin, which flows and covers entirely the freshly-made layer. However, this is unattainable in our application, since the viscosity of the mixture is totally different.

As it is presented in Fig. 2.4, a simple supporting structure for the UV led lamp was assembled, together with a raising module for the building platform. In order to shift it downwards after each layer creation, a pack of sheets was placed beneath it. In fact, it has been noticed that each paper had more or less the same thickness of the thinnest layer we were able to create with a manual scraper (approx. $60 - 80\mu m$).

From now on, these experiments will be referred as 'Physical-mask samples', in order to differentiate them from the samples made with dynamic mask projections. (Chap. 5.1)

Three different samples were created with 20 layers of material, with UV exposure times respectively equal to: 30s, 60s, and 90s (respectively sample 1, 2 and 3 of Fig. 2.6. Each layer was then exposed to a heat flux, generated by a 1500W heat gun (60-600°C with three power levels) for a period of 4s. This time was the maximum allowable before generating extreme distortion in the layers, with possible cracking or wrong adhesion of the following one. After this step, a fourth sample was created with an exposure time equal to 60s, since it was the one for which the curing seemed to have the best quality, but removing the heating phase.

Due to the many manual and time-consuming phases, it was not possible to use the same mixture batch for all the sample, since the mixture tends to become more viscous at ambient temperature. Therefore, four different mixtures have been created, trying to keep the percentage as close as possible, as presented in Tab. 2.3.

	SAMPLES			
PROPERTIES	1	2	3	4
Binder mass (g)	41,38	43,39	39,66	39,68
Resin mass (g)	6,20	6,51	5,94	5,93
IPA mass (g)	1,17	1,24	1,12	1,1
Binder mass % (g)	84,88%	84,85%	84,89%	84,95%
Resin mass % (g)	12,72%	12,73%	12,71%	12,70%
IPA mass % (g)	2,40%	2,42%	2,40%	2,35%
UV exposure (s)	30	60	90	60
Heat exposure (s)	4	4	4	NO

Table 2.3: Experiments parameters

After the realization of the samples, they have been placed into a furnace so as to entirely get rid of the resin (debinding process) and to sinter them. The graph representing the sintering cycle is shown in Fig. 2.5.

The samples obtained are shown in Fig. 2.6.

As it can be observed in the figure, the best results in terms of binder curing and metal sintering have been obtained for an exposure time equal to 60s. This can be stated looking at the absence of delayering and at the general good compactness. The blur contours are easily explained considering that the metal mask used for creating the circular shape had to be replaced in position after the creation of each layer, with the consequent misalignment imprecision.

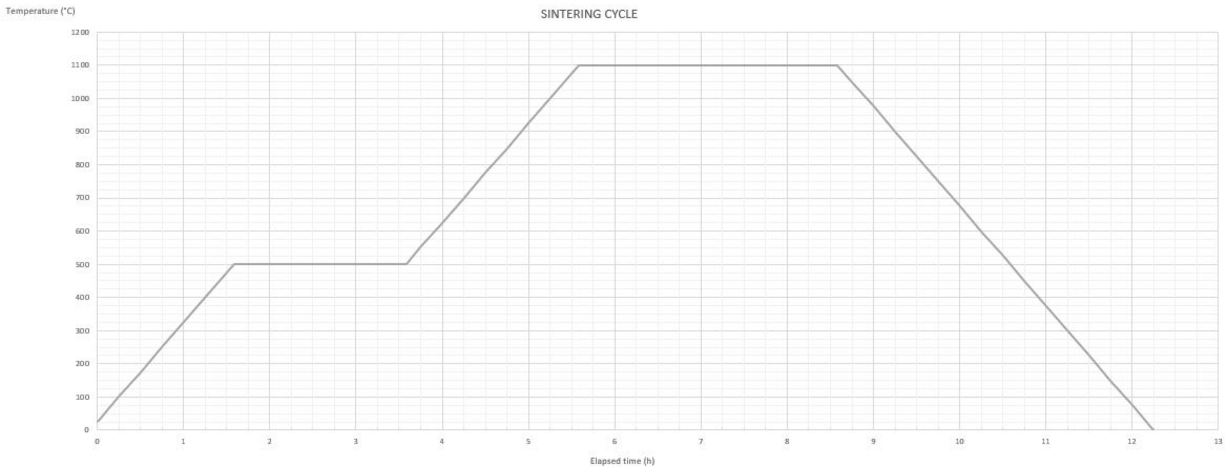

Figure 2.5: Sintering cycle

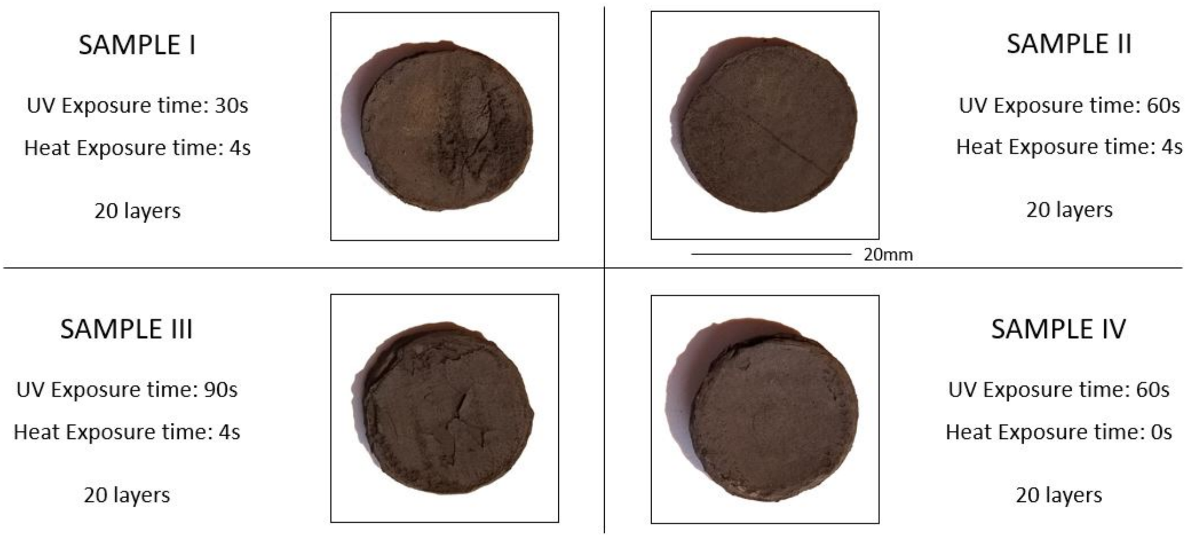

Figure 2.6: Samples showing the influence of process parameters

2.3.4 Characteristics of the Mixture Powder-Binder

After having computed a rough estimation of the process parameters, several tests, where different percentages of powder, resin and IPA were mixed together looking for the theoretical ideal composition to obtain the desired viscosity, have been performed, with the final result of:

- SS316, approx. 89.5%.
- Resin, approx 8.5%
- IPA, approx. 2%.

The starting point was the composition utilized for the process parameter tests. We then increased the powder amount constantly, in order to obtain steps of 0.5% in its relative percentage mass, therefore keeping constant the ratio between resin and IPA. This has been done in order to prevent any possible inhibition of the photopolymerization of the resin.

The parameters that have been taken into account are:

- The optimal viscosity, to allow the creation of uniform layers of limited thickness. Consequently, the related parameters that have been taken into account were the easiness in blending the mixture and its flowability.
- The capacity of being cured in the correct way, so as to obtain a the final part without possible delayering.

It has to be underlined that all the aforementioned parameters require a subsequent validation, that will be performed with the assembled prototype, since the structure assembled for these tests can have had a significant influence on the final results. This can be easily explained if we consider that all the steps have been performed manually, with the obvious human errors, and that many of the components firstly used in the initial tests, have been replaced by similar ones throughout the experimental phase because of several issues.

Chapter 3

DESIGN DEVELOPMENT

3.1 INITIAL DRAFT

The design of the novel hybrid machine started from the basic concept of a traditional binder jetting AM machine. In many applications, the main structure is constituted by a building platform, which is shifted vertically by a piston or similar mechanisms. New layers of powder are spread over it, an injection system deposits the binder and the cycle repeats until all the layers are created. (See Fig. 3.1)

As it has been proved by experimental results [18], the system which produces the best results in terms of layer accuracy and compactness of the powder bed is the counter-rolling spreader, together with its translating system.

However, after some simple manual tests, it has been observed that it would have not been the optimal solution in our case. In fact, the mixture tends to stick against the roller, due to the viscosity of the binder, and results in non-uniform layers. For this reason, it was decided to adopt a static blade, or scraper, with better results.

The powder bed is often contained in one or two tanks, positioned one per side of the building bed. (See Fig. 3.1) In the latter case they both act alternatively as supply and collecting bed. In other terms, during the cyclic building process, one supply platform is raised in order to allow the spreading system to collect enough powder to create a new layer on the building platform, which meanwhile is lowered of one layer thickness. The spreading system then pushes the material in excess towards the second supply platform, which of course has to be lowered, so as to be able to receive it. After the deposition of the binder and its heating, the process is repeated in the opposite direction.

As it has been mentioned in the objectives, one of the main goals of our project was to reduce the building time, starting from the elimination of the jetting process. The idea behind our novel machine was the pre-mix of the powder and the binder, with the substitution of the conventional binder with a low-viscosity UV-curable one. For this reason, the conventional radiating heating system has been substituted by an UV-emitting system. In this way, it would have been possible to avoid the long-lasting high-precision jetting, as well as the long-lasting heating phase.

One of the main concern faced during the design process was the flowability of the binder in the mixture powder-binder. Since the resin is in liquid state, the capillary pressure would tend to push it towards the lower part of the holding container. This could strongly affect the characteristics of the final product, especially for what concerns the first layers. In fact, as it has been mentioned in chapter 2.1.2, the presence of insufficient binder could generate an inadequate bonding of the layers. For this reason, it was decided to add an automatic stirring system, in order to have a mixture as homogeneous as possible. The initial basic design of the printer is shown in Figure 3.1.

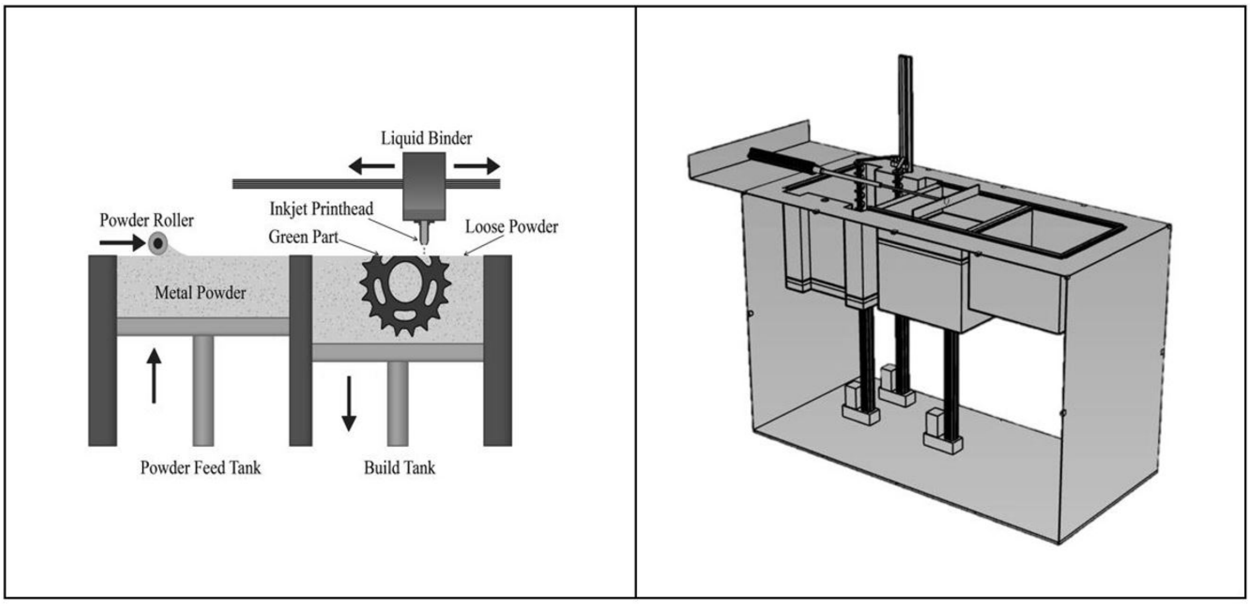

Figure 3.1: Working principle and initial draft of the machine

3.2 FIRST PHASE

After the evaluation of the viscosity of the mixture and with some basic tests on replications of the tank-building bed contact, it was observed that an optimal sealing of the building was hardly obtainable. In fact, even though a seal, sliding against the walls of the containers, had been applied all over the edges of the platforms, a small part of the mixture was able to escape, spilling over the base of the container and creating friction issues.

Considering also the dimensions of the vibration-damped table (height=1m) upon which the machine would have been placed, as well as the dimensions of the desired building volume (approximately a 20in. cube) the following modifications were applied to the initial design (as shown in Figure 3.2):

- The supply bed was substituted by an overhead hopper, with a thin opening, characterized by a width large enough to cover the width of the building platform, in order to have a uniform mixture deposition.

- The mechanism for the moving building platform was substituted. Instead of using a pneumatic cylinder pushing from the bottom surface, a mechanism was designed, constituted by a ball screw and some connecting plates. Since the ball screw cannot enter in contact with the powder bed, in order to avoid any possible malfunctioning, it was decided to add two bars, which would have been welded at the platform sides, so as to allow a connection placed far from the mixture.

- A structure able to withstand the loads coming from the ball screw was added in the assembly.

- An external industrial stirrer, together with a screw conveyor, was placed on the side of the table. This should be fixedly connected to the volume created to collect the material in excess, in order to allow a continuous recirculation.

In this way, a significant reduction in the height of the building platform and a secure sealing of the different containers were achieved.

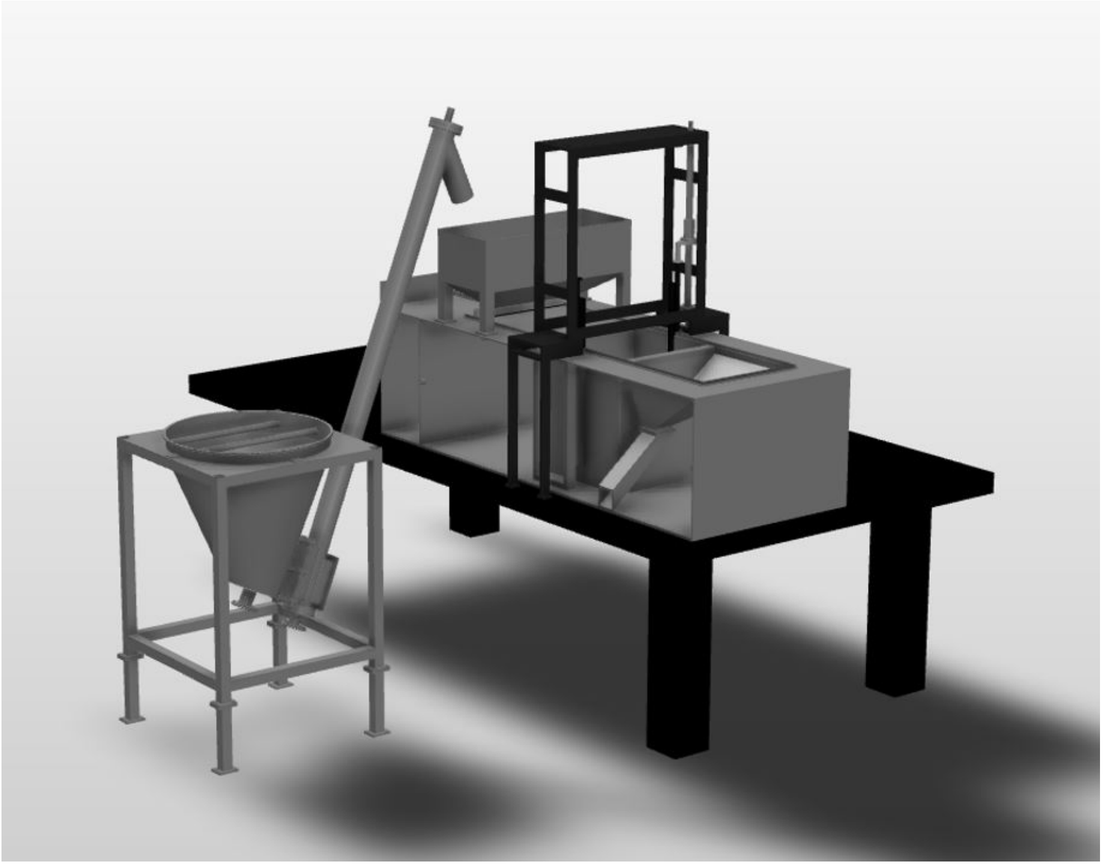

Figure 3.2: Design phase 1

After the completion of this step, some static analysis has been made, with particular attention to the main support structure and the related components designed to withstand the screws ball and the loads applied to.

As first step it has been necessary to compute the maximum load acting on the system. Even though the main application of the machine is to work with the mixture previously described, in order to be as conservative as possible, the density of Nickel has been taken into account. The reason behind this choice is that Nickel is one of the heaviest material whose particles are used in AM for the production of metal components.

With building container characterized by a volume of $8000in^3$ and the Nickel density approximately equal to $0.322lb/in^3$ the maximum powder weight is equal to:

$Max\ powder\ mass = 2570lb$

Considering to use steel alloy for the construction of the building platform its mass is approximately equal to:

$Platform\ mass = 112lb$

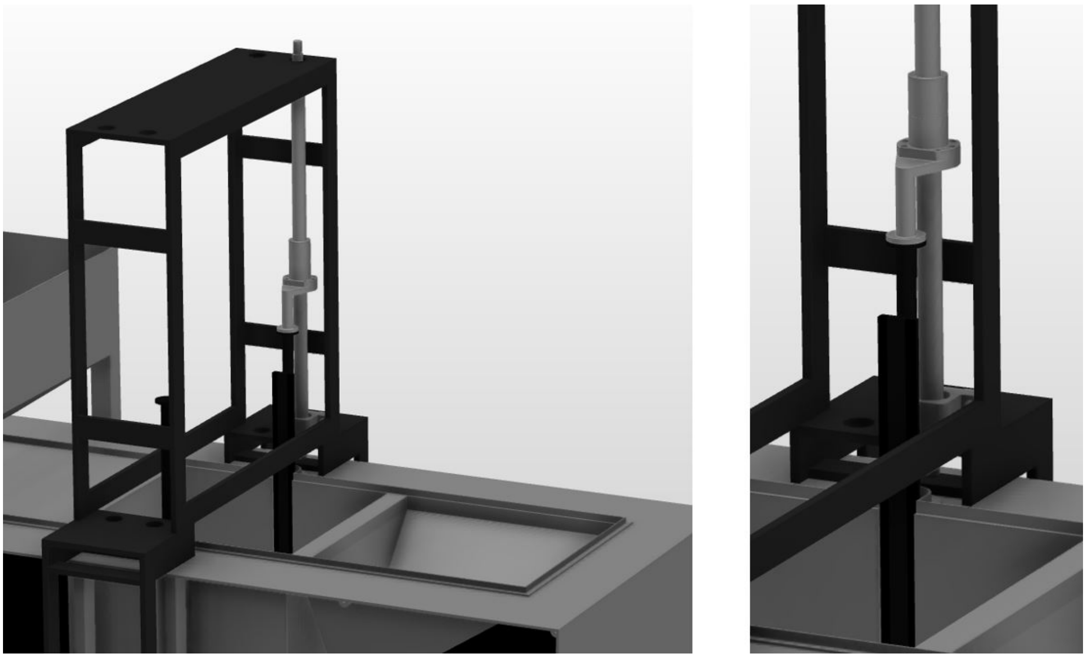

Figure 3.3: Details of phase 1

Considering the aforementioned weights, the deformation obtained by the simulation was higher than the tolerable value. In fact, it has been noticed that also with 2 screws ball, the vertical deformation generated on the connectors between the welded bars and the ball-screw mechanism was several times higher than the desired precision. This is related to the needed layer thickness for the manufacturing of components, which has been defined equal to $80-100\mu m$, which is a common resolution for many AM printers. It's also one of the most influential parameters in the final product quality: the thinner is the layer the better is the final result, both in terms of geometrical precision, surface roughness, mechanical properties etc.

A second issues was the flexion of the threaded bar, caused by the moment generated by the powder weight, whose application point is offset for a distance equal to the length of the connector. The bending of the bar can cause unwanted friction in the moving mechanism, as well as a loss of precision in the motion itself.

Some test were made changing the structure of the frame, but no significant results were obtained. Only the application of four different screws ball, placed close to the corners of the building platform and a much more robust frame allowed us to obtain a remarkable improvement. Unfortunately, an extremely precise coordination of four ball crews could be really problematic and expensive.

3.3 PROVISIONAL DESIGN

For this reason, as well as due to the extreme overall height of the machine, it has been necessary to modify again the design, moving back to the initial idea for some details:

- It has been decided not to use the vibrating table, in order to same approximately 1 meter in vertical dimension.
- The moving mechanism of the platform has been replaced again with an electric actuator, so as to avoid unwanted bending moment and have a precise control on the vertical position (Industrial actuators have a precision up to $30\mu m$).
- The main frame has been substituted with an assembly of aluminum bars, together with cross-bars in order to increase the rigidity of the system, give support to the main actuator and reduce the overall weight.

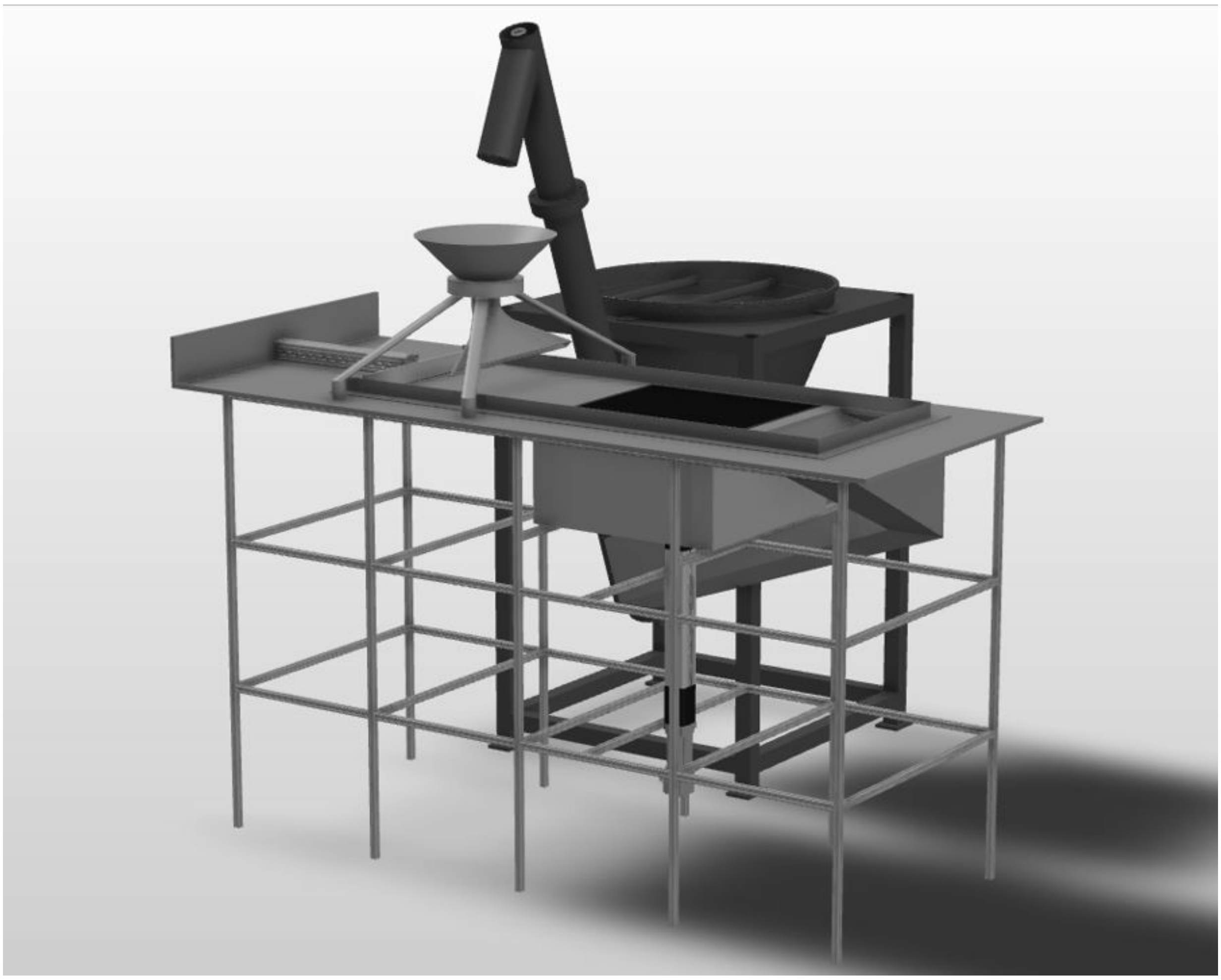

Figure 3.4: Provisional design

3.4 PROTOTYPE DESIGN

Before proceeding with the search for the expensive components of the 3D printer, it has been determined to realize a smaller prototype, with a maximum budget of $10'000. In this way, first of all it has been possible to test the functioning of all the components required for the manufacturing process, avoiding the direct involvement of a significant amount of money. Secondly, it was also considered that, thanks to the creation of an automated system, the experiments performed on the mixture and on the process parameters would have been much more robust and less time-consuming, since it would have replaced all the manual actions.

The first inputs for the design of the 3D printer prototype were:

- The prototype should have been as automated as possible.
- The prototype should have replicated all the basic motions/mechanism thought for the realization of the main printer.
- The building bed should have had a dimension of 4x4in.

3.4.1 Initial Draft

As first step, a basic layout of the prototype has been made, as it can be seen from Fig 3.5.

Following the basic structure of the main printer, two generic linear actuators were placed to allow the movements of the scraper and of the building platform. Due to the limited dimensions of the prototype, there was no point in using a screw conveyor to move the mixture. Therefore, the hopper was placed overhead the printer and its design was changed, meant also to room an auger in order to cover the mixing function as well.

Finally, a system moved by a belt and an electrical engine was created. This was meant to rotate supporting arms and the IR and UV lamps mounted on them. In this way, it would have been possible to guarantee the correct positioning of the lamps exactly above the building bed, as well as the avoidance of any interference among the different moving elements of the system.

Only in a second moment, thanks to the manual experiments, it was understood that the heating phase was not strictly needed and the UV lamp would have been unnecessary and replaced by a DLP projector. Consequently, we got rid of both supporting arms and the overall design was changed.

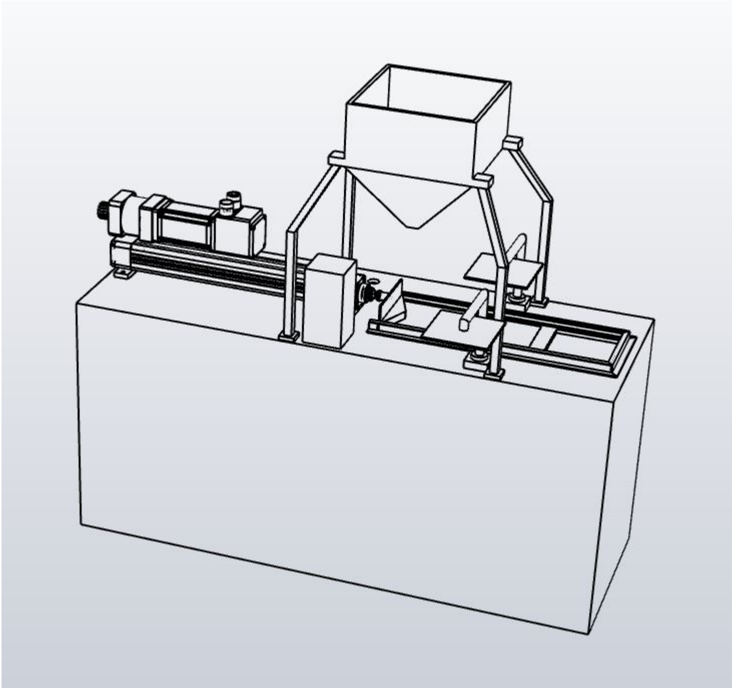

Figure 3.5: Initial layout of the prototype

3.4.2 Selection and Search for Components

Following the aforementioned considerations, the search for the suitable components started.

First of all, the maximum load acting on the system was computed using the same formulas used for the full-scale printer.

With the building container characterized by a volume of $64in^3$ and the Nickel density approximately equal to $0.322lb/in^3$, the maximum powder weight is equal to:

$$Max\ powder\ weight = 20.5lb$$

Considering the weight of the carbon steel platform approximately equal to $1.5lb$ and applying a safety factor equal to 2, in order to take into account all the friction forces and any other possible interaction, the needed power applied by the linear actuator is equal to:

$$Needed\ power\ = (20.5 + 1.5)lb \cdot 0.453\frac{kg}{lb} \cdot 2 \cdot 9.81\frac{m}{s^2} \cong 200N$$

For the purpose of research on American websites, the equivalent force of $44lbf$ has also been taken into account.

Our first efforts were dedicated to most complex parts: the main frame, the linear actuator for the building platform and the industrial mixer.

Main Linear Actuator

Three different RFQ[1] have been requested to the following companies: Tolomatic, Ultramotion and Parker. The parameters taken into account to look for the right product were:

- The maximum desired height for components produced with the prototype was 4in. Therefore the useful needed stroke should have been equal or greater to that value.
- The minimum peak force required is equal to 200N, necessary to lift the platform in case it is packed with Ni powder.
- The average powder particle dimension is $50\mu m$, then a repeatability equal or smaller is necessary.
- Since a perfect sealing in the contact building platform and support walls cannot be guaranteed, the linear actuator should have been provided with protection against contamination.
- If possible, due to the characteristics of the building cycle, a system which can standstill without the need of constant power supply is preferable.

The quotation about three different products were received, with the characteristics and prices presented in Tab. 3.1.

Table 3.1: Linear actuators characteristics

CHARACTERISTICS	TOLOMATIC	ULTRAMOTION	PARKER
Product name	ERD	Series A2 Servo Cylinder	ETH32
Product code	ERD15 BNM05 SM152.400 LMI AMI3C1A1 CR57 IP67	#A2NZ9C-B0M0E0	ETH032M05A1XPDJMN0150A;HTS:8501F2400
Useful stroke	6in	5,75in	150mm
Continuos force	200lbf	41lbf	1130N
Peak force	200lbf	82lbf	3600N
Feedback	Multiple solutions	Phase index absolute position	Multiple solutions
Contamination protection	IP-67	IP-65	IP-65
Repeteability	25µm	30µm	30µm
Motor	Servo	Brushless DC	Servo
Supply voltage	230VAC	8-36VDC	120VAC
Mechanism	Ball screw	Ball screw	Ball screw
Drive and Electronics	IMA33 RN05 SM152.400 MV23 DT1A1B IP67	Integrated	S063V2F12I11T30M00
Power supply	Integrated	#PS-1X2A	Integrated
TOTAL PRICE	$7700	$3420	$4650

[1]Request for Quotation

Even though the cheapest product is the A2 servocylinder offered by Ultramotion, it has been decided to purchase the linear actuator from Parker, due to the greater reliability and precision offered by a servo motor. Additionally, it is worth to note that the employment of a linear actuator with a DC brushless motor would have required the constant supply of power for standstill positions, which are the most frequent in our production process, where the platform is lowered step-by-step with long waiting times among them for the layer fabrication.

SUPPORTING FRAME

For the frame, two different local machine shops have been contacted. Since both quotations were higher than $1500, and considering also the simplicity of the structure, we decided to produce the component internally.

While looking on Servocity website for the linear actuators[2], we found out they also sell aluminum extruded structural bars. Together with these, the company offers an entire set of components to create the proper links.

Considering the savings, in terms of overall weight and cost, as well as the flexibility offered by an assembled frame if compared to a welded one, it has been determined to purchase all the components necessary for both the frames[3] from Servocity, saving at least $1000 compared to the first quotation.

INDUSTRIAL MIXER

For what concerned the mixer, the main problem has been to find an industrial product with suitable dimensions, which unfortunately are relatively small. The most economical quotation we were able to get was approximate $6000, with a lead time greater than a month. We, therefore, decided to design it upon our needs and require a quotation from the local machine shops as well.

While almost the main part of the mechanism was assessed as efficient and effective for the tasks they were required to performed, great attention was given to the refinement of the geometries and the correct functioning of the hopper-stirrer.

[2]Necessary to move the scraper for the layer creation and the discharge port of the industrial mixer

[3]The main one is meant to hold the building surface, while the secondary one, shown in later pictures, is meant to support the projection system, needed to replace the original UV-light source.

The following considerations were taken into account:

- The height of the deposition opening of the hopper should have been as little as possible. This aspect prevents the overflow of material or a non-uniform deposition of the mixture because of the impact speed.
- The position of the discharge port could have a relevant influence on its uniformity. For this reason, a central position, as well as a width equal to or greater than the building bed are preferable.
- Since the photo-polymeric binder is curable also when exposed to a common light source, the deposition should have been as quick as possible, or at least through an enclosed system in order to avoid unwanted and untimely curing. Following this principle also the flow over an inclined connection has to be evaluated.

Analyzing all the mentioned variables, the different alternatives shown in Fig 3.6, were created.

The first alternative is constituted by a cylindrical case, tapered towards the circular discharge port, placed at its bottom. The auger is vertical and is actuated by a DC motor placed on the top of the mixer cover, not represented in the shown design. A linear actuator is placed on one side of the mixer in order to allow the sliding motion of the horizontal discharge port.

In the second alternative the mixer (right picture of Fig. 3.6) is still placed above the building bed with a discharge port on its bottom, but the shape has been modified. The auger is positioned horizontally, with a length equal to the width of the machine and the discharge port is still operated by a linear actuator, mounted along the main direction of the printer case.

For the last alternative, the basic concept is taken from building concrete mixers. The auger is still mounted horizontally, with a small inclination angle and is operated by an adequate DC motor. The discharge port is positioned on one corner of the mixer and the material flows outwards thanks to the slope and the rotating motion of the blade. A chute creates the connection for the deposition of material in the middle of the building platform. A similar design was created simply positioning the mixer aligned with the main direction of the platform case.

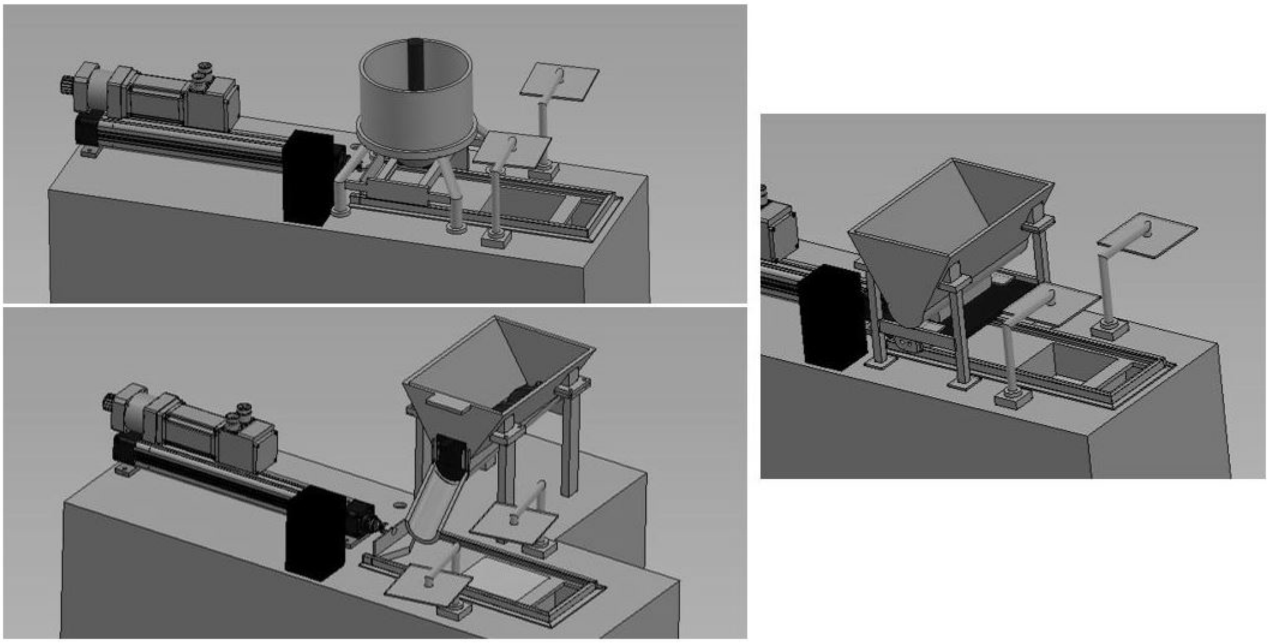

Figure 3.6: Alternatives for the hopper design

After the considerations done earlier, it was decided to adopt a completely overhead solution, in order to eliminate the time for mixture flow over the inclined connection and have more precise control over the deposition. Therefore the lowest solution was immediately discarded.

Between the other two alternatives, especially considering the possible problems related to the fabrication and the possible lack of accuracy connected to, the first design was considered as the optimal.

This can be easily explained considering that a hopper with such geometry could be obtained through precise cuts of bars, tubes and pipes, together with some simple welds.

After the RFQ to the same machine shops contacted for the frame, due to the high prices charged for the fabrication of the component, respectively \$2500 and \$2950, it was decided to produce it internally.

For the main body a piece of PVC pipe was used, for the conical part and the auger, needed to mix the binder and the metal powder together, a 3D printer was used, while the frame for the blender was made out of wooden strips. Part of the process is shown in Fig. 4.1

OTHER COMPONENTS and BOM

The research continued with the remaining linear actuators. Since there were not precise requirements on their precision, their functioning or any other additional function, the only considered characteristics have been:

- Minimum force 100N.
- Useful stroke equal to 4in for the mixer discharge port and 12in for the scraper.

The companies taken into account were: Servocity and Progressive Automation.

Since the characteristics and the prices were similar, it has been deiced to purchase everything from Servocity, in order to reduce as much as possible the number of suppliers, getting in this way also a better price on the final amount.

Together with the linear actuators, many other components are necessary for their correct functioning. For this reason, starting from the characteristics of the chosen actuators, shown in Tab. 3.2, the suitable electronics was sought, as well as the needed supports.

Product Weight	38.2 oz
Voltage Range (Recommended)	6V - 12V
Operating Temperature	-26°C ~ +65°C
Speed (No Load)*	2.00" per second
Speed (Max Load)*	1.37" per second
Dynamic Thrust*	25 lbs
Static Load	500 lbs
Current Drain (No-Load)*	800mA
Current Drain (Max Load)*	3.8A
Current Drain (Stall)*	15A
Motor Type	3 Pole Ferrite
Feedback Style	10KΩ Potentiometer
Potentiometer Tolerance	± 5%
Potentiometer Linearity	± 0.25%
Feedback Density	5KΩ / inch
Gear Ratio	05:01
Gear Material	Metal Gear Train, Nylon Pinion
Gearbox Style	Straight Cut Spur
Wire Length	24"
Ingress Protection (IP)	IP54
Duty Cycle	25% (25% on, 75% off)
Housing Material	Zinc Alloy
Lead Screw Type	3mm pitch, single thread

Table 3.2: Servocity linear actuators characteristics

Considering the stall current equal to 15A and the max load current equal to 3.8A, it has been determined to use a Sabertooth 2x12A. This board can control two bidirectional motor via multiple independent control interfaces, such as radio control (RC), servo pulses, analog voltage, and serial communication. Its maximum peak current per channel is 25A, while the maximum continuous is 12A, therefore suitable for our application.

Lastly, in order to be able to control the electronic board with the correct commands, as well as to create coordination between the microprocessor and the servo drive IPA04, it was thought to employ the controller NI MyRIO, already available within the department.

Therefore, complying with required characteristics for our prototype, summed up in the Tab. 3.3, all the components were chosen and purchased from different suppliers.

NEEDED COMPONENTS	MINIMUM CHARACTERISTICS/REQUIRED FUNCTIONS
Linear actuator for the building platform	3in stroke
	200N pushing force
	±50µm repeatability
	Standstill position without power supply
	Contamination protection
Linear actuator for the scraper	10in stroke
	100N pushing force
Linear actuator for the discharge port	3in stroke
	10N pushing force
Electronics for the actuators	Peak current per actuator channel 15A (stall current)
	Continuos current per actuator channel 3,8A
	Peak current for Gear Motor 20A (stall current)
	Continuos current for Gear Motor - Unknown

NEEDED PARTS TO BE FABRICATED	MINIMUM CHARACTERISTICS/REQUIRED FUNCTIONS
Main structure	Able to withstand all the loads with deformations lower than 50µm
	Perpendicularity and parallelis geometric tolerances lower than 0.2
Industrial blender	64in^3 capacity
	Continuos stirring suitable for wet powders

Table 3.3: Minimum requirements for the prototype components

The final Bill Of Materials (BOM) is shown in the following page, in Tab. 3.4.

The electrical and electronic connections among the different components is also presented in Fig. 3.7.

SECONDARY ACTUATORS						
COMPONENT DESCRIPTION	MANUFACTURER	PRODUCT	SPECIFIC CODE	UNIT PRICE ($)	QUANTITY	PRICE ($)
Actuator for the scraper	Servocity	HDA12-2	HDA12-2	129,99	1	129,99
Mounting	Servocity	HDM250	HDM250	12,99	1	12,99
Actuator for the slider	Servocity	HDA4-2	HDA4-2	129,99	1	129,99
Mounting	Servocity	HDM250	HDM250	12,99	1	12,99
45 RPM HD premium gear motor	Servocity	638270	638270	39,99	1	39,99
HD Premium Planetary Gear Motor Mount	Servocity	555174	555174	4,99	1	4,99
Gear Motor Input Board D	Servocity	605120	605120	0,99	1	0,99
ELECTRIC/ELECTRONIC COMPONENTS						
COMPONENT DESCRIPTION	MANUFACTURER	PRODUCT	SPECIFIC CODE	UNIT PRICE ($)	QUANTITY	PRICE ($)
Dual Motor controller	Servocity	Sabertooth 2x12A	RB-Dim-42	72	2	144
DLP projector	Optoma	Optoma S343	B07FZSRVWV	289,00	1	289
Microcontroller	National Instruments	myRIO-1900	782692-01	548,00	1	548
Female-mle wires	Servocity	Jumper wires	607042	0,2	40	8
MAIN ACTUATOR						
COMPONENT DESCRIPTION	MANUFACTURER	PRODUCT	SPECIFIC CODE	UNIT PRICE ($)	QUANTITY	PRICE ($)
Actuator for the platform	Parker	ETH032 with servo	805-1410A	2775	1	2775
Controller and drive	Parker	IPA controller	IPA04-HC	1196	1	1196
MECHANICAL COMPONENTS						
COMPONENT DESCRIPTION	MANUFACTURER	PRODUCT	SPECIFIC CODE	UNIT PRICE ($)	QUANTITY	PRICE ($)
Support structure	Paradise machining	Hollow box		340	1	340
Hopper	Paradise machining	Platform		250	1	250
	Paradise machining	Countertop		465	1	465
Support structure	AltroSteel	plate 5/16 (15x40in)+ angle (40inx0.75x0.125) A36		230	1	230
	Servocity	plate 4.5x12	585004	13,99	1	13,99
	Servocity	12in xrail	565046	4,79	4	19,16
	Servocity	36in xrail (for 30)	565078	9,99	8	79,92
	Servocity	9in xrail	565038	4,29	17	72,93
	Servocity	flush raised perp mount	585074	3,49	38	132,62
	Servocity	screw	632110	1,89	12	22,68
	Servocity	2x screw plate	585757	4,99	19	94,81
	Servocity	2x 3/8" X-Rail Gusset	585071	3,99	15	59,85
	Servocity	4x X-Rail Nut	585756	4,99	9	44,91
Projector structure	Servocity	21in xrail	565070	7,09	4	28,36
	Servocity	9in xrail	565038	4,29	4	17,16
	Servocity	4.5in xrail	565026	3,69	4	14,76
	Servocity	raised perp mount	585074	3,49	20	69,8
	Servocity	2x screw plate	585757	4,99	10	49,9
	Servocity	screw	632110	1,89	5	9,45
	Servocity	plate 9x12in	585006	16,99	1	16,99
TOTAL						7324,22

Table 3.4: Bill Of Materials

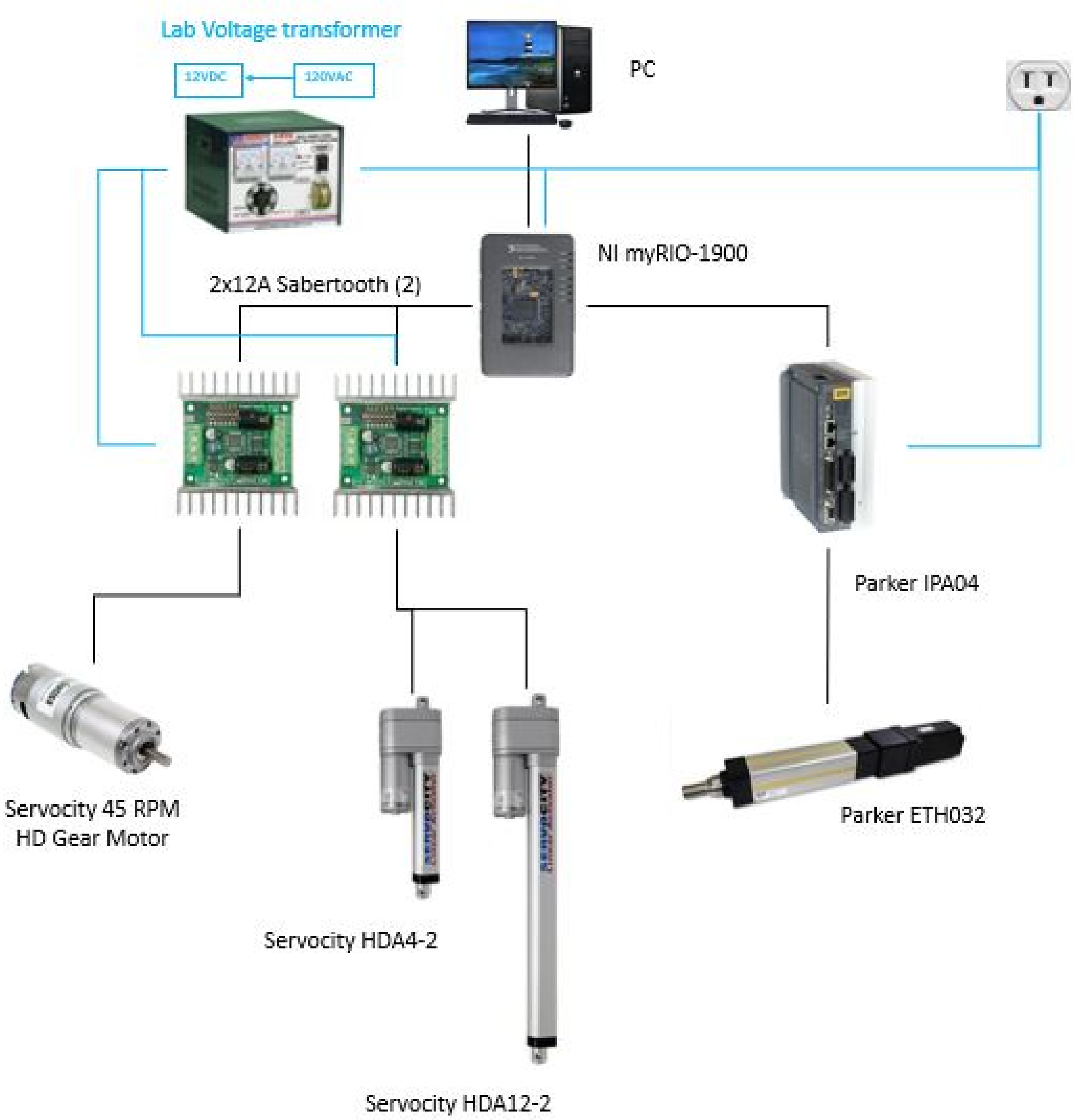

Figure 3.7: Electrical and electronic connections among the components

3.4.3 Prototype Final Design

First Version

Starting from the aforementioned considerations, the design was precisely refined:

- The main structure, initially designed with $1/2in$ A-36 plates has been substituted by a frame of extruded aluminum structural bars, supplied by Servocity, and of a half-inch thick aluminum plate, machined and supplied by a local machine shop.
- Its design has been adapted in order to accommodate the Parker ETH 032 and the Servocity electric linear actuators, integrating all the elements required to increase the frame stiffness, so as to withstand any possible load coming from them.
- The design of the industrial mixer was modified, in order not to have interference with the motion of the scraper, to fit within the available space and to accommodate the HDA4-2, for the motion of the discharge port.

The design of the prototype, as well as some details, can be seen in Fig. 3.8, 3.9.

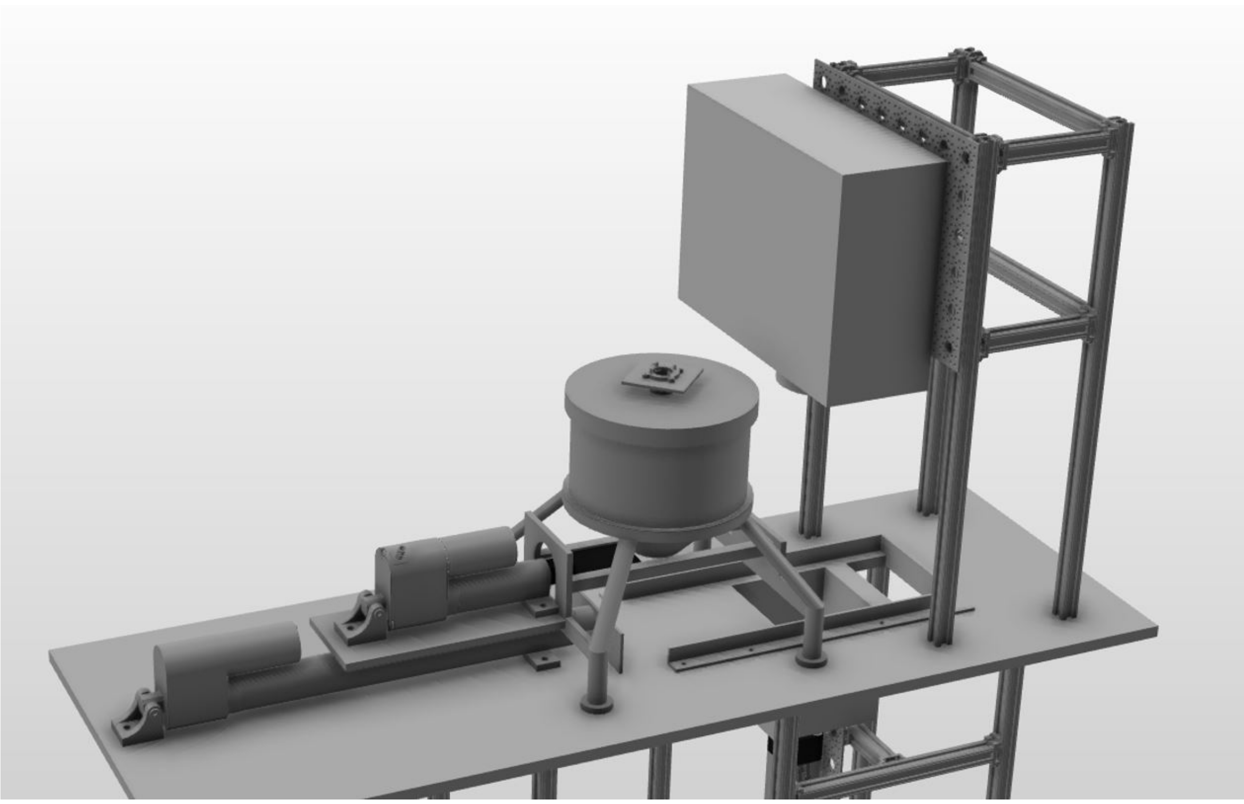

Figure 3.8: Superior part of the prototype, first version

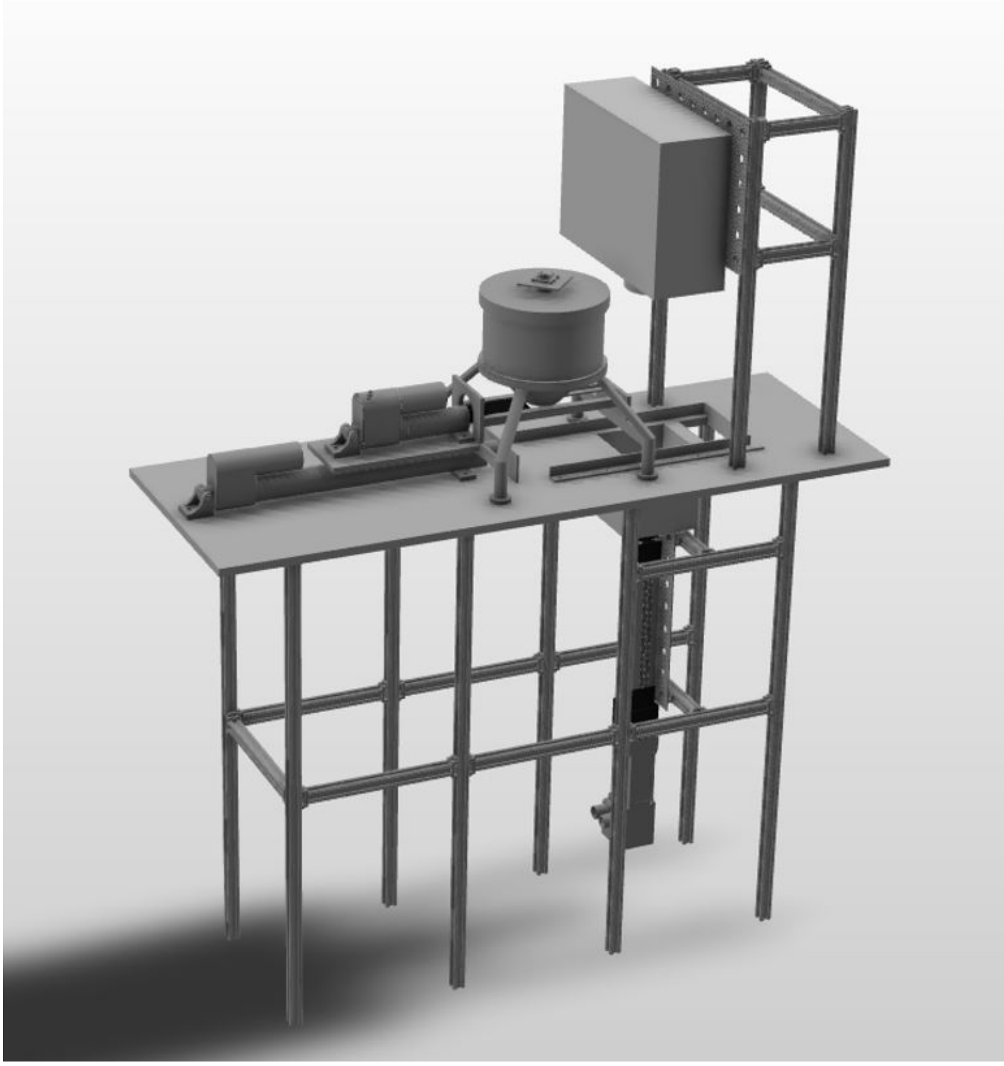

Figure 3.9: Final design of the prototype, first version

Second Version

In spite of the fact that the BOM respected the determined budget, we received the request for cutting even more the total amount. For this reason, we decided to get rid of the extruded aluminum structure and we have been provided with the steel structure of an working table.

As a consequence, we had to adapt the design of every component to the new dimensions. We had to replace the aluminum frame for the projector as well, making use of wooden strips and screws, losing in this way the possibility of adjusting the distances of the several cross-bars in case of need.

We decided anyway to leave the previous chapter, in order to let the reader having a finite design and a complete components list, ready to be used to replicate the prototype for any possible different application.

By replacing the aluminum bars, we were able to save other \$900, reducing the total amount approximately to \$6400. Considering also that the microcontroller MyRIO and the drives Sabertooth 2x12A were already owned by the department, the actual amount spent on the purchase of new component was approximately \$ 5750.

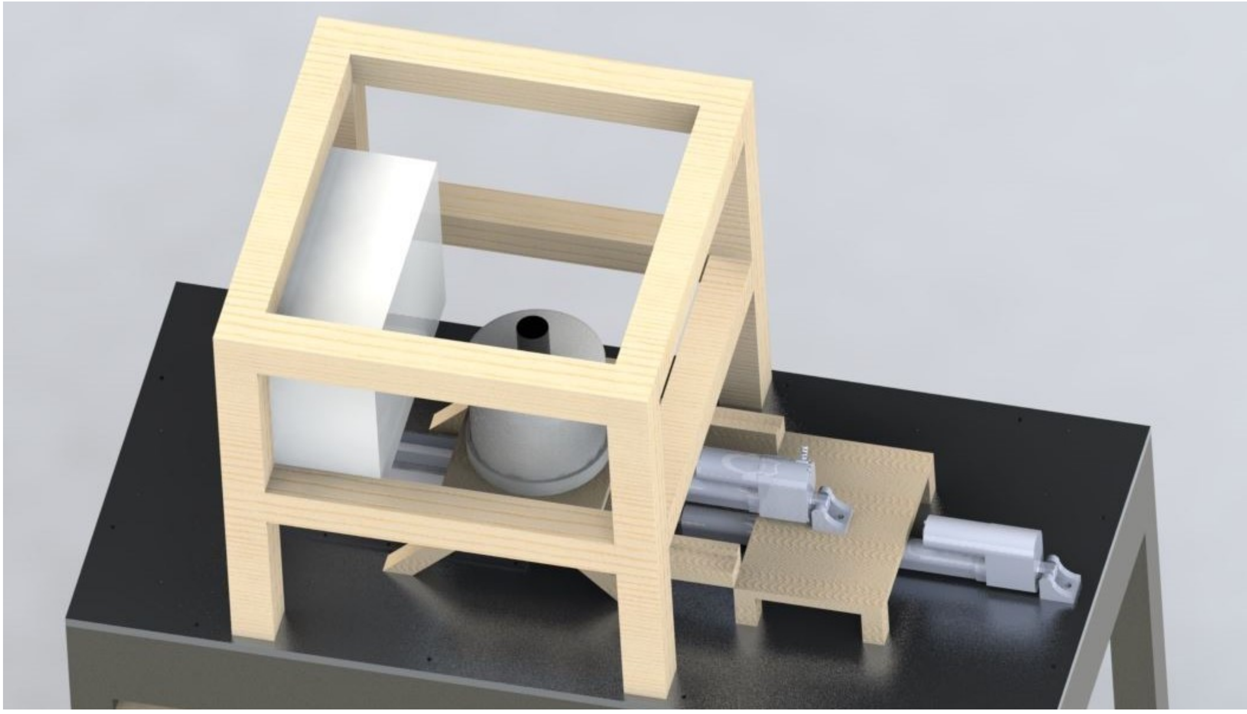

Figure 3.10: Superior part of the final design, version 2

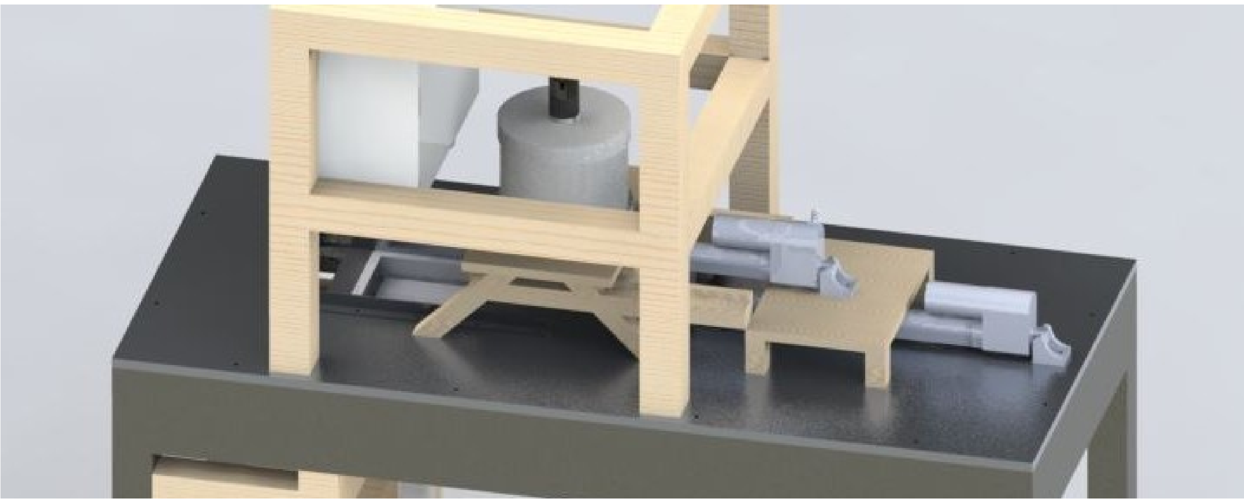

Figure 3.11: Superior part of the final design, version 2

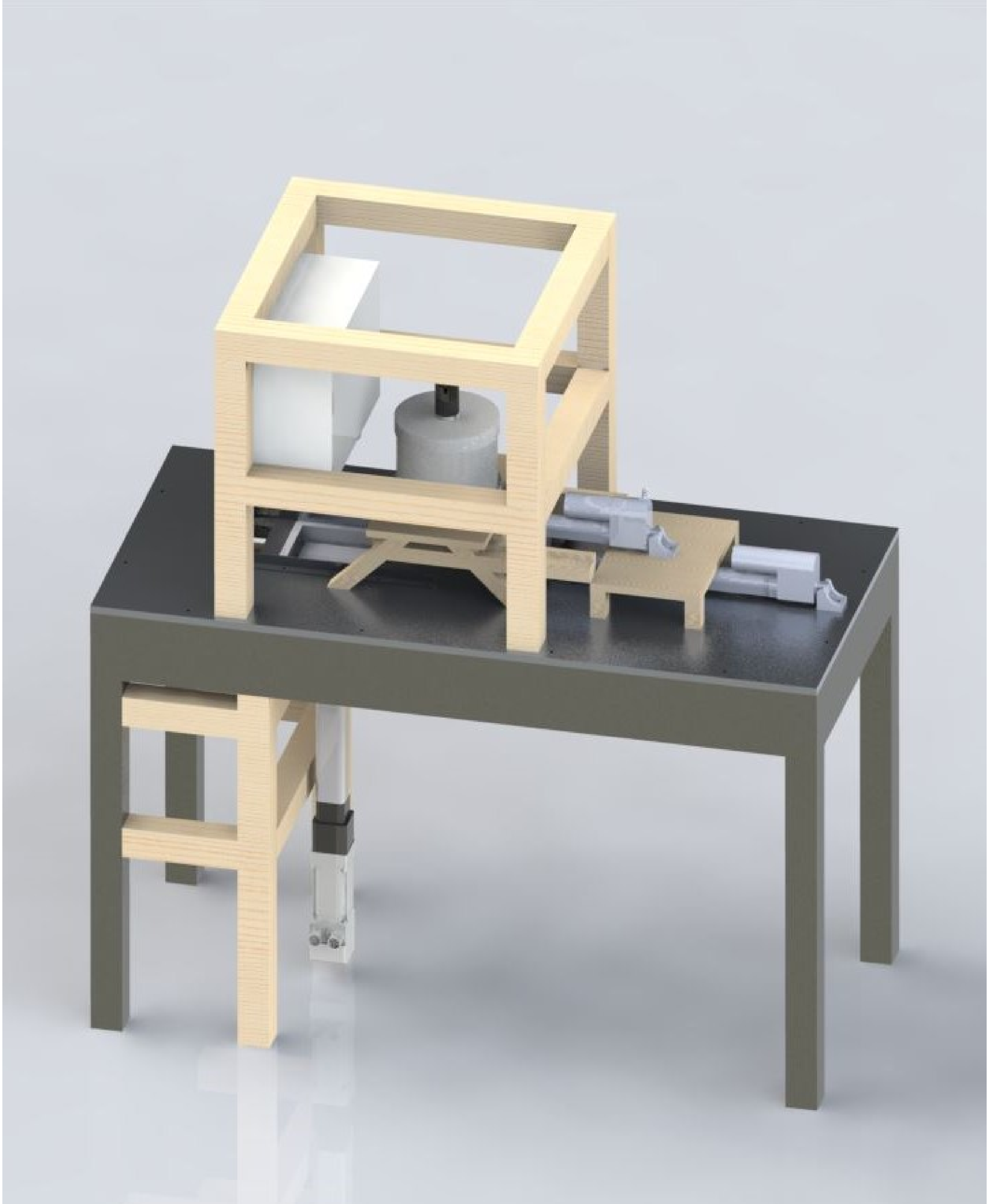

Figure 3.12: Final design of the prototype, version 2

Chapter 4

CONSTRUCTION AND ASSEMBLY

Once the final design was completed, all the equipment needed for the realization of the system was ordered, while the raw materials were purchased from local suppliers. The parts that have been built at the MSU machine shop by ourselves were:

- Projector frame
- Electronics support structure
- Blending system
- Connections for the different motors/linear actuators
- Slide rails.

The materials used for the construction were mainly wood (plates and bars of different dimensions), aluminum (plates, sheets and bars of different dimensions), PVC tubes and pipes, screws, nails and others.

The equipment employed for the realization of the system has been:

- Vertical and drop saw
- Shearing machine
- Vertical drill and manual tools
- Extrusion-based 3D printer

In the following pages some pictures of the different steps are shown.

The scheme of the electronic connection created to power the linear actuators, the DC motor, the potentiometers and the encoder is shown in Fig. 4.2.

The built prototype, lacking only of the Parker linear actuator, is shown in Fig. 4.3.

The LabVIEW code used to run the prototype following the fabrication process presented in Fig. 5.1, is shown in Fig. 4.4, 4.5, 4.6 and 4.7. The reader can find a detailed description of the code in Appendix A.

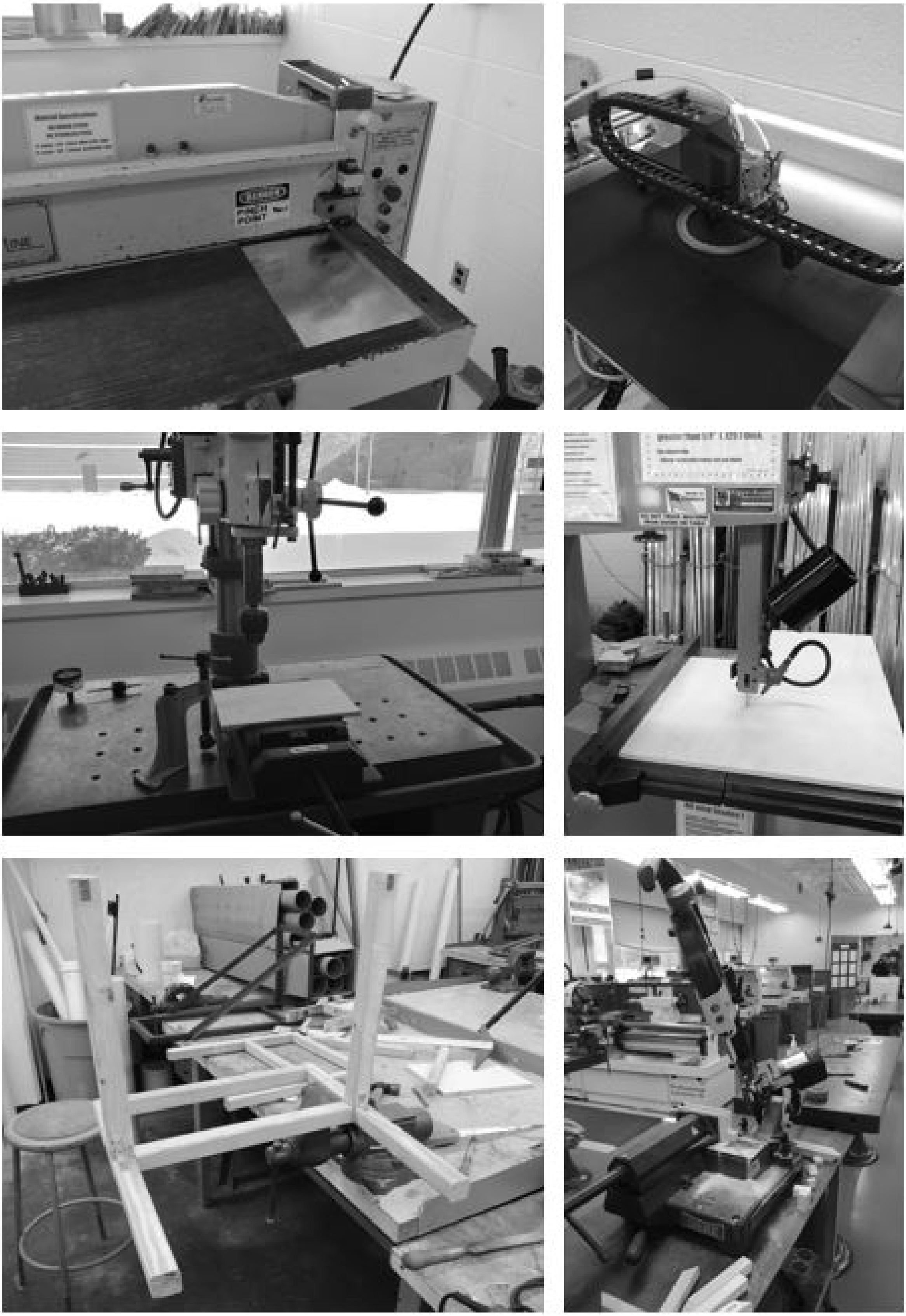

Figure 4.1: Different steps and equipment used for the realization of some parts

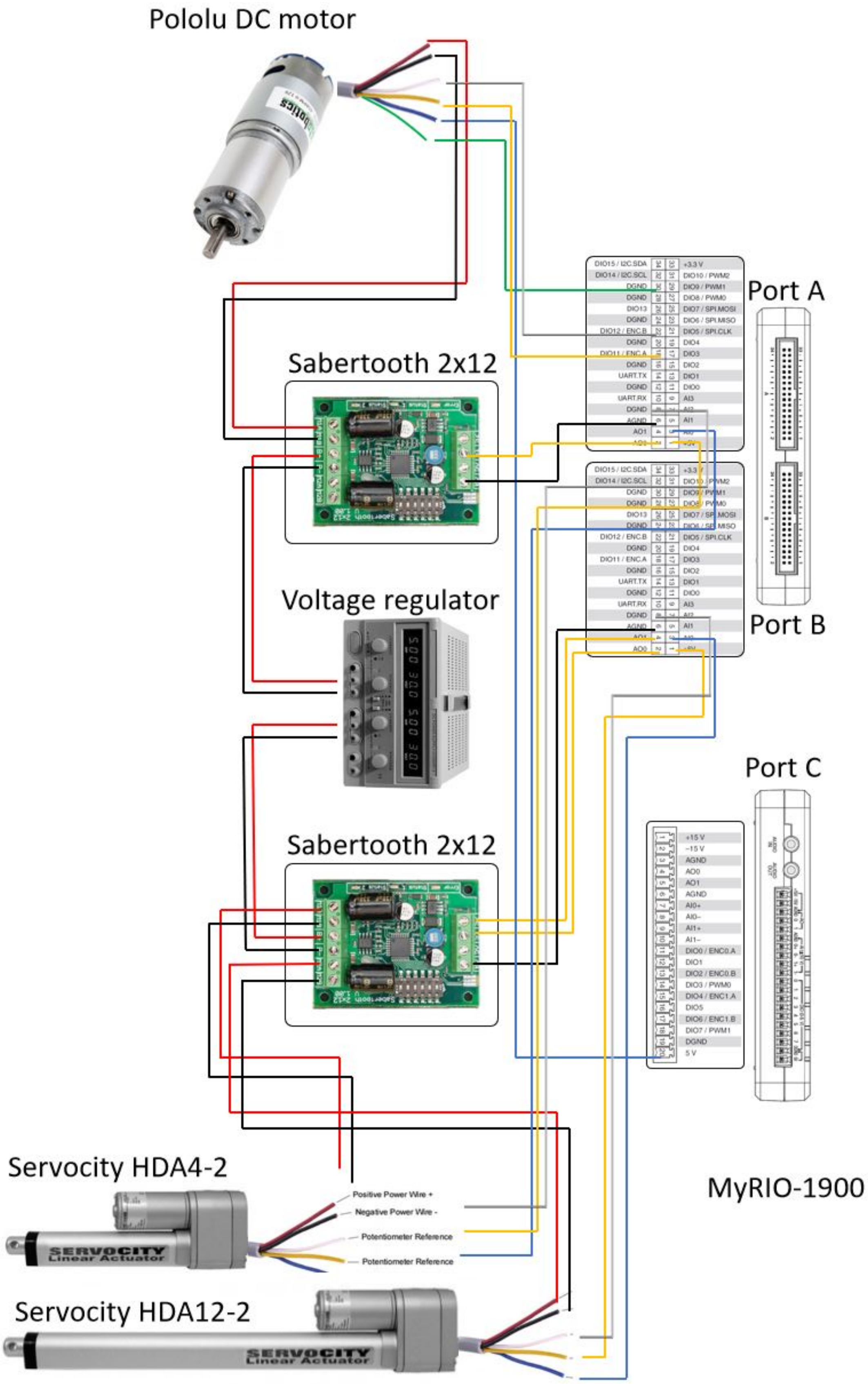

Figure 4.2: Scheme of the electronic connections

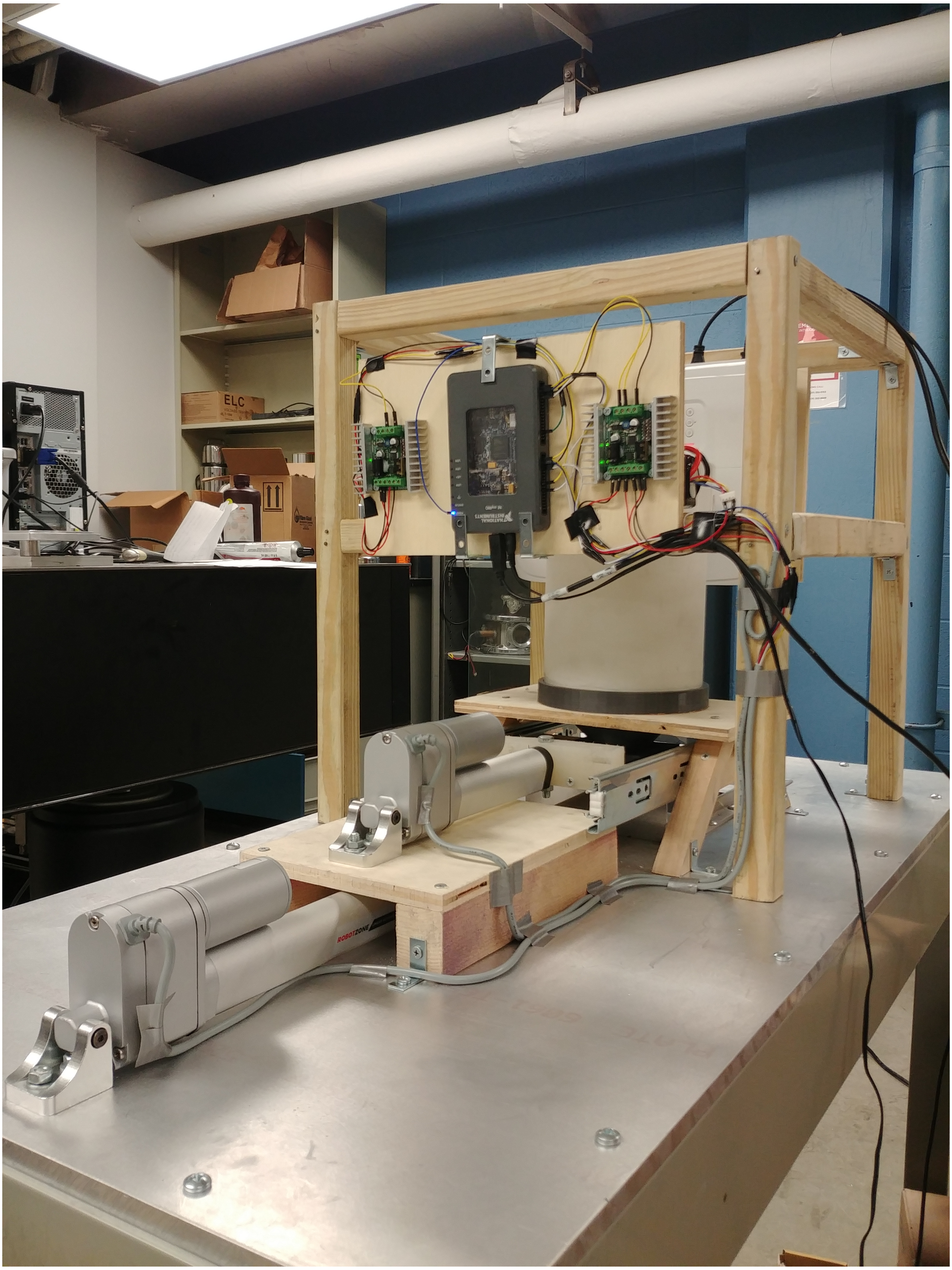

Figure 4.3: Superior part of the built prototype

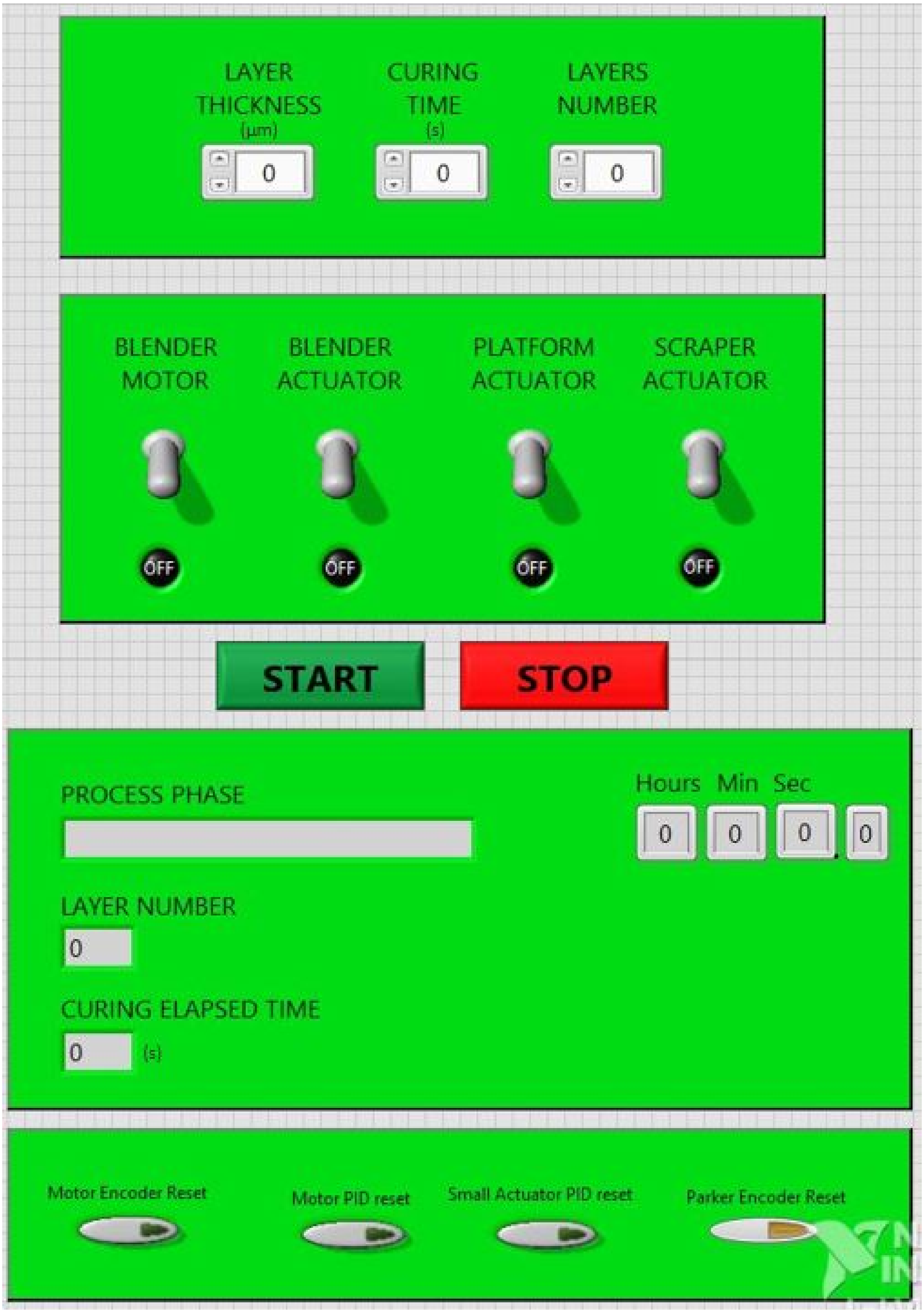

Figure 4.4: LabVIEW code, Front panel

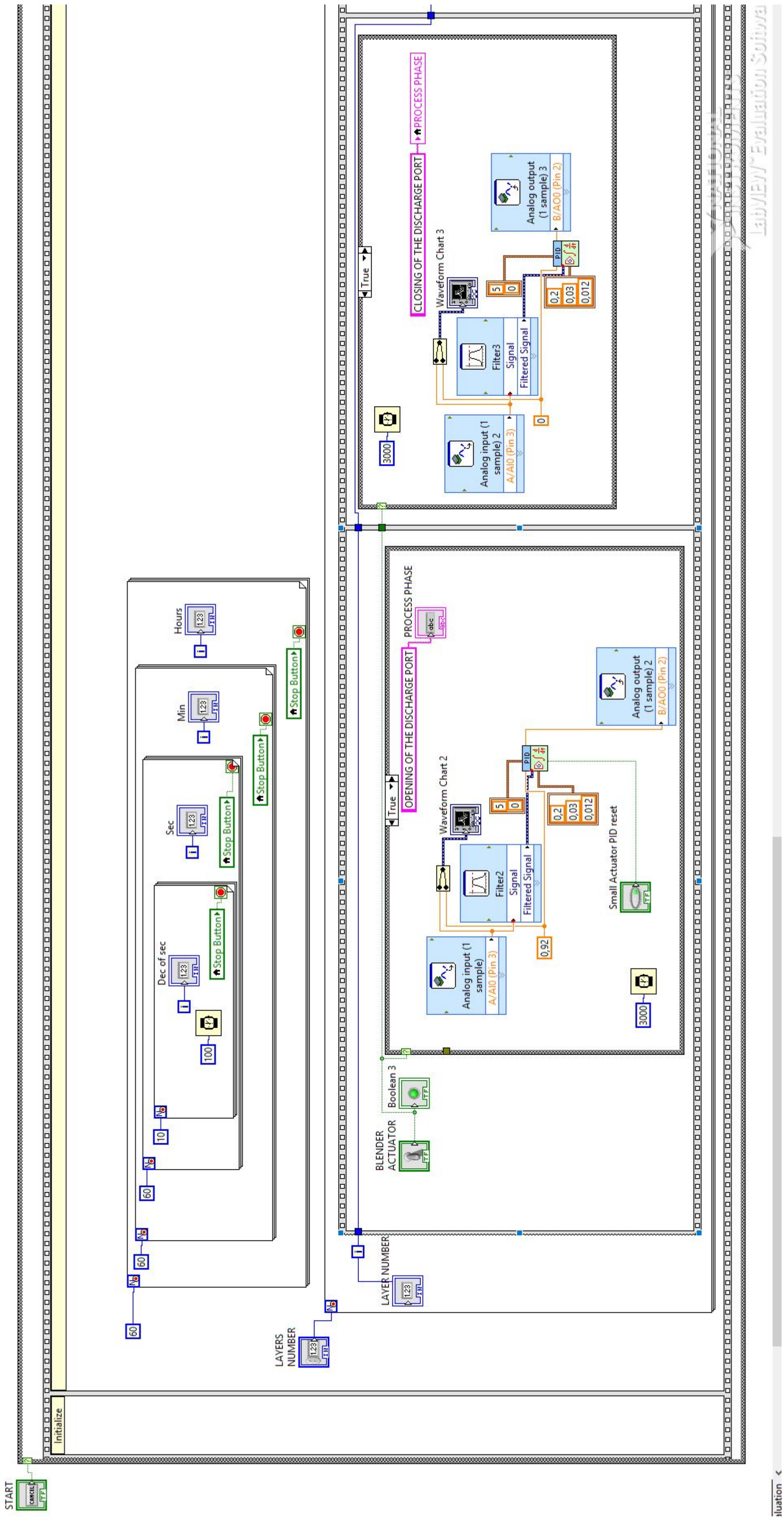

Figure 4.5: LabVIEW code, Part 1

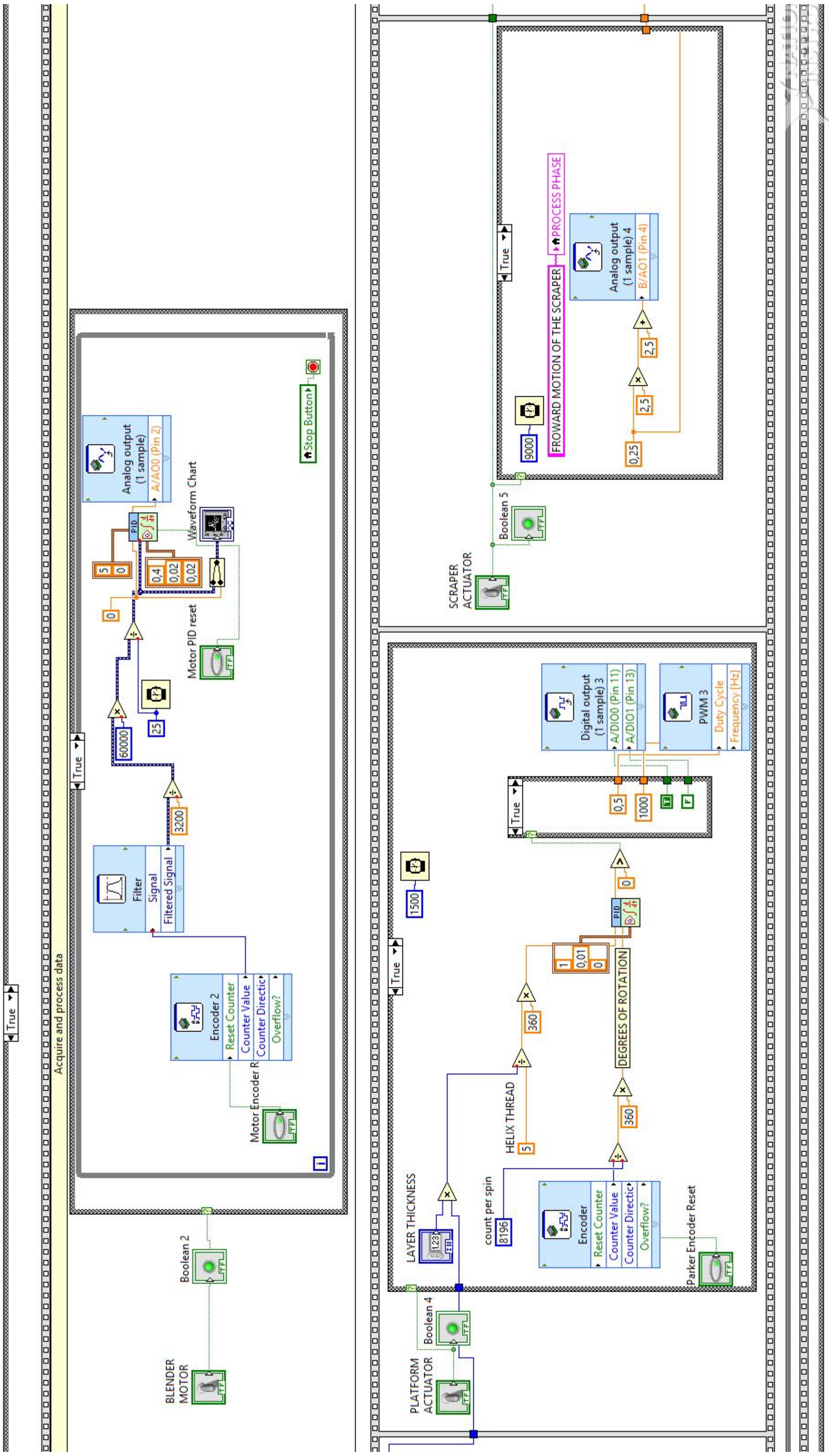

Figure 4.6: LabVIEW code, Part 2

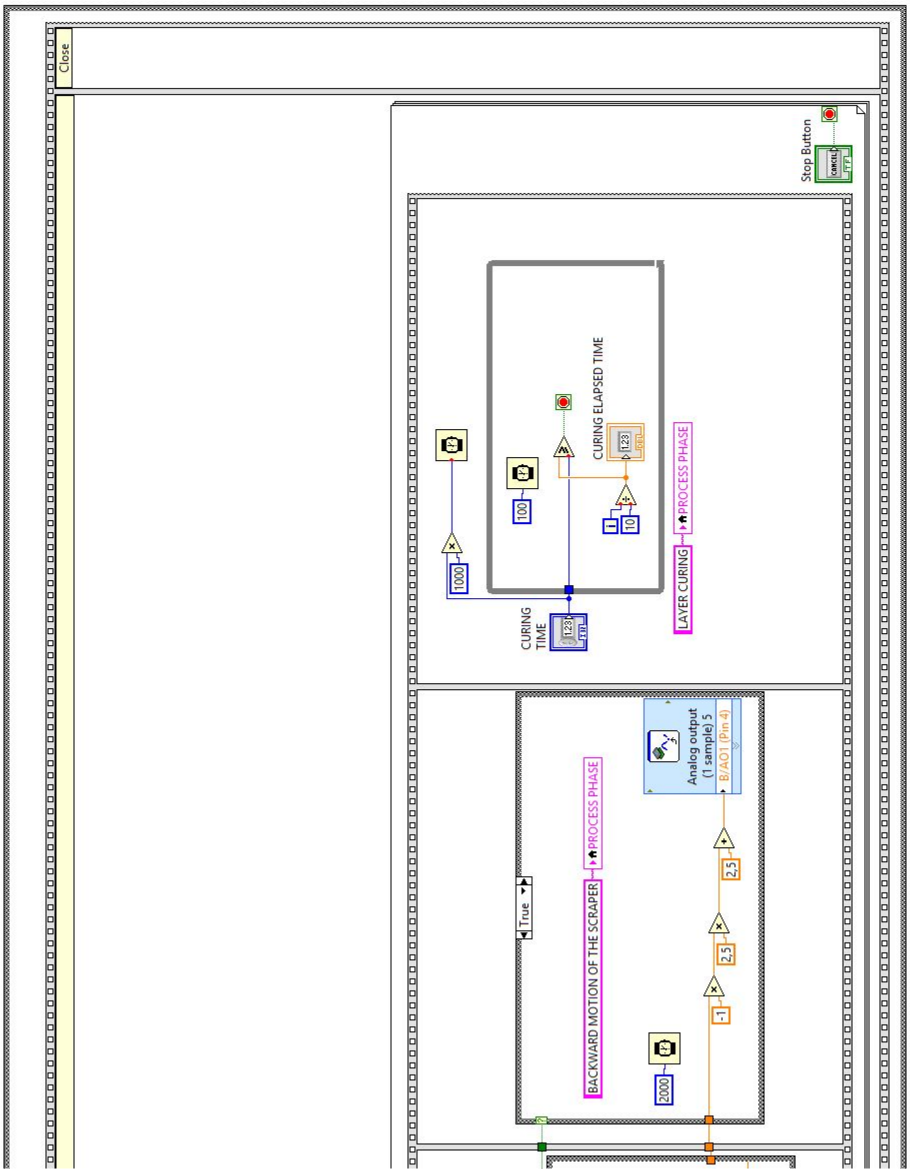

Figure 4.7: LabVIEW code, Part 3

Chapter 5

TESTING THE MANUFACT. PROCESS

Any manufacturing process requires a precise definition of its structure. The different steps and parameters have to be organized in a reliable way, that allows complying with the given requirements, so as to have the same products, with the same quality, anytime the process is repeated with the same parameters.

Therefore, all the involved variables, which could be either defined every time or fixed for any fabrication process, need to be analyzed carefully. A hasty selection of the process parameters could generate a waste of time, material and money. This because it has a direct influence on the products' properties, which could result to be quite different from the requirements, or in the worse scenario it can lead to damage or destruction of some components.

This is certainly pivotal for mass production processes, where the efficiency of any involved activity is absolutely necessary to guarantee the competitiveness of a company. Nevertheless, it is also relevant for a project like ours.

In fact, within a university department, the available resources, in terms of time and available budget, are limited. Therefore, it is important to make the best possible use of them.

For this reason, it was believed necessary to define and follow a detailed process planning method, in order to obtain the correct identification and selection of all the variables.

The conceptual scheme, presented in Fig. 5.1, was followed during the creation of the code in Labview.

While waiting to receive all the components to assemble the complete prototype, other manual experiments, necessary to have a deeper insight in the fabrication feasibility and in the manufacturing process variables, have been done and they are presented in Chapt. 5.1

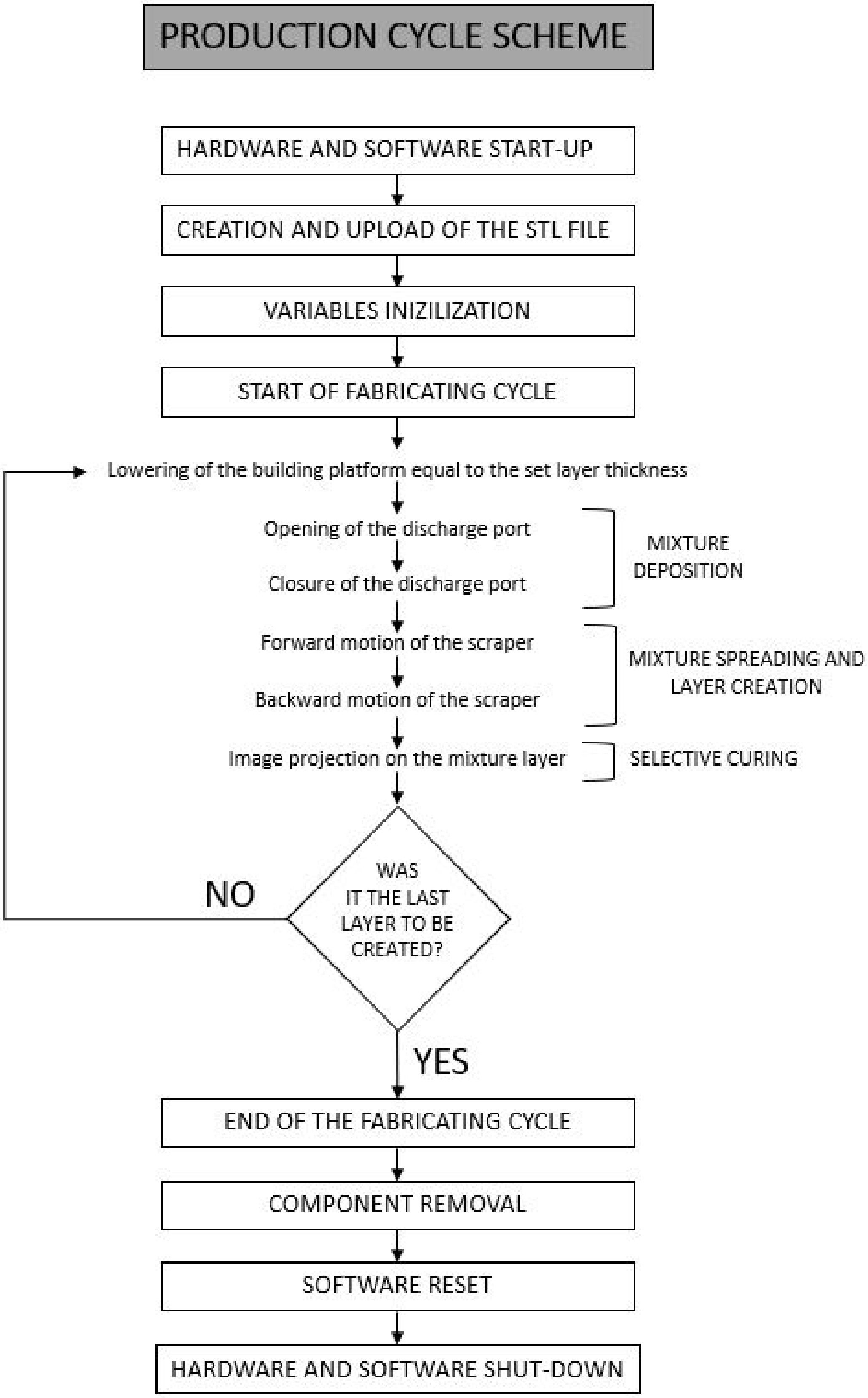

Figure 5.1: Production Cycle Scheme

5.1 DYNAMIC MASK PROJECTION

As it has been mentioned in the introductory chapter, in SLA MPVP the two main systems for image projection are LCDandr DLP[1] systems. Because of the great availability of economical alternatives, it was decided to start testing the use of commercial projectors.

In a LCD projector, as it can be observed in Fig. 5.2, a beam of high-intensity light is emitted by a source, which can be constituted by several different typologies of lamps. It is patterned, often by optic reflective systems, through two different dichroic mirrors, which are coated in a particular film that reflects the light of a specific wavelength range, allowing the remaining part to pass through. Since the dichroic mirrors are usually designed to reflect the red and the green parts of light spectrum, the remaining is mainly constituted by wavelengths close to the blue color range.

All three components of light are patterned through as many LCD displays and then conjoined back in a single beam by a dichroic prism. The prism, therefore, allows the superposition of three images which are identical in shape, but different in colors, obtaining the fully colored image which we are used to look at on screens.

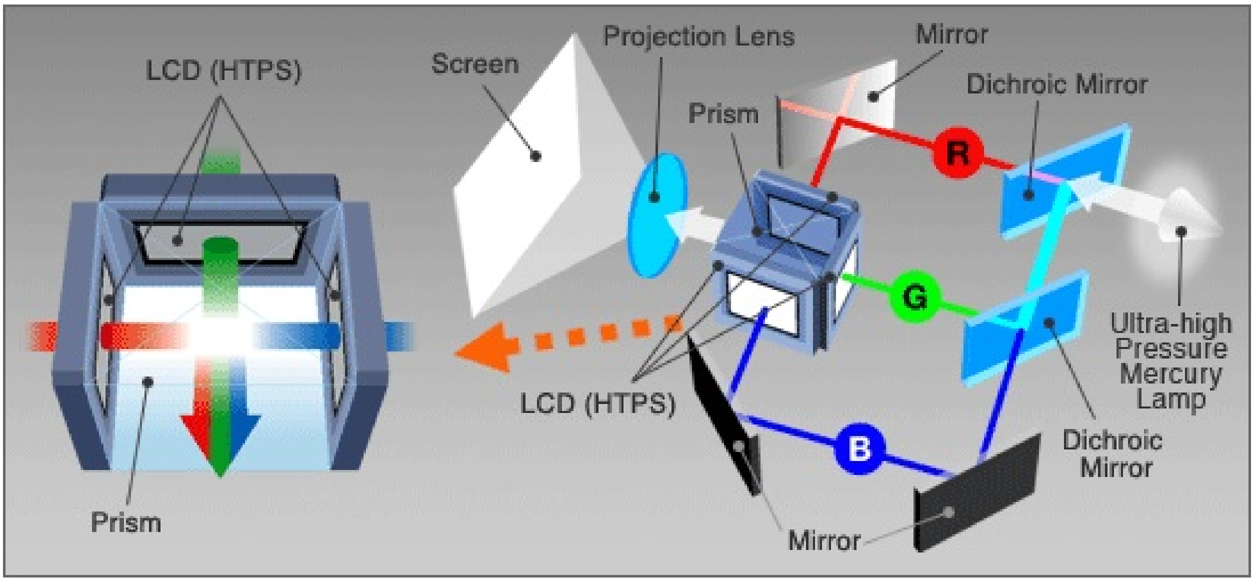

Figure 5.2: Internal structure of a LCD projector

[1]Digital Light Processing

On the other hand, as it can be also observed in Fig. 5.3, a DLP projector, in particular in its simplest version, has a quite different structure. The beam emitted by a light source is condensed, thanks to a dedicated lens into a single point beam, which is forced to pass through a spinning color filter. Just after it, there is a second lens which reshapes the light to the appropriate beam dimension. This is patterned towards the DMD and then reflected to the projection lenses, through which the final image exits the projector.

If we analyze in detail the structure of a DMD, the advanced system developed by Texas Instruments and shown in Fig. 5.3, we can notice that it is made of an array of highly reflective aluminum micro-mirrors, characterized by a tilting capacity usually equal to $\pm 12°$. The rotation is controlled electro-mechanically, up to 5000 times per second, and it is at the base of the image projection. In fact, each of the mirrors corresponds to a pixel[2] and only in the ON state they reflect the received light towards the projection lenses, otherwise discarded in a different direction. The perfect synchronization control on the desired micro-mirrors and the color wheel spin, generated by the DLP board, allows creating perfect images.

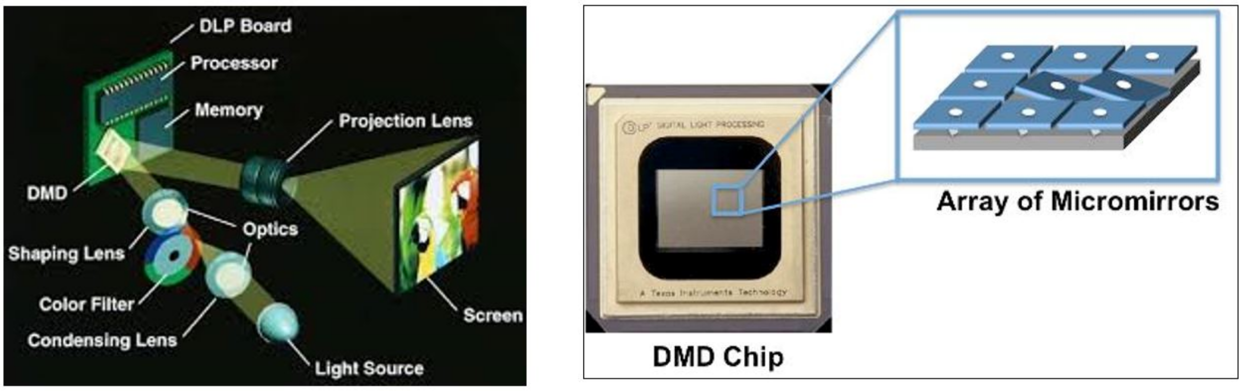

Figure 5.3: Internal structure of a DLP projector and of a DMD chip

It becomes clear why DLP projectors are on average much more expensive than LCD projector, in particular in the most advanced configuration, made of three different DMD, one for each primary color, in a concept similar to the one explained for LCD projectors.

Consequently, in order to keep the purchase costs as low as possible, it was decided to start running some rough experiments employing a used commercial LCD projector, which was available within the department.

[2]In a FullHD DLP then there are more than 2 millions micromirrors

5.1.1 Tests criteria

Considering that this was a preparatory part, the main goal in this phase was to test the effectiveness of the projecting system in curing our mixture made of resin and metal powder. For this reason, the accuracy in the realized parts, as well as their superficial aspect, or any mechanical properties were not among the main evaluation criteria.

What we were mainly looking for was the creation of a solid layer, capable of undergoing a complete production process with the superposition of several layers on the top of it.

In second place, it was desirable having a curing time as low as possible. In fact, we need to keep in mind that the main objective of this project is to realize a system capable of reducing the fabrication time, thus 5 min or longer for the curing of each layer could have been unacceptable results.

It was determined to start testing the curing of the resin by itself. It is quite straightforward that if the light source with the dynamic mask is not capable of curing the resin when employed alone, it is impossible to obtain its photopolymerization when mixed with metal powder, thus generating a reduction in its concentration.

In case of positive results from the first part of the tests, we proceeded withthe second, employing and running experiments with the mixture resin-metal powder.

For all the experiments, the maximum number of variables taken into account was 3:

- Time of exposure. Starting with a minimum time equal to 30s, if we did not get the desired result we would have increased it by multiples of 30s.
- Distance from light source. The ideal condition is to get good curing, placing the mixture at the minimum focal distance from the projector. If this was not obtained, following the principles discussed in the previous chapter, the distance was reduced to the minimum possible, in order to observe if the increased radiating flux was capable of photo-polymerize the resin.
- Mixture weight percentages. For what concerns the experiments related to the mixture resin-metal power, a third variable was the weight percentage of its two main components. Starting from the ideal mixture with 90% of weight constituted by metal particles, in case of negative results, we would have reduced its amount following steps of 10% up to a minimum with 50% metal particle and 50% resin.

In other words, for each test, we started seeking for the ideal conditions:

- Minimum curing time, so as to reduce as much as possible the lead time of the fabrication process.
- Building bed placed at the minimum focal distance. In this way we would obtain the perfect trade-off between irradiating flux and resolution, since the part would not have been too far from the light source, perfectly in focus on the building bed.
- Mixture composition with the highest metal powder percentage possible. This is a desirable result. In fact, it results in a significantly high final density, in a lower shrinkage percentage, and more in general in a better mechanical characterization.

For what concerns the curing of resin by itself, the simplest parameter to change is the time of exposure. As a matter of fact, since our testing assembly was not enclosed, the building bed was directly observable and the parts could be taken out with ease.

Consequently, if the curing was not reached we simply increased the exposure time, up to the set maximum of 3 min. If also the longer exposure time was not sufficient for the photopolymerization, we would have decreased the distance between the building bed and the lens to a minimum of 1 cm.

The scheme followed for the experiments is presented in Tab. 5.1, where the order can be easily followed along the arrow, or in other words with a columnar pattern.

Whenever the desired curing was reached, the experiment would have been stopped and the following experiment would have been set up.

			II PARAMETER: MIXTURE COMPOSITION	
			1° STEP	2° STEP
			85% metal powder-15% resin	87% metal powder-13% resin
I PARAMETER: EXPOSURE TIME (s)	1° STEP	15	NO	NO
	2° STEP	30	PARTIAL	NO
	3° STEP	45	YES	PARTIAL
	4° STEP	60	YES	YES
	5° STEP	75	YES	YES
	6° STEP	90	YES	YES

Table 5.1: Process parameters for the resin curing

For what concerns the experiments with the mixture, the approach followed was slightly different. Having three different variables to take into account, the mixture composition was assessed as the most time-consuming to be changed. As a consequence, it was determined to start fixing a certain mixture composition, make all the possible experiments with that mixture sample and, in case of negative results, move on with a different composition.

For the management of the other two variables, time of exposure and distance from focal lens, the procedure followed was the same as for the resin. Initially, the mixture was positioned at the correct focal distance and the different times of exposures were tested. If the 3 min exposure was not sufficient, the part building platform would have been raised close to the lens in order to get the maximum luminous radiation possible.

The order of experiments for the mixture is shown in Tab. 5.2, and it can be easily followed along the columns, as it has been done for the experiments with the resins.

			II PARAMETER: DISTANCE FROM LENS (cm)							
			1° STEP	2° STEP	1° STEP	2° STEP	1° STEP	2° STEP	1° STEP	2° STEP
			25 cm	1 cm	25 cm	1 cm	25 cm	1 cm	25 cm	1 cm
I PARAMETER: EXPOSURE TIME (s)	1° STEP	30	1	7	13	19	25	31	37	43
	2° STEP	60	2	8	14	20	26	32	38	44
	3° STEP	90	3	9	15	21	27	33	39	45
	4° STEP	120	4	10	16	22	28	34	40	46
	5° STEP	150	5	11	17	23	29	35	41	47
	6° STEP	180	6	12	18	24	30	36	42	48
			90/10	90/10	80/20	80/20	70/30	70/30	60/40	60/40
			1° STEP	1° STEP	2° STEP	2° STEP	3° STEP	3° STEP	4° STEP	4° STEP
			III PARAMETER: WEIGHT PERCENTAGES OF THE MIXTURE (METAL POWDER %-RESIN %)							

Table 5.2: Process parameters for the mixture curing

5.1.2 Experiments with the LCD Projector

As already mentioned, in order to keep the purchase costs as low as possible, it was decided to start running some rough experiments employing a used commercial LCD projector, which was available within the department. Without modifying its basic structure, in order to obtain a radiation of light as close as possible to ultraviolet wavelengths ($< 400nm$), a simple circular image, colored in ultraviolet (RGB: 158,0,255), on a black background, was created through a graphic software.

A simple structure to hold both the projector and the building platform, similar to the one shown in Fig. 5.6, was also assembled.

In any test, the initial exposure time was equal to 30s. However, if no curing was obtained after 30s, we considered exposure times equal to multiples of 30s, up to a maximum of 3 min. The firsts attempts regarded only the curing of the resin, which succeeded only partially after 1 min and at a very close distance. However, whenever mixed together with the metal powder in any percentage, no polymerization was observed, even after 3 min of exposure.

In order to determine if the lack of curing could have been related to the chemical composition of the resin, the same tests were repeated with the employment of the Anycubic resin, specifically designed for curing at UV led light with wavelength equal to 405nm[3].

For the same reasons, the tests were also made with the Ferrolite Iron Resin, a UV curable resin containing iron. The manufacturer, Tethon 3D, claims that after sintering all parts can reach a state with 100% iron, which unfortunately has never been observed in any test performed at MSU lab. It also has the inconvenient of not being able to control the kind of metal powder, as well as the mixture characteristics, therefore not suitable to meet the goals of our project.

However, the results obtained with all the resin employed have always been very similar to each other, as it can be observed from the Tab. 5.3. This can be explained as there is not a significant influence of the chemical composition of the binder on the curing, since they are designed to cure with approximately the same kind of light source (in terms of power and wavelength).

Considering the structure of a LCD projector, the incapacity of obtaining an acceptable curing was then thought to be attributable to the optic systems, which can have caused a significant reduction in the exposure power. This, accompanied by a narrowing of the light bandpass due to the dichroic mirrors, could have prevented to reach the critical exposure value and consequently the curing of the layer.

For this reason, the experiments continued with the substitution of the LCD projector with different light generating system.

[3]This resin was not taken into account as possible binder for our application due to the much higher viscosity (550cP vs 55cP), which could have resulted in a not complete wetting of the metal particles or not-homogeneous mixture, with the consequent curing-related issues.

5.1.3 Experiments with UV LED Light and LCD Display

It was then decided to attempt to make use of the components available in the Anycubic Photon 3D printer. In fact, even though the light source of this printer is not really powerful (40W, 405nm), its simple assembly, designed to cure parts positioned close to the UV bulb and therefore lacking of many optic systems, should have an higher curing capability.

As a matter of fact, we could observe the partial curing of thin layers of mixture powder-binder, in particular for those with great percentage of resin, with exposure times inversely proportional. Nevertheless, the amount of time necessary and the stiffness of the created bonds were absolutely unacceptable for our project.

As a result, it was decided to disassemble the Anycubic Photon 3D printer, in order to be able to make use of its curing system. Hence, it was possible to flip it upside-down, so as to avoid the use of the transparent FEP film used at bottom of the vat which could have had a certain influence on the light transmittance, and in case of negative results, to be able to substitute the light chip, increasing its power or changing the wavelength.

As it was expected, the influence of the FEP film was almost null and the outcomes of the experiments were the same.

The original light was then substituted by UV LED chips, connected to a heatsink and to a fan, in order to keep the temperatures as low as possible, as it can be observed from Fig. 5.4. The two different UV LED chips were:

- Chanzon 50W 395nm
- Chanzon 100W 405nm

The first chip was purchased in order to observe the influence of the wavelength over the curing. In theory, the shorter is the wavelength the better curing we have, since the resin is UV photo-curable and the UV range has its upper boundary at 400nm.

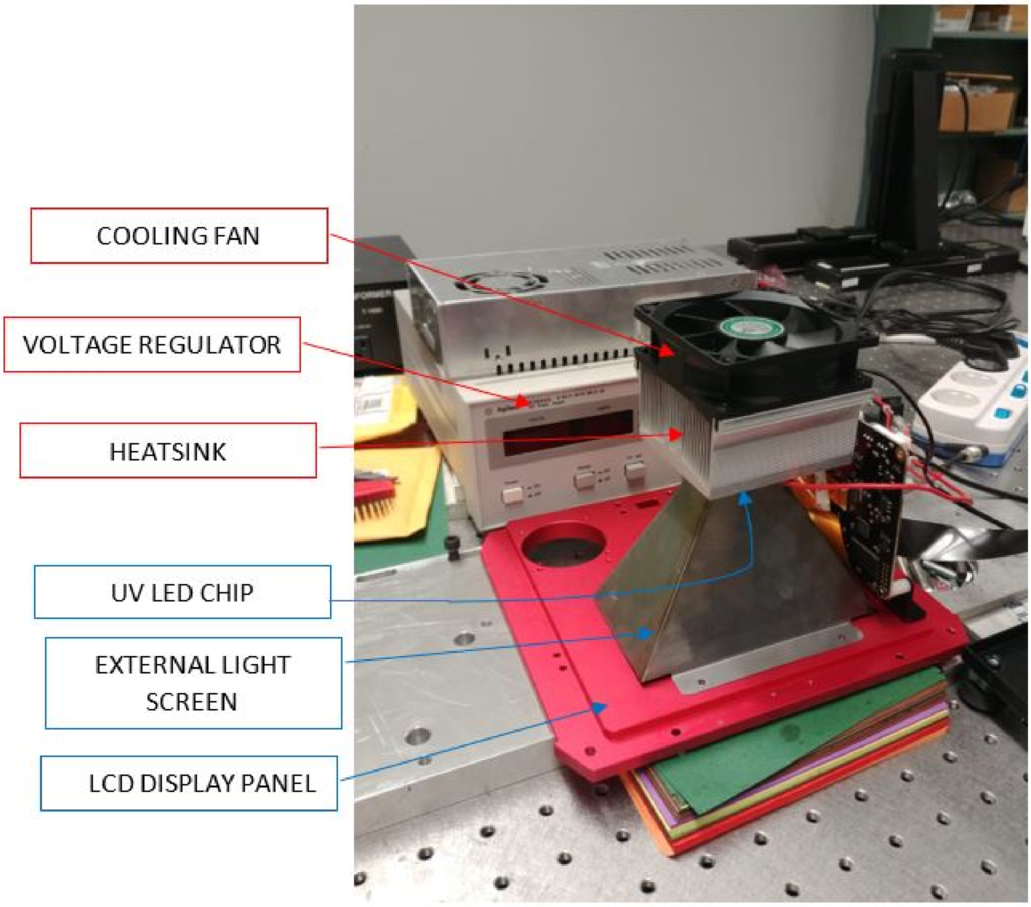

Figure 5.4: Set-up used for the experiments with the UV LED Light and LCD Display

However, no curing, even for the resin by itself, was noticed while using the assembly described earlier and the UV LED chip 50W and 395nm. This can be reconnected to the internal structure of an LCD display, presented in Fig. 5.5.

As it can be easily understood, even in a simple LCD display there are many different components and layer, which affect light transmittance. Most of all, after the vertical polarization, light passes through the liquid crystals, which are manipulated electrically, with the application of a certain voltage to the transistor film. However, even if they are switched to ON state, the filter placed in front of each subpixel only allows through a range of wavelengths (Source: Samsung).

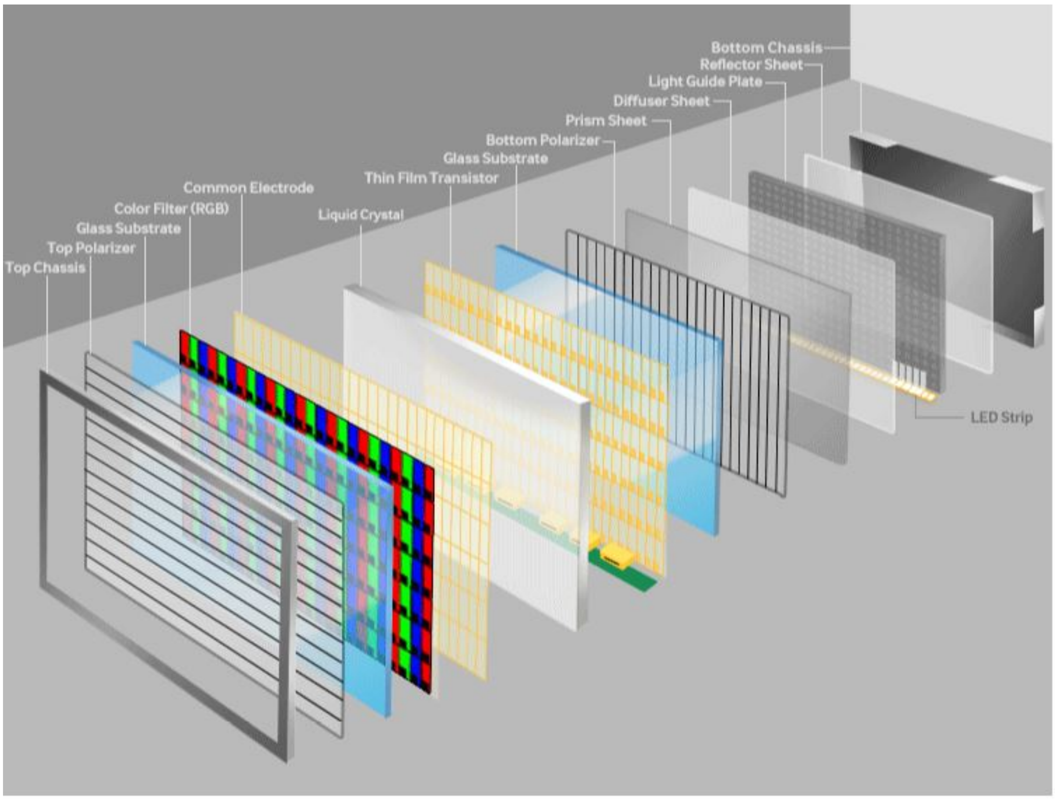

Figure 5.5: Structure of a LCD display, courtesy of Samsung

Since the hazard associated with exposure to UV light is widely known, usually all filters are meant to block light with wavelengths shorter than 400nm. For this reason, even if the chip employed was more powerful than the original bulb and in the desired wavelength range, no curing could have been obtained due to the LCD display screening.

For what concerns the second chip (405nm, 100W) we managed to obtain some partial curing of the mixture, reaching also mass percentage close to 80%-20% (metal-resin), in particular for long exposure times and with the UV LED chip placed close to the LCD. Anyway the results were not optimal and overheating issues were noticed both in the chip and in the LCD screen.

All the results are summarized in Tab. 5.3.

The sub-cases are not reported in order not to make the read ponderous and also because the desired results were not obtained, therefore it would result in a useless addition of information.

	Curing with physical mask (405nm-50W)	Curing with LCD projector	Curing from bottom with LCD (405nm-40W)	Curing from top with LCD (405nm-40W)	Curing from top with LCD (395nm-50W)	Curing from top with LCD (405nm-100W)
Green resin only	YES	PARTIAL	YES	YES	NO	YES
Low viscosity resin only	YES	PARTIAL	YES	YES	NO	YES
Green resin with powder (80/20)	YES	NO	PARTIAL	PARTIAL	NO	PARTIAL
Low viscosity resin with powder (90/10, 80/20, 60/40)	YES	NO	NO	NO	NO	PARTIAL
Low viscosity resin with powder (50/50)	YES	NO	PARTIAL	PARTIAL	NO	PARTIAL
Ferrolite resin	YES	NO	PARTIAL	PARTIAL	NO	PARTIAL

Table 5.3: Summary of all the experiments results

5.1.4 Experiments with DLP projector

Since the cheapest solution showed not to be suitable and effective for our application, it was settled to proceed trying out a DLP projector. The possibility of assembling a system by ourselves was discarded due to the lack of available time and to all the precision-related issues that were likely to be generated.

In order to select the projector among all the alternatives, the following criteria have been taken into account:

- The available budget for the purchase was set equal to $500.
- Since the projector was meant only for testing the prototype and not to be mounted on the final printer, the resolution was not among the primary requirements.
- It should have had the highest contrast and luminous flux possible[4].

At the end of the research, the Optoma S343 SVGA DLP Projector was purchased. Its characteristics are presented in Tab. 5.4.

Manufacturer	Optoma
Model	s343 SVGA
Part code	B07FZQCV77
Contrast	22'000:1
Luminous Flux	3600 lumen
Resolution	800x600
Throw Ratio	1,94-2,15:1
Image Size	27,7"-304,4"

Table 5.4: Characteristics of the DLP projector

The primitive system assembled in order to run the experiments is shown in Fig. 5.6. The variables taken into account were the same of the previous experiments. The starting point was the exposure to light for 30s or multiples, in case of failure in curing the resin. The first experiments concerned the use of only resins, while as a second step we proceeded in analyzing the curing behavior of the mixture, with different percentages.

[4]The luminous flux is not the equivalent of the radiant flux. Nonetheless, it is the parameter usually provided by the projectors manufacturers and it's still a measure of the power generated by the system

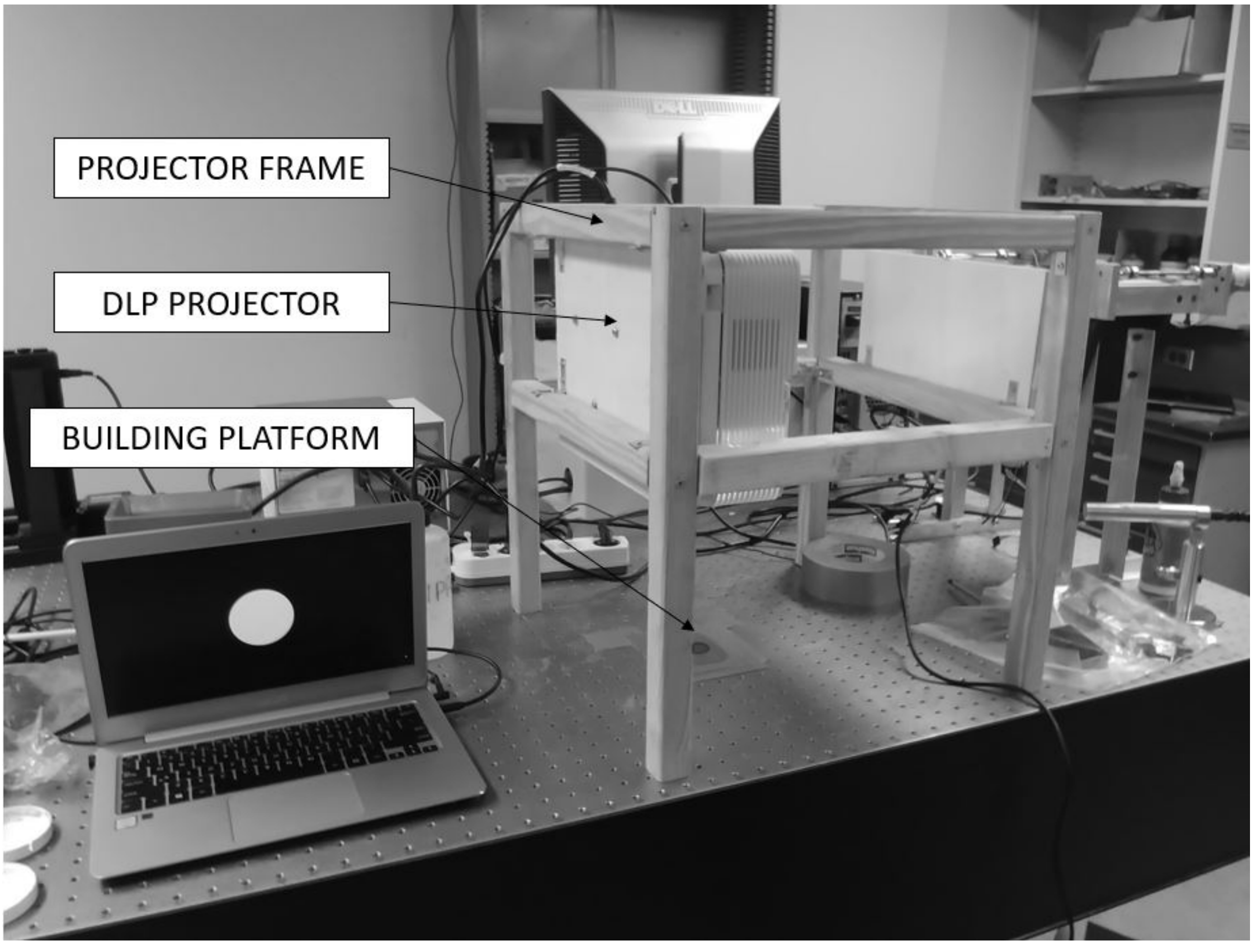

Figure 5.6: Set-up used for the experiments with the LCD and DLP projectors

The increase in the radiating flux, compared to the previous systems, was immediately observed. Not only did the resin cured immediately, but also an important distortion was observed after only a couple of seconds.

As a consequence, when the mixture was tested close to the lens, the photopolymerization of an extremely thin layer was observed. However, its strength was still unacceptable for our application.

In order to try to increase even more the output power, some experiments were performed after having removed some optical components from the projector.

The first step was the removal of the color wheel. After this modification, we could obtain a quite solid layer after 2 min of exposure, with the building platform close to the lens. The position of the building platform was changed and put close to the lend after some unsatisfactory outcomes were obtained at the original distance. The proximity, of course, resulted in a loss of precision along the contours of the created shape (a simple disc), due to the lack of focus of the projected image.

A significant improvement was obtained with the second step, which consisted in the removal of the only light filter easily accessible[5] Immediately at the first test, with a mixture 85% metal powder-15% resin and at the correct distance from the lens, we obtained a cured layer much better, in terms of consistency, accuracy and superficial aspect, than what we could obtain with the highest metal powder amount possible in the mixture, positioned at 1 cm from the lens for the previous case.

This can be easily seen in Fig. 5.7, where the two samples can be compared.

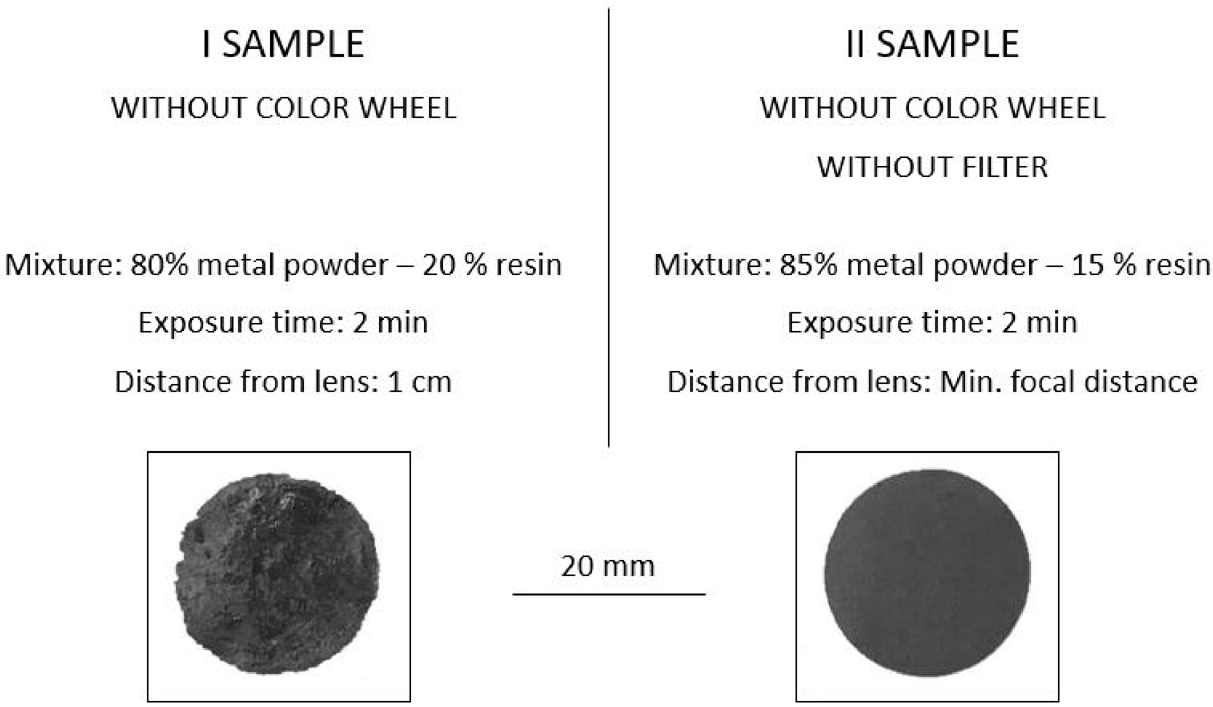

Figure 5.7: Samples obtained after the modifications made on the projector

[5]Theoretically other lens/filters are present within the optical case of the projector. However

Some considerations were then made on the functionality of the removed light filter, in order to understand the feasibility of the procedure. In fact, the original filter was meant to let only the visible light pass through, while stopping the UV and IR rays, emitted by the lamp, so as to prevent any possible harm for the human sight and increasing the lifetime of the projector components. In particular, the technological DMD chip can be easily damaged after long exposure to UV light, as warned by a TI technical.

Concerned about the integrity of the projector and aware that the needed radiation range for the curing of the resin was in the UV spectrum, we thought that limiting the overall spectrum, we could reduce the heat flux and, as a consequence, also the temperature increase of the components.

For this reason, the filter THORLAB FGB37S was bought and cut into shape to fit into the projector. Its bandpass can be observed in Fig. 5.8. It two main characteristics are:

- A good portion of the UV-radiation, in other terms any light with wavelength smaller than 400 nm, needed for the curing of the resin, is transmitted.
- The biggest part of IR light, as well as the portion of the visible light above 600 nm, almost completely useless in our application, is blocked.

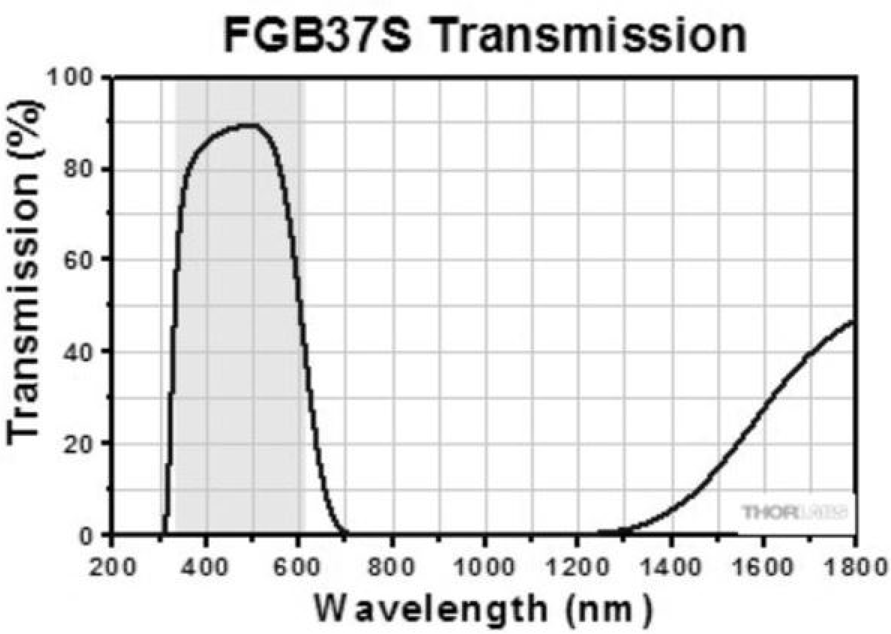

Figure 5.8: Transmission chart of the THORLAB FGB37S

Unfortunately, after only some seconds of use, the filter cracked, emitting the typical sound of broken glass. After its removal from the projector it was observed that, together with the fracture, an important thermal deformation occurred, as noticeable in Fig. 5.10. This means that the heat flux:

- Raised the temperature over the glass-transition temperature, generating a local melting of the central part of the filter, due to the braking of the internal structure bonds.
- The raise in temperature was so high the thermal expansion of the filter, caused the internal stress to overcome the value withstandable by the glass.

No countermeasures were thought to be able to avoid these results, and it was stated to purchase a second filter, and more specifically the Newport FSQ-KG5, with the bandpass shown in Fig 5.9. With a bandpass similar to the THORLAB filter and commercialized as a 'Heat Absorbing Glass Filter' it was believed to have a structure suitable to resist to any possible temperature increase. Despite that, similarly to what happened for the first filter, a cracking sound was emitted, approximately 20s after the turn-on of the projector. On the other hand, no deformation was noticed after the removing of the filter and the fracture did not alter the projection by any mean. As a consequence, the tests made on the resin and on the mixture were positive.

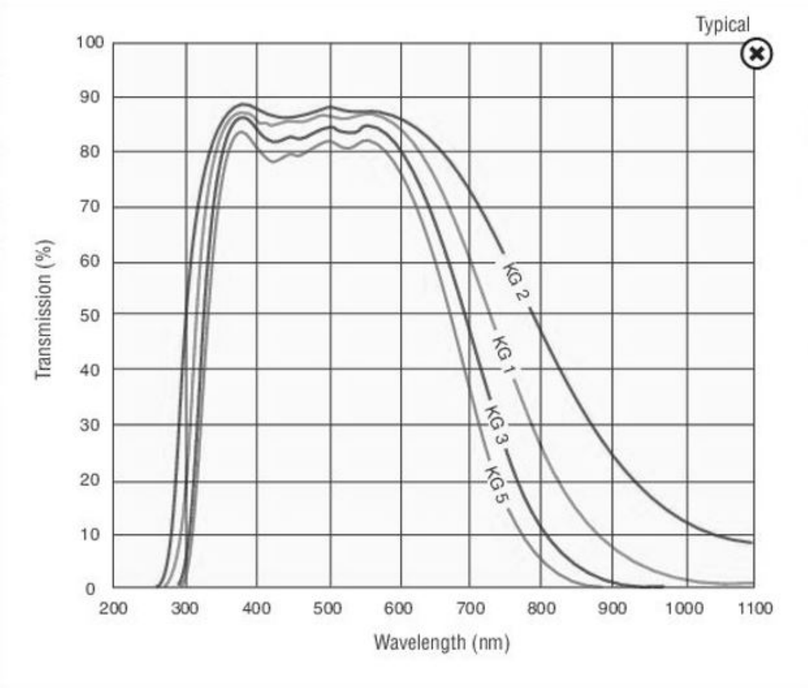

Figure 5.9: Transmission chart of the Newport FSQ-KG5

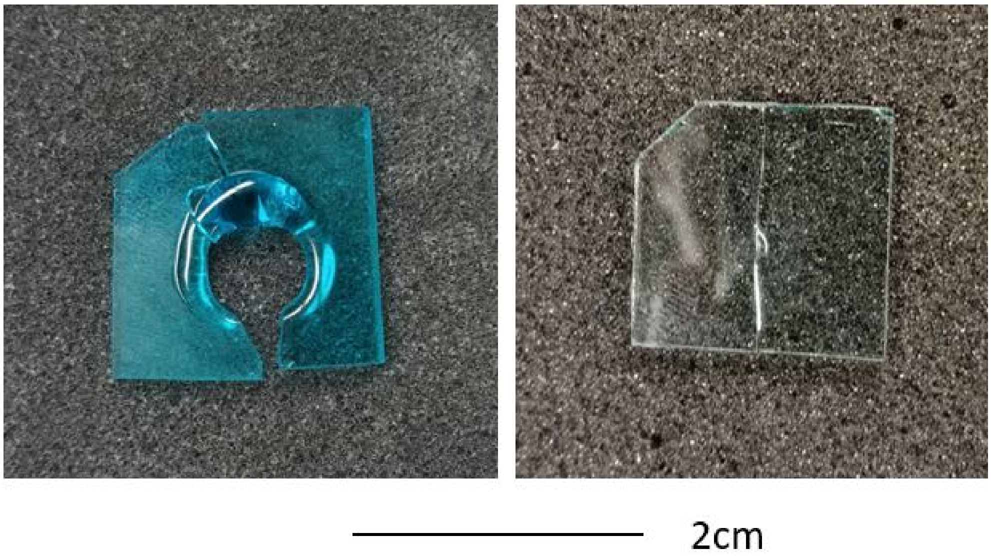

Figure 5.10: Damages to the THORLAB and Newport filters

However, totally different results were obtained after a new bottle of resin was used. With the same environmental conditions the resin of the new bottle, even though it was of the same kind and production lot, showed a different viscosity, being much more liquid, and could not cure with the same easiness as before.

Therefore, it was thought that a minimal polymerization of the resin contained in the first bottle occurred due to the exposure to natural light. This probably happened because, even though great attention was paid during all the experiments, for a relevant amount of time it was needed to use it out of its container.

The partial curing of the first bottle of resin is thought to be connected with the easy solidification of the mixture. Since the resin was partially cured, much less energy was required for the completion of the polymerization of the mixture, obtained after 60s and almost completed after 90/120s. With the resin of the new bottle, longer times were required to obtain the same result. Woefully, these were not acceptable for our needs.

While removing the second filter, in order to test again the projection without any filter, a small deformation was noticed (see Fig. 5.10). As a result, it was understood that also the Newport FSQ-KG5 faced a raise in temperature over the glass-transition T after prolonged exposure to the projector light.

As a last attempt, a third filter was purchased, more specifically the ROSCO # 4200, with the bandpass shown in Fig. 5.11.

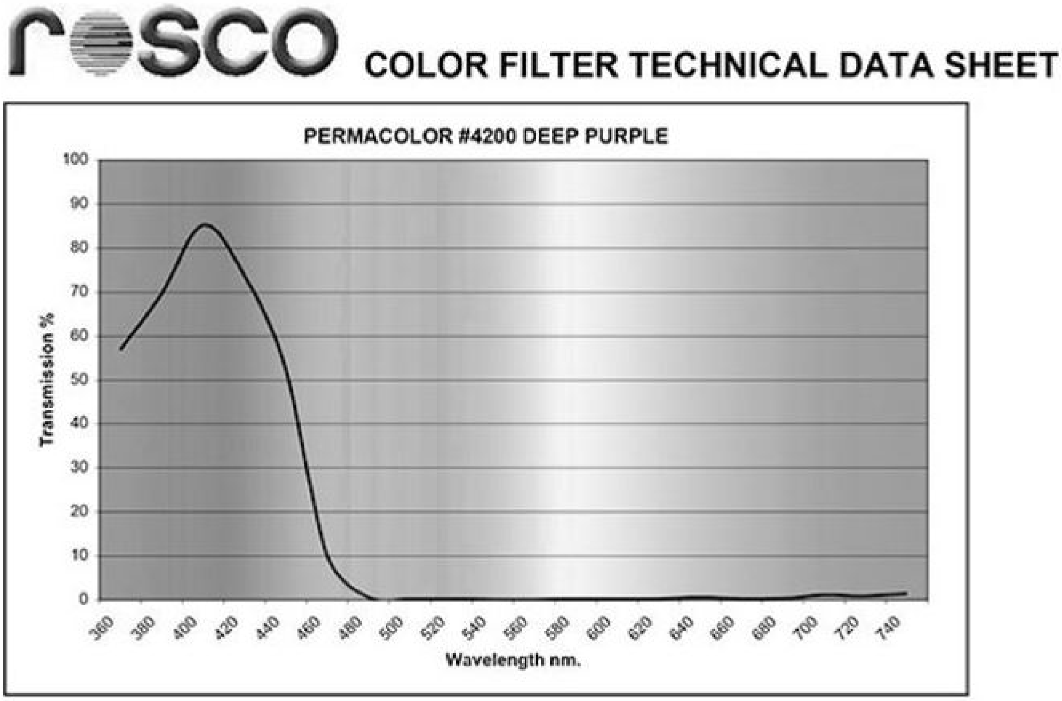

nm.	360	380	400	420	440	460	480	500	520	540	560
trans %	57	70	85	74	52	10	1	0	0	0	0

Figure 5.11: Transmission chart of the Rosco # 4200

Although the bandpass was as desired, the special treatment on the filter prevented to have a good light transmissibility. A vivid purple light was visible after the filter but the radiating flux was not sufficient to observe any curing of the resin when used in the mixture.

Since no filter was strong enough to withstand the temperature increase or comply with our needs, the decision of running the same experiments performed with the physical mask, avoiding the installation of any filter, was made.

The parameters considered to be influential on the final products were:

- Mixture composition in terms of weight proportion.
- Exposure time in projected light.
- Presence of IPA in the mixture.
- Presence of heating phase after the creation of each layer.

For the last experimental phase, instead of evaluating the variables singularly, we decided to consider first of all the manufacturing process steps, so as to understand which were the best parameters to obtain the optimal results in each of them.

Optimal miscibility and flowability

Having built, at this time of the prototype development, all the parts involved in the mixing of the raw materials, in its deposition and in the spreading to create the building layers, the research group had a clearer understanding of the required process parameters. It was clearly known that the first constraints were related to the easiness in mixing and in creating the layer itself, more than to its photopolymerization.

While using a mixture made of resin and metal powder only, the proper proportion was sought, starting from a mixture 80/20, with a step of 1%. The upper limit for the metal powder, in order to have a good flowability for the deposition and the spreading of the material, has been determined equal to 87%. Thanks to the extremely low viscosity of the resin, it is obvious that the higher is resin amount in the mixture, the lower is its viscosity, hence the greater ease in all operations.

On the other hand, the greatest amount of metal powder is desired to increase the final density of the part, in order to get close to the ideal 100%, and to reduce the distortions generated by the free space, after the elimination of the resin particles during the debinding phase.

The 87% could be increased by the addition of small percentages of IPA, in replacement of part of the binder. Some trials have been made, but no satisfactory results were obtained, due to the following considerations:

- The densities of the two liquid are not completely different (0.79g/ml vs 1.16g/ml), which means that, even if the viscosity is lower (2cP vs 55cP), no significant change can be obtained by replacing small percentages of resin with IPA.
- The amount of replaceable resin is strictly limited by the inhibition of curability. It has been observed that reducing the amount of resin below the 12/3% curing issues arise, with strong influences on the final green part quality.

It has also been observed that for mixture with metal powder weight percentage lower than 85% the mixture becomes even more liquid than needed, since it could result in problems in uniformly spreading it or in leaking. As a consequence, no further experiments were made with mixture characterized by metal powder percentage greater than 87% or lower than 85%, considered as upper and lower boundaries.

Curability of the resin

As a second step, the easiness in curing was assessed, considering two samples of mixture, respectively 85% and 87%. For each of them, we tested the curing of a single layer, starting from an exposure time equal to 15s and increasing it with a step of 15s, stopping only when a visibly solid disc was obtained. The results can be read in Tab. 5.5.

			II PARAMETER: MIXTURE COMPOSITION	
			1° STEP	2° STEP
			85% metal powder-15% resin	87% metal powder-13% resin
I PARAMETER: EXPOSURE TIME (s)	1° STEP	15	NO	NO
	2° STEP	30	PARTIAL	NO
	3° STEP	45	YES	PARTIAL
	4° STEP	60	YES	YES
	5° STEP	75	YES	YES
	6° STEP	90	YES	YES

Table 5.5: Obtained curing depending on the parameters combination considered

We mainly considered the lower and the upper limits earlier defined in order to accentuate any possible difference, which were quite evident:

- The higher is the amount of resin in the mixture, the shorter is the time needed to obtain the same level of curing. The difference in time is approximately equal to 15s.
- The sample with the higher amount of resin seemed to allow a much easier removal from the platform.

On the other hand, no relevant differences where noticed in the strength of the cured layer, as expected since we were creating single-layer parts, too fragile to give any feedback on this matter.

Stiffness of the green part

The third manufacturing process factor taken into account has been the stiffness of the part being produced, both while and after its fabrication. In fact, before moving the green parts to the furnace in order to sinter them, we need to guarantee a reliable manufacturing process and an internal structure strong enough to withstand the stress which occurs during the removal from the platform, as well as during any possible manipulation.

The possible issues related to the fragility of the single layer or of the green part.

The first inconvenience would result in the fracturing of the just created layer while spreading the material for the following one, while the second in the part bending while striving to separate it from the building platform, or, in the worst case scenario, in a complete cracking.

Consequently, after having determined the required time exposure for the curing of a layer, similarly to what done during the first experiments, we started fabricating a disc made of 20 layers, together with a second part, so as to show more precisely the fabricating accuracy with shapes different from a simple circle. For this reason, the geometries of a subsized tensile bar, according to the standard ASTM E 8M-04[6] [12], was taken into account, reducing only the radius of curvature to 2mm, so as to increase even more the fabrication complexity.

E 8M – 04

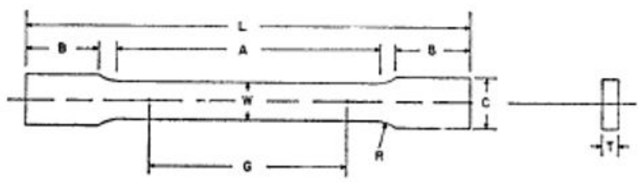

Dimensions, mm			
Nominal Width	Standard Specimens		Subsize Specimen
	Plate-Type 40 mm	Sheet-Type 12.5 mm	6 mm
G— Gage length (Note 1 and Note 2)	200.0 ± 0.2	50.0 ± 0.1	25.0 ± 0.1
W— Width (Note 3 and Note 4)	40.0 ± 2.0	12.5 ± 0.2	6.0 ± 0.1
T— Thickness (Note 5)		thickness of material	
R— Radius of fillet, min (Note 6)	25	12.5	6
L— Overall length, (Note 2, Note 7 and Note 8)	450	200	100
A— Length of reduced section, min	225	57	32
B— Length of grip section, (Note 8)	75	50	30
C— Width of grip section, approximate (Note 4 and Note 9)	50	20	10

Figure 5.12: ASTM E 8M-04 standard

[6]withdrawn in 2008 and replaced by the dual standard E 8/E 8M

Starting from the outcomes of the previous step we tried to build some parts. It became soon clear that the exposure times were not sufficient to complete the whole process. As a matter of fact, the layers were not completely cured and almost completely crumbled after the first layers.

As a consequence, we had to increase the exposure time, with steps of 15s, until we managed to create a complete part. The results can be summarized stating that we had to increase of approximately 30s the exposure time for both the sample mixtures.

After having determined the minimum exposure times for the fabrication, it was decided to make four samples, varying only a parameter at time, so as to understand any possible direct influence of the several manufacturing variables. The combination of variables taken into account and a short description of the results is summarized in Tab. 5.6, while the pictures of the parts are collected in Fig. 5.13 and 5.14.

SAMPLE NUMBER	MIXTURE COMPOSITION	EXPOSURE TIME (s)	HEATING TIME (s)	FABRICATED PART CHARACTERISTICS
1	87% METAL POWDER-13% RESIN	90	0	The overall quality is acceptable, as well as the precision. Some curing problem in the upper part of the tensile bar, as for all the other samples (black circles). Minimal delayering.
2	87% METAL POWDER-13% RESIN	**120**	0	The overall quality is acceptable, similar to Sample 1. No relevant improvements.
3	**85% METAL POWDER-15% RESIN**	90	0	The overall quality is acceptable, similar to Sample 1. Improvements in curing, as expected, and in the easiness of removing.
4	87% METAL POWDER-13% RESIN	90	**15**	Relevant problems: strong delayering and curling of the layers (red and black circles). Unacceptable overall quality.

Table 5.6: Obtained results with complete fabrication, depending on the parameters combination considered

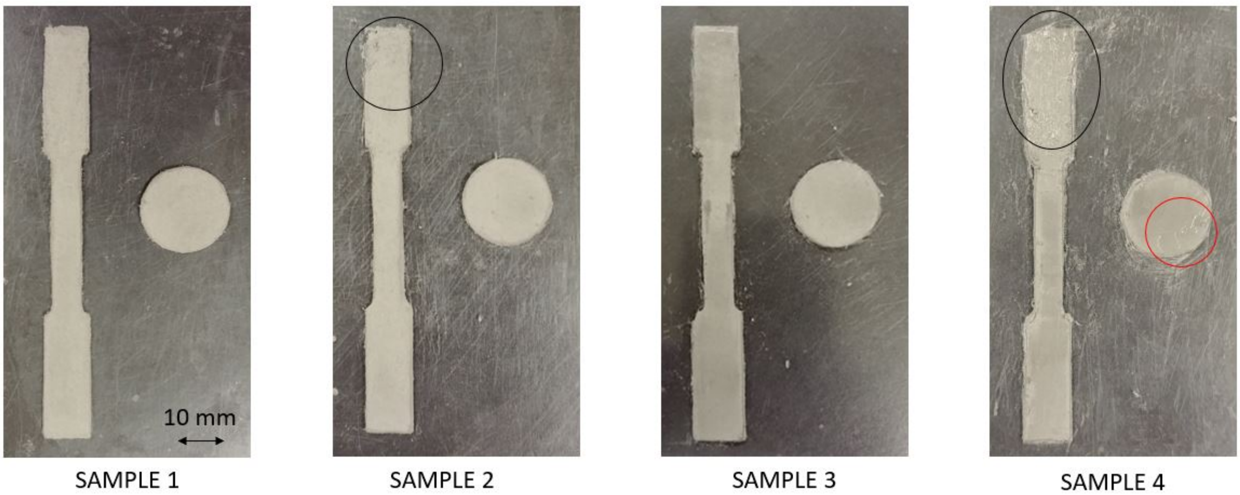

Figure 5.13: Pictures of Samples 1-4 after the manufacturing cycle, before removal

It is worth to note that in all the experiments, even in the following ones, it was noticed that the upper part of the tensile bar always faced problems in curing, together with a partial crumbling. This is particularly evident in Sample 2 and 4, highlighted with black circles, but it has been observed also in other samples. This issues can be related either to the human factor, certainly present in any manual test, or more likely to a less luminous spot in the projection, which results in a lower radiating energy in that specific region.

As a matter of fact, while removing the parts from the building platform, all the tensile bars broke, with different extent, in the upper part, where the curing issues were noticed. Additionally, a second smaller fracture propagated in Sample 1 and 2 in a different area of the tensile bar, indicating that the internal structure was not strong enough to withstand the load. Sample 3 did not face that problem, probably thanks to the noticeable greater flexibility given by the higher amount of resin.

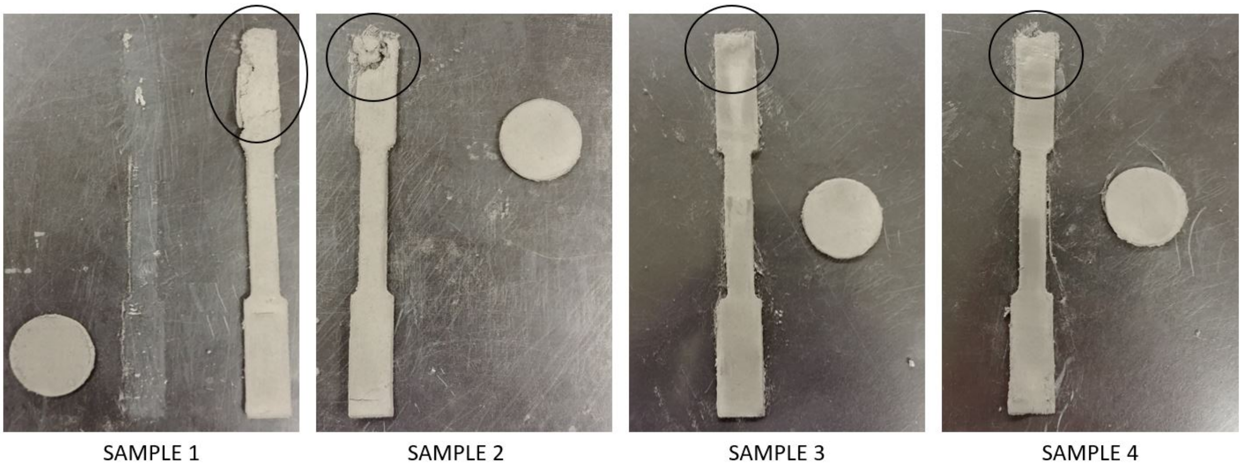

Figure 5.14: Pictures of Samples 1-4 after removal

Due to the poor quality of the sample exposed to a heating phase (Sample 4), the hypothesis of this additional step in the manufacturing process was discarded and, related to this variable, no other tests were performed.

Although the samples showed an undesirable fragility, it was decided to proceed with the sintering, so as to understand the general characterization of the structure after such a process.

All the samples turned out to be too weak to undergo complete sintering, cracking in several points, bending and deforming extensively, therefore showing the total inefficiency of the process.

As a consequence, we decided to test longer exposure times, so as to see if possible better curing could have a great influence on the final results. Two other samples were made, still employing the mixture with 87% of metal powder and 13% of resin, with exposure times equal to 180 and 240s. The characteristics of the sample are collected in Tab. 5.7, while Fig. 5.15 shows their pictures. In Fig. 6.1 then same details are enlarged in order to show the accuracy of the smallest part, such as 90° angles or the 2mm radius curvature.

SAMPLE NUMBER	MIXTURE COMPOSITION	EXPOSURE TIME (s)	HEATING TIME (s)	FABRICATED PART CHARACTERISTICS
5	87% METAL POWDER-13% RESIN	**180**	0	The overall quality has significantly improved, as well as the precision. The parts seems to be stiffer and more robust. The details, such as the 2mm curve, are much more define. Almost no curing problem, was noticed. Minimal delayering.
6	87% METAL POWDER-13% RESIN	**240**	0	The characteristics of this sample are approximately identical to Sample 5's ones.

Table 5.7: Obtained results with complete fabrication, depending on the parameters combination considered

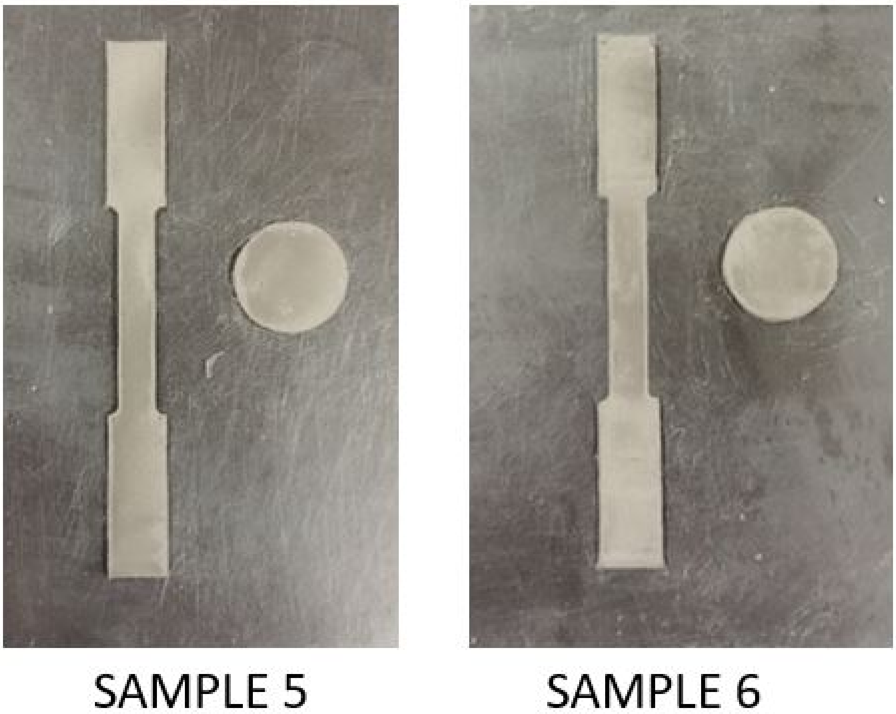

Figure 5.15: Pictures of Samples 5-6 after the manufacturing cycle, before removal

As it can be clearly noticed, the improvement obtained from the previous test is quite impressive.

Chapter 6

RESULTS AND DISCUSSION

Fabrication Quality

Starting from what experienced during the creation of the samples and also looking at the enlargement of some Sample 6 details, shown in Fig. 6.1, the following considerations could be made:

- Almost no issues have been faced during the fabrication. The layers were strong enough to withstand any load and any wear generated by the motion of the scraper. The upper part of the tensile bar still felt weaker than the rest, confirming the aforementioned hypothesis. The optimal curing resulted in a solid final structure, without cracks, superficial or lateral defects. Furthermore, no significant delayering was noticed in any part of the samples.

- The final hardness was high enough to prevent any superficial scratch from the knife used to clean the contours and remove the material in excess. Additionally, neither fractures nor distortions were generated during the removing from the platform.

- The general accuracy, quality and superficial roughness have incredibly improved.

  Because of no relevant difference could be noticed between Sample 5 and 6, the curing time taken as reference was the one employed for Sample 5, equal to 3 min, which allows a significant save in processing time, especially when the number of layers will not be 20 as in our project, but thousands.

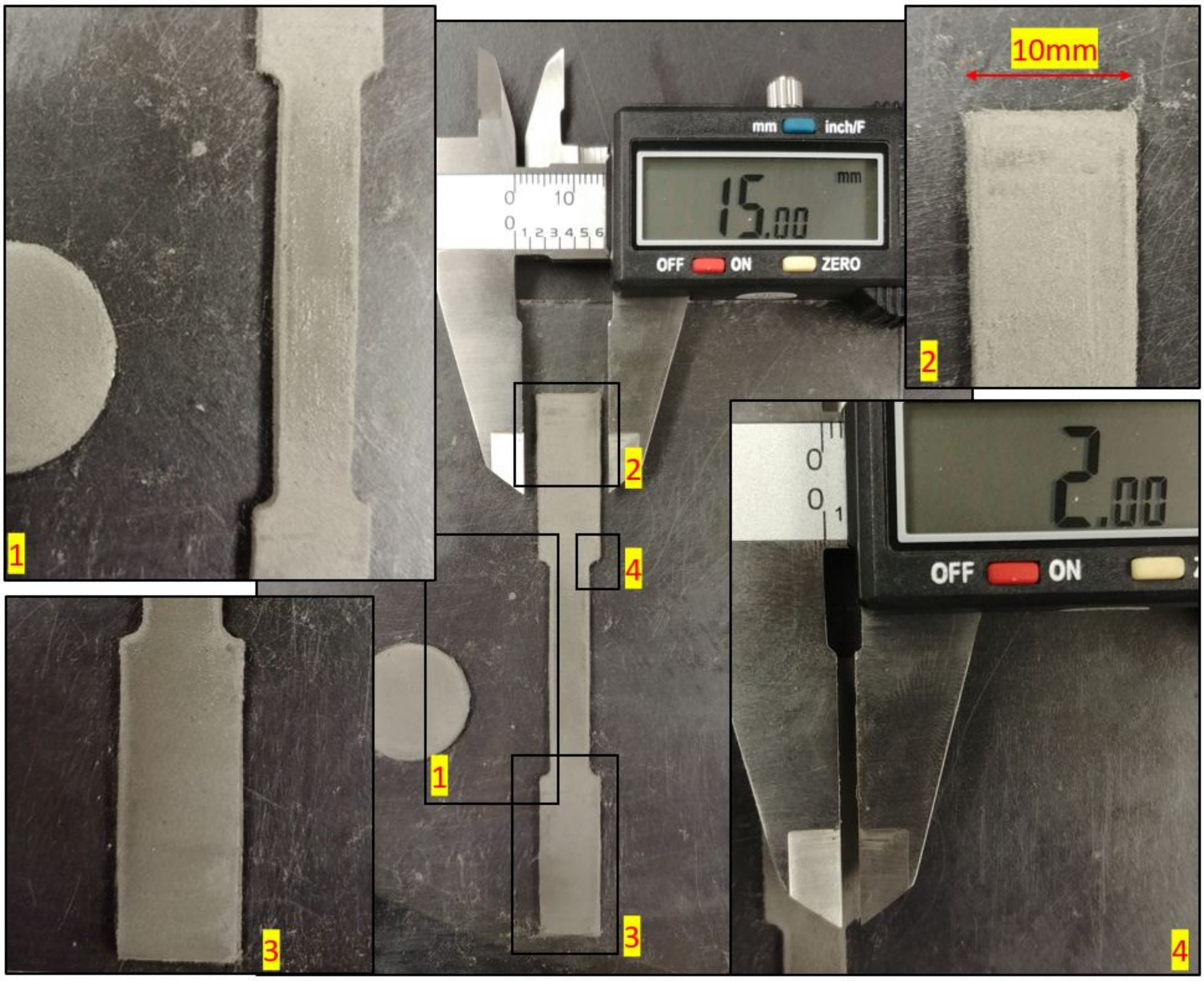

Figure 6.1: Details of Sample 6 after removal

Quality after Post-processing

After having removed the parts from the building platform, the samples were put into an air furnace and post-processed as explained in Chapt. 2.2.3 (debinding phase at 500°C and final sintering at 1100°C). The outcomes are shown in Fig. 6.2.

As it can be noticed:

- The main dimensions of the samples were maintained, with a maximum precision uncertainty of 10%, noticed in the tensile bar width (corresponding approximately to 1mm). Even though it is a relevant amount, in particular when larger dimensions are taken into account, it has to be underlined that the imprecision is mainly to be related to the manual fabrication of the parts, and not to the accuracy of the process.

  In fact, small misalignment errors during the replacing of the building platform under the projector, after the material spreading for the new layer, were unavoidable.

- The strength of the internal bonds was high enough to allow proper sintering, without visible fractures or significant delayering.

- A certain distortion occurred, in particular in Sample 6. The distortion particularly visible is along the main dimension of the tensile bar. It is worth to note that the average thickness of the sample is smaller than 1 mm.

  As a consequence, the distortion can be considered acceptable and it is not likely to happen in larger and thicker components, which will probably face only a certain amount of internal stress.

- Probably, the most relevant defect is the superficial roughness. Many circular irregularities, with an average diameter of 1mm, appeared on all the samples (from 1 to 6). It is worth to note that they are mainly present in the upper surface, while there is almost no trace in the back of the samples.

  Anyway, no significant differences were noticed among the samples, and as a consequence, it is also hard to make some hypothesis. Probably, the main reason behind this unwanted effect has to be related to the post-processing itself. A possible cause is a too short or wrong debinding phase, which could have resulted in a incomplete burning of the resin. This may have been expelled during the sintering phase abruptly, generating the superficial defects. Some further experiments will be performed once the prototype will be completed.

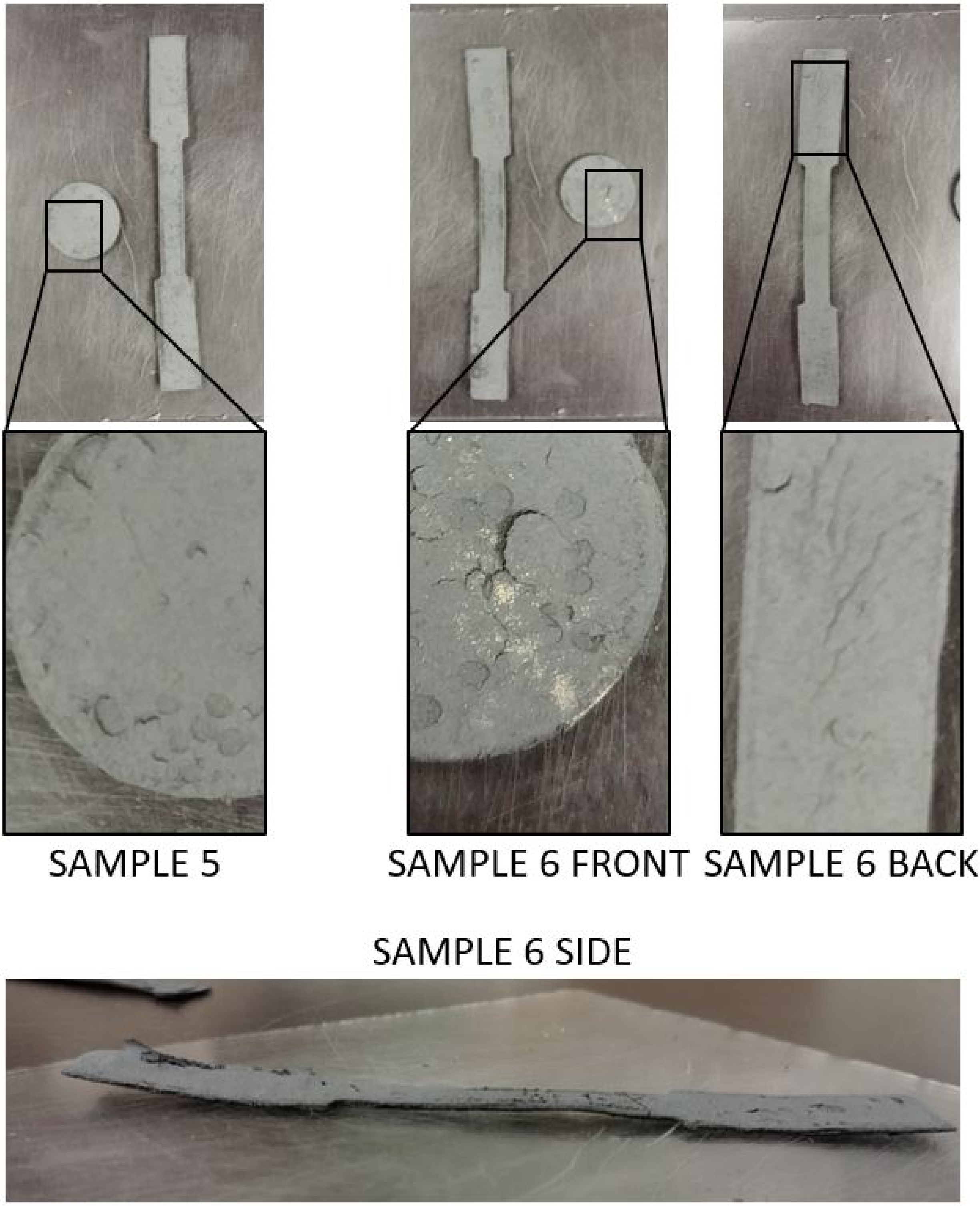

Figure 6.2: Pictures of Sample 5-6 after sintering

Chapter 7

CONCLUSIONS

Thanks to the work developed in 6 months at Michigan State University, we succeeded in our first and primary objective: proving the feasibility of a novel hybrid 3D printing technique for metal parts, named Selective Binder Curing.

Starting from the mere idea of building a new 3D printing machine, considering the base structure of a binder jetting printer and the core components of SLAs, we have been able to merge some of their characteristics, together with some innovative components and mechanisms, making use of their strong points and getting rid, or at least limiting, some of their drawbacks.

The first positive result obtained during the experimental phase is related to the 'physical-mask projection' part, Chap. 2.3. Employing a simple UV-light LED chip, we managed to cure the photopolymerizable resin, even when mixed with significant weight percentage of metal powder, fabricating solid discs.

However, this was only a preliminary test with a primitive structure. In fact, the physical mask has the enormous limitation of obliging the user to create parts with fixed cross-section, which prevents its application into a real manufacturing context.

Nevertheless, it was a good starting point. It was clear that with the proper light source, 3D parts could be easily made. We only had to substitute the system, in order to have a dynamic projection, which allows having the desired cross-section layer after layer.

Throughout the experiments with different kinds of light generating systems, we failed many times. Nonetheless, we eventually got the desired outcomes while testing an extremely economical DLP projector, after having removed some of its internal components.

Therefore, having proved the resin curing with a dynamic system, we moved to the analysis of the fabricating process parameters, shown in details in Chap. 5.1.3.

In the end, we showed that a good printing process, with the components and the technologies employed in our study, can be obtained with a 3 min exposure time, avoiding the use of a heating phase, with a mixture made of the 87% of metal powder and the 13% of photopolymerizable resin (Sigma-Aldrich CPS 1030 UV).

No significant changes have been noticed reducing the metal powder amount to 85%, or replacing small percentages of resin with IPA, which could have had the benefit of increasing the flowability of the mixture.

The second relevant part of the work has been dedicated to the creation of a prototype for this novel technique, developed simultaneously with the experimental phase.

Starting from a rough sketch of the imagined system, the general design has undergone several refinement cycles, due to the identification of new needs, requirements and constraints throughout the project. A selection of the needed components has been made, with a total cost approximately equal to $7300, lower than the $10'000 available budget.

However, considering the components already available at MSU and the last-second changes, requested by the project advisors, the expense amounted to approximately $5700. After the definition of the Bill Of Materials, thanks to the detailed dimensions of each component, a final design has been made. Starting from this, we had the possibility to build the missing parts, with the proper dimensions, using the equipment available at the MSU machine shop.

The second all the components were available, we completed the assembly and we tested the LabVIEW code, designed to run all the components according to the manufacturing cycle, shown in Fig. 5.1. After having checked the correct functioning, the feedback parameters, together with some small parts of the code, have been optimized so as to calibrate the performance of the prototype, according to specific manufacturing needs.

If we analyze the final outcomes of the project, we can state that the Selective Binder Curing technology has been tested and its feasibility has been proved.

However, it certainly needs a further and deeper refinement.

The process parameters have been determined and they are significant for a preliminary study like ours. Unfortunately, they are unacceptable for a real industrial application and they must be improved during future experimental analysis.

- The 3 min exposure time for each layer is to be reduced.

  For instance, the ExOne x-1 ProLab, available at MSU, takes on average 1 min to complete the jetting phase and an additional minute to heat it up, with a building platform of 40x60mm. It is also worth to note that it is an economical 3D printer for lab applications, while industrial printers take even shorter times.

  As a consequence, in future works, it will be mandatory to look for a reduction of the needed exposure time, and, as a consequence, of the overall fabricating time, in order to make the process suitable for industrial requirements.

  Good results are likely to be obtained replacing the cheap DLP projector with a dedicated curing system, requiring, on the other hand, greater investments, which we could not afford at this time of the development phase.

- The accuracy of the produced samples was remarkable. Even the smaller curvatures were precisely defined and no significant errors in the shape have been detected. The error in the overall dimensions, as already stated, is to be related to misalign errors, unavoidably generated during the manual steps of the experimental phase.

  For this reason, they are believed to disappear as soon as the experiments will be performed making use of the assembled prototype.

- The aforementioned superficial defects and the partial delayering observed in some samples may be related to the post-processing phase. Thanks to the just assembled prototype, further experiments will be completed in shorter times, allowing to test many different variables and different furnaces, while looking for the ideal combination.

- Thanks to the prototype, in future experiments it will also be possible to overcome the time-related issues faced during the manual tests, permitting the creation of larger and taller components. In this way, my future colleagues will have the opportunity to check possible distortions and test the actual stiffness of components made via SBC in a reliable way.

In the end, we can state that this novel hybrid 3D printing technique still has some issues which are to be solved in future experiments, but the feasibility of the process has been clearly proved and the technology has undoubtedly the potential to become an alternative to classic industrial applications. Certainly, its strong points, if compared to other 3D printing technologies for metal parts, will not be the perfect dimensional accuracy or the mechanical properties of the manufactured parts, since SLS, SLM and EBM are hardly replicable. They will be the cost-effectiveness, the flexibility, in terms of dimensions and material, and, possibly, a great productivity, especially when used in a modular way.

Appendix A

LabVIEW CODE

In order to give a clearer understanding of the LabVIEW code used to run the prototype, we believed this chapter could be useful to the reader.

A.1 Front Panel

Analyzing the front panel, shown in Fig. 4.4, a straightforward subdivision of the controls can be noticed:

- The first box is dedicated to the process parameters which need to be defined by the user (thickness of each layer, curing time and number of layers, depending on the vertical dimension of the part to be built).
- The second box contains the controls which allow the user to deactivate a particular component of the prototype, for particular applications.
- The third box collects the indicators of the fabricating process, so as to give information, such as the phase of the cycle (material deposition, layer creation, curing etc.), the number of layers already created, the elapsed time etc.
- The last box contains the reset buttons for each encoder or PID control.

A.2 Main Code

Observing Fig. 4.5, the upper block is simply a series of for loops meant to measure the elapsed time in the format hours:min:sec.

On the other hand, the lower part of the picture is occupied by the actual control block. The outer part is constituted by a for loop, where the stop condition is controlled by the number of layers received as input from the front panel.

Inside the for loop, a flat sequence has been placed in order to have a precise control on the operations sequence, which is to be followed. The backbone of the process has been presented in Fig. 5.1. The first block is represented by the opening and the closure of the discharge port, in order to allow the deposition of material.

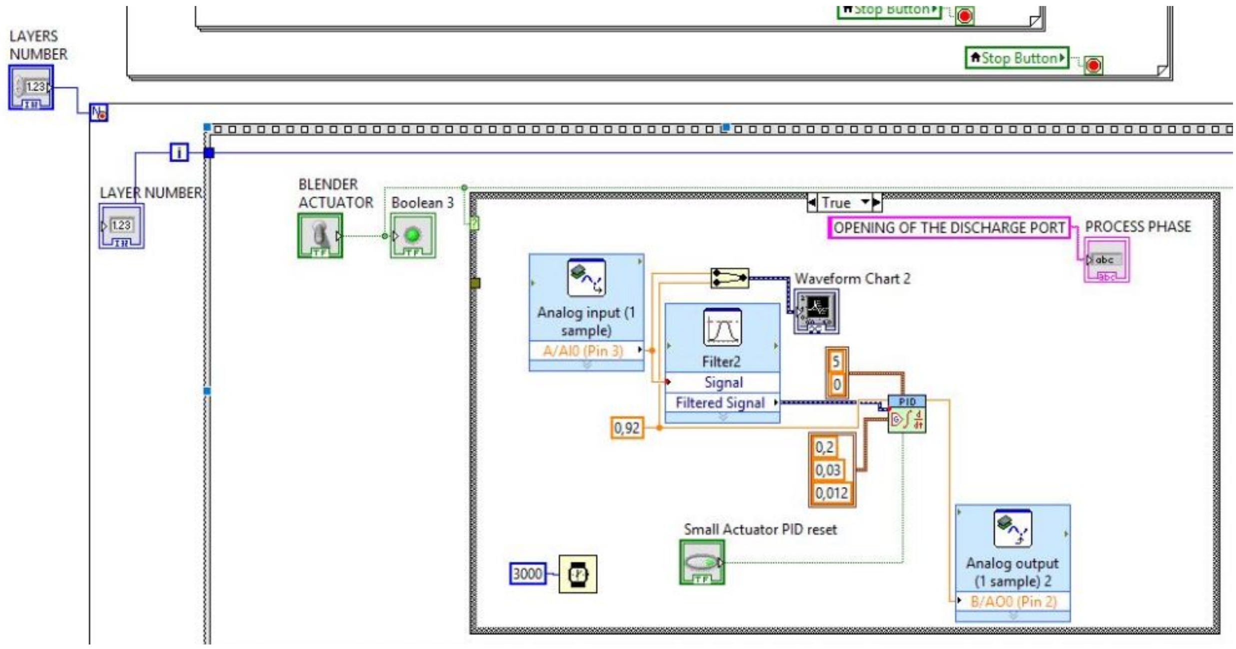

Figure A.1: Detail of the LabVIEW code

If we take a closure look at the code, with the help of Fig. A.1 the following elements can be effortlessly noticed:

- The switch control on the actuator of the discharge port controls the condition of the case structure, set as true in this example. In case of false condition, the case structure is empty and the software simply proceeds with the following step.
- Within the true case structure, the first element to appear is the analog input, which relates to the analog voltage generated by the potentiometer of the linear actuator and received through Pin 3 of Port A (as it can also be double-checked on Fig 4.2).
- The voltage relates to the position of the linear actuator, but needs a filter to reduce the unwanted signal noise.

- After the filtration, the signal can be used for the PID control, in comparison with the desired position value. In this case it was set to 0,92, which is not a spatial value but a voltage correspondence, where 0V relates to the linear actuator in rest position, while 1,4V to the maximum extension, linked to a linear behaviour.
- The two orange boxes, wired to the PID control, represent respectively the expected output values (from 0 to 5V) and the value of the proportional, integral and derivative constants, determined experimentally.
- The last elements linked to the PID control are the analog output, so as to generate the desired voltage to control the actuator, and the reset button to clear the stored values of the control.
- The waveform chart was meant to show the difference between the desired position of the actuator of the discharge port and its measured value from the potentiometer.
- The purple elements are simply the written information that we want to read on the indicators of the front panel.
- The timer represents the time given to complete this part of the flat sequence.

Analyzing Fig. 4.6, the presented structures are really similar to what just described. In the upper part the reader can notice the case structure for the mixing motor, with the only difference that the PID is based on a encoder feedback. The filtered input value has to be corrected, according to the number of counts per revolution and the considered time interval, in order to control directly the rotational speed in RPM.

In the lower part a similar control is applied for the position of the building platform, with some corrections so as to consider the different influence of the encoder value on the variable under control (vertical position).

In the last corner of the picture we can notice the direct linear control on the speed of the scraper actuator. It is constituted by a simple proportion with the output voltages, considering that 5V corresponds to the maximum forward speed, while 0V to the minimum backward speed.

Observing Fig. 4.7, we can finally have a glance at the control on the backward motion speed of the scraper and at the flat sequence block dedicated to the curing phase, where the main element is controlled by the input set by the user.

BIBLIOGRAPHY

[1] Samuel M Allen and Emanuel M Sachs. Three-dimensional printing of metal parts for tooling and other applications. *Metals and Materials*, 6(6):589–594, 2000.

[2] Flaviana Calignano, Diego Manfredi, Elisa Paola Ambrosio, Sara Biamino, Mariangela Lombardi, Eleonora Atzeni, Alessandro Salmi, Paolo Minetola, Luca Iuliano, and Paolo Fino. Overview on additive manufacturing technologies. *Proceedings of the IEEE*, 105(4):593–612, 2017.

[3] Han Chen and Yaoyao Fiona Zhao. Process parameters optimization for improving surface quality and manufacturing accuracy of binder jetting additive manufacturing process. *Rapid Prototyping Journal*, 22(3):527–538, 2016.

[4] Zhou Chi. *Optimized mask image projection for large-area based additive manufacturing process*. PhD thesis, University of Southern California, 2011.

[5] Truong Do, Patrick Kwon, and Chang Seop Shin. Process development toward full-density stainless steel parts with binder jetting printing. *International Journal of Machine Tools and Manufacture*, 121:50–60, 2017.

[6] Truong Do, Chang Seop Shin, Dalton Stetsko, Grayson VanConant, Aleksandr Vartanian, Shenli Pei, and Patrick Kwon. Improving structural integrity with boron-based additives for 3d printed 420 stainless steel. *Procedia Manufacturing*, 1:263–272, 2015.

[7] Daniel Feldt, Petra Hedberg, Asker Jarlöv, Elsa Persson, Mikael Svensson, Filippa Vennberg, and Therese You. Independent project in chemical engineering and materials engineering: A literature study of powder-based additive manufacturing, 2018.

[8] Jean-Pierre Fouassier and Jan F Rabek. *Radiation curing in polymer science and technology: Practical aspects and applications*, volume 4. Springer Science & Business Media, 1993.

[9] Wei Gao, Yunbo Zhang, Devarajan Ramanujan, Karthik Ramani, Yong Chen, Christopher B Williams, Charlie CL Wang, Yung C Shin, Song Zhang, and Pablo D

Zavattieri. The status, challenges, and future of additive manufacturing in engineering. *Computer-Aided Design*, 69:65–89, 2015.

[10] Ian Gibson, David Rosen, and Brent Stucker. *Additive Manufacturing Technologies.* Springer, 2015.

[11] Prashanth Konda Gokuldoss, Sri Kolla, and Jürgen Eckert. Additive manufacturing processes: Selective laser melting, electron beam melting and binder jetting—selection guidelines. *Materials*, 10(6):672, 2017.

[12] ASTM International. *ASTM E8-04 Standard Test Methods for Tension Testing of Metallic Materials.*

[13] ASTM International. *ASTM F2792-12a, Standard Terminology for Additive Manufacturing Technologies.*

[14] Paul Francis Jacobs. *Rapid prototyping & manufacturing: fundamentals of stereolithography.* Society of Manufacturing Engineers, 1992.

[15] Jim H Lee, Robert K Prud'Homme, and Ilhan A Aksay. Cure depth in photopolymerization: experiments and theory. *Journal of Materials Research*, 16(12):3536–3544, 2001.

[16] Ameya Limaye and DW Rosen. Process planning to build mask projection stereolithography parts with accurate vertical dimensions. In *International Solid Freeform Fabrication Symposium, The University of Texas at Austin*, 2007.

[17] Zhanjie Liu, Yifan Wang, Fernando J Muzzio, Gerardo Callegari, and German Drazer. Capillary drop penetration method to characterize the liquid wetting of powders. *Langmuir*, 33(1):56–65, 2016.

[18] Hadi Miyanaji, Morgan Orth, Junaid Muhammad Akbar, and Li Yang. Process development for green part printing using binder jetting additive manufacturing. *Frontiers of Mechanical Engineering*, pages 1–9.

[19] Hadi Miyanaji, Shanshan Zhang, and Li Yang. A new physics-based model for equilibrium saturation determination in binder jetting additive manufacturing process. *International Journal of Machine Tools and Manufacture*, 124:1–11, 2018.

[20] Gerhard Pahl and Wolfgang Beitz. *Engineering design: a systematic approach*. Springer Science & Business Media, 2007.

[21] Yayue Pan, Chi Zhou, and Yong Chen. A fast mask projection stereolithography process for fabricating digital models in minutes. *Journal of Manufacturing Science and Engineering*, 134(5):051011, 2012.

[22] Duc Truong Pham and Rosemary S Gault. A comparison of rapid prototyping technologies. *International Journal of machine tools and manufacture*, 38(10-11):1257–1287, 1998.

[23] Issa Rishmawi, Mehrnaz Salarian, and Mihaela Vlasea. Tailoring green and sintered density of pure iron parts using binder jetting additive manufacturing. *Additive Manufacturing*, 2018.

[24] C Sun, N Fang, DM Wu, and X Zhang. Projection micro-stereolithography using digital micro-mirror dynamic mask. *Sensors and Actuators A: Physical*, 121(1):113–120, 2005.

[25] Beatrice Vanzo. L'avvento della stampa 3d. implicazioni e nuove possibilità per la manifattura. 2017.

[26] Yujia Wang and Yaoyao Fiona Zhao. Investigation of sintering shrinkage in binder jetting additive manufacturing process. *Procedia Manufacturing*, 10:779–790, 2017.

[27] Chi Zhou, Hang Ye, and Feng Zhang. A novel low-cost stereolithography process based on vector scanning and mask projection for high-accuracy, high-speed, high-throughput, and large-area fabrication. *Journal of Computing and Information Science in Engineering*, 15(1):011003, 2015.